JOURNAL OF FLUID MECHANICS

UNIV OF MICHIGAN
SEP 1957
ENGINEERING LIBRARY

VOLUME 2 PART 5

JULY 1957

Printed and Published by

TAYLOR & FRANCIS LTD

RED LION COURT, FLEET STREET, LONDON, E.C.4

The JOURNAL OF FLUID MECHANICS exists for the publication of theoretical and experimental investigations of all aspects of the mechanics of fluids, and is issued in six parts per volume.

Editor:

Dr. G. K. BATCHELOR, Cavendish Laboratory, University of Cambridge, Cambridge, England.

Assistant Editors:

Dr. T. B. BENJAMIN, Dr. I. PROUDMAN.

Associate Editors:

Prof. G. F. CARRIER, Pierce Hall, Harvard University, Cambridge 38, Massachusetts, U.S.A.

Dr. W. C. GRIFFITH, Research and Development Laboratory, Missile Systems Division, Lockheed Aircraft Corporation, Palo Alto, California, U.S.A.

Prof. M. J. LIGHTHILL, Department of Mathematics, The University, Manchester, England.

Authors wishing to have papers published in the JOURNAL should communicate them to any one of the persons named above, choosing one in their own country where possible.

Authors are urged to ensure that their papers are written clearly and attractively, in order that their work will be readily accessible to readers.

Manuscripts should be typed in double spacing on one side of the paper only, with references listed at the end in alphabetical order of authors. Drawings should be done on a large scale in Indian ink on tracing cloth or drawing paper, captions being typed on a separate sheet. Proofs of papers from overseas will usually be despatched to authors by airmail. Authors are entitled to receive 50 offprints of a paper in the JOURNAL free of charge, and additional offprints can be purchased from the publisher.

PRICE £1 ($2.80) per part

Subscription, £5 10s. 0d. per volume of six parts, post free ($15.40 in U.S.A. and Canada)

Agents for U.S.A. and Canada:

Academic Press Inc., 111 Fifth Avenue, New York 3, N.Y., U.S.A.

On the generation of waves by turbulent wind

By O. M. PHILLIPS
St. John's College, Cambridge

(*Received* 18 *February* 1957)

CONTENTS

1. Introduction.
2. The approach to the problem.
   2.1 The physical background.
   2.2. The equations of motion.
3. The initial stage of wave development.
   3.1. The initial response of the water surface.
   3.2. Resonance waves.
   3.3. The question of $U_{\min}$.
4. The principal stage of development.
   4.1. The wave spectral function.
   4.2. Termination of the principal stage of development.
   4.3. Comparison with observations on the wave field.

SUMMARY

A theory is initiated for the generation of waves upon a water surface, originally at rest, by a random distribution of normal pressure associated with the onset of a turbulent wind. Correlations between air and water motions are neglected and the water is assumed to be inviscid, so that the motion of the water, starting from rest, is irrotational. It is found that waves develop most rapidly by means of a resonance mechanism which occurs when a component of the surface pressure distribution moves at the same speed as the free surface wave with the same wavenumber.

The development of the waves is conveniently considered in two stages, in which the time elapsed is respectively less or greater than the time of development of the pressure fluctuations. An expression is given for the wave spectrum in the initial stage of development (§ 3.2), and it is shown that the most prominent waves are ripples of wavelength $\lambda_{cr} = 1{\cdot}7$ cm, corresponding to the minimum phase velocity $c = (4gT/\rho)^{1/4}$ and moving in directions $\cos^{-1}(c/U_c)$ to that of the mean wind, where U_c is the 'convection velocity' of the surface pressure fluctuations of length scale λ_{cr} or approximately the mean wind speed at a height λ_{cr} above the surface. Observations by Roll (1951) have shown the existence under appropriate conditions, of waves qualitatively similar to those predicted by the theory.

Most of the growth of gravity waves occurs in the second, or principal stage of development, which continues until the waves grow so high that non-linear effects become important. An expression for the wave spectrum is derived (§ 4.1), from which follows the result

$$\overline{\xi^2} \sim \frac{\overline{p^2} t}{2\sqrt{2}\rho^2 U_c g},$$

where $\overline{\xi^2}$ is the mean square surface displacement, $\overline{p^2}$ the mean square turbulent pressure on the water surface, t the elapsed time, U_c the convection speed of the surface pressure fluctuations, and ρ the water density. This prediction is consistent with published oceanographic measurements (§ 4.3).

It is suggested that this resonance mechanism is more effective than those suggested by Jeffreys (1924, 1925) and Eckart (1953), and may provide the principal means whereby energy is transferred from the wind to the waves.

1. Introduction

In the following pages, a theory is proposed to account for the generation of waves by wind. The problem has attracted attention for many years, during which time many experimental studies have been made and many hypotheses advanced to account for the results of these observations. However, no really satisfactory explanation of the phenomenon has been offered and not even the physical processes involved can be regarded as known. Although casual observations of wind-generated waves must have been made by almost everyone, thorough experimental investigations are difficult, and our understanding of the subject has consequently been very limited. The best known of the various hypotheses put forward are those due to Jeffreys (1924, 1925) and Sverdrup & Munk (1947), which are described in a valuable review of the subject by Ursell (1956). Jeffreys's sheltering hypothesis is the very reasonable one that the wind passing over any waves already existing on the surface induces a variable pressure distribution, and that the component which is in phase with the wave slope supplies further energy to the wave, resulting in its continued development. The predictions from this hypothesis involve a sheltering coefficient s, which, for a wave in which the energy gain from the wind just balances the viscous dissipation, is required to have a value of approximately 0·27. However, experimental measurements of s made on solid wave models gave values which were smaller by an order of magnitude, so that it must be concluded that the effect of sheltering, though undoubtedly present to some degree, is not efficient enough to account for the observed wave growth. The failure of this hypothesis led Sverdrup & Munk and others to consider the effect of the tangential stresses set up on the water surface. By assuming that *all* the energy communicated to the water by these stresses appears in waves and none in currents, they were able to account for the order of

magnitude of the observed wave heights. But such theories, based upon energy considerations alone, are hardly satisfactory; and, as a means of producing the irrotational motion associated with surface waves, the shear stresses seem intuitively to be singularly inefficient, particularly in the early stages of wave growth. It seems more plausible to suppose that the initiation and early development of waves is a consequence of fluctuations in the normal pressure upon the surface, which under natural conditions are always present on account of the invariably turbulent character of the wind. As the waves develop, the influence of the shear stresses upon the wave pattern may not remain negligible, though it is difficult to give an *a priori* estimate of their importance. However, it will be seen later that the observed wave heights can be explained in terms of the pressure fluctuations alone, so that it seems possible that the effects of the shear stresses are rarely, under natural conditions, dominant in the wave growth.

The present approach is developed without specific empirical assumptions, such as the sheltering hypothesis of Jeffreys or the assumptions of energy transfer involved in the work of Sverdrup & Munk. The mathematical problem can be formulated as follows. Given that at an initial instant a turbulent wind commences to blow across an infinite sheet of deep (inviscid) water originally at rest, generating a distribution of fluctuating pressure on the surface which is a stationary random function of position and time, the aim is to study the properties of the surface displacement at subsequent times.

An attempt to solve the problem in a manner similar to this was made by Eckart (1953). He represented the pressure distribution associated with the turbulent wind in a very specific way, i.e. as an aggregate of pressure points of a given size and duration over a finite storm area. It is very likely that this representation is too specific to give an adequate description of the randomness of the fluctuations in pressure associated with the turbulent wind. It will be seen later that this randomness is essential, since the water surface selects from the whole range of wave-numbers in the applied pressure distribution certain ones whose amplitude increases most rapidly by a mechanism involving a type of resonance. The inadequacy of Eckart's representation in this respect is probably the most important cause of the failure of his theory to explain the observed wave heights; his predicted values are an order of magnitude too small.

It is clear from the way the problem has been formulated that the present treatment is not a stability theory, such as the Kelvin–Helmholtz model (see, for example, Ursell 1956). It is found that waves can grow not only through an instability but by this mechanism of resonance between the components of the surface pressure distribution and the free surface waves. It cannot be claimed that this resonance effect, whose nature will be explained more fully below, is the only one capable of generating waves; for instabilities of the Kelvin–Helmholtz type will almost certainly occur if the wind velocity is sufficiently high and established sufficiently rapidly (perhaps producing the capillary ripples observed in strong gusts of wind),

and in some circumstances the effects of sheltering and shear-stress action may not be negligible. However, it does account in a natural way for a variety of observed phenomena, though a true appreciation of its scope and limitations must await the results of further investigations, particularly on the effects of the non-linearities which become important when the wave slopes become appreciable.

My understanding of the problems involved in the generation of waves by wind has been greatly helped by discussions with Dr M. S. Longuet-Higgins of the National Institute of Oceanography, Surrey, and with Mr F. Ursell and Dr A. A. Townsend at Cambridge; it is a pleasure to acknowledge my indebtedness to them for their constructive comments upon this work.

2. The approach to the problem

2.1. *The physical background*

It is a matter of common observation that winds, blowing over the ground or over water, do not consist of streams of air in steady and uniform motion but rather of an irregular series of 'puffs' and 'lulls' carrying eddies and swirls distributed in a disordered manner. In the language of the fluid dynamicist, the wind is not laminar, but invariably turbulent. This turbulent nature of the wind will be found to result in the birth and growth of waves upon a water surface. The atmospheric eddies, or random velocity fluctuations in the air, are associated with random stress fluctuations on the surface, both pressures (i.e. normal stresses) and tangential shear stresses. The eddies are borne forward by the mean velocity of the wind, and at the same time they develop, interact and decay, so that the associated stress distribution f both moves across the surface with a certain convection velocity dependent upon the velocity of the wind and evolves in time as it does so. An overall convection velocity of the stress fluctuations can be defined mathematically as *the velocity of the frame of reference in which their frequency scale is least*, or their time scale greatest. This least frequency scale is characteristic of the evolution of the stress distribution, whereas the frequencies observed, say at a fixed point, are invariably greater because of added contributions from the sweeping of the stress pattern past the point.

The stress distribution contains components with a very large range of wave-numbers, and as might be expected, Fourier components with very different wave-numbers $\boldsymbol{\kappa}$ are convected at different speeds. The surface stress fluctuations of any given length scale can be attributed to turbulent eddies near the surface whose length scale is of the same order of magnitude, and the larger eddies will be convected by the mean wind with a greater speed than the smaller stress-generating eddies lying near the surface. A definition to express this slightly more refined concept can be given as follows. If $F(\boldsymbol{\kappa}, t)$ is the two-dimensional spatial Fourier transform of the surface stress covariance $\overline{f(\mathbf{x}', t')f(\mathbf{x}' + \mathbf{x}, t' + t)}$, then the convection velocity

$\mathbf{U}_c(\boldsymbol{\varkappa})$ for the components of wave-number $\boldsymbol{\varkappa}$ is the velocity of the frame of reference in which the time scale

$$[F(\boldsymbol{\varkappa}, 0)]^{-1} \int_0^\infty F(\boldsymbol{\varkappa}, t)\, dt$$

is greatest. That is, we take axes moving with velocity $\mathbf{u}$, and in this frame of reference (see § 4.1)

$$F(\boldsymbol{\varkappa}, t, \mathbf{u}) = [F(\boldsymbol{\varkappa}, t)]_{\mathbf{u}=0} \cos(\boldsymbol{\varkappa} . \mathbf{u}\, t).$$

The convection velocity $\mathbf{U}_c(\boldsymbol{\varkappa})$ is the value of $\mathbf{u}$ for which

$$\int_0^\infty [F(\boldsymbol{\varkappa}, t)]_{\mathbf{u}=0} \cos(\boldsymbol{\varkappa} . \mathbf{u}\, t)\, dt$$

is a maximum. This maximum time scale, or development time of the stress fluctuations, which appears later in the analysis, will be denoted by $\Theta(\boldsymbol{\varkappa})$. In the frame of reference convected with velocity $\mathbf{U}_c$, the time dependence is slowest and is determined by the growth and decay of the eddies as they are carried along.

The convection velocity $\mathbf{U}_c$ defined in this way must be related to the mean velocity of the wind measured at a certain height above the surface. The physical picture of the convection of the stress-generating eddies mentioned above suggests that $\mathbf{U}_c(\boldsymbol{\varkappa})$ is of the same order as the mean velocity of the wind at a height κ^{-1} above the surface. Now, the mean velocity profile of the wind $U(z)$ is determined by the friction velocity u_* ($=(\tau_0/\rho_a)^{1/2}$ where τ_0 is the mean horizontal shear stress at the surface, and ρ_a the density of the air), by the roughness length z_0, and by the kinematic viscosity ν, and is of the form

$$\frac{U(z)}{u_*} = 2{\cdot}3\left[\log\frac{z}{z_0} + B\left(\frac{u_* z_0}{\nu}\right)\right]. \tag{2.1}$$

In aerodynamically rough flow, the function B is in effect zero, and the roughness length z_0 for a water surface is probably related to u_* by an expression of the type $u_*^2 \propto g z_0$ and for moderate winds is of order 0·1 cm. The velocity profile of the wind over a water surface is discussed in recent review articles by Ellison (1956) and Ursell (1956); the reader is referred to these accounts if further detail is required. However, the important point in this connection is that when z/z_0 is large, the variation of mean velocity with height is slow, so that for the components of the stress distribution whose length scale is of the order of several metres, the convection velocity $U_c(\boldsymbol{\varkappa})$ is very nearly equal to the wind velocity as usually measured from a ship. For the very much smaller components, however, it may be considerably less.

Our problem is to discover the nature of the action between this stress distribution and the water surface, and the investigation of this is described in the following sections. However, it will perhaps be clearer if some of the

salient features are described first in physical terms, although this will necessitate anticipation of some of the analysis to be developed later. This background will, it is hoped, make the direction and implications of the subsequent mathematics more evident.

We have assumed that the fluctuating pressure upon the water surface is responsible for the birth and early growth of waves. If a Fourier analysis were to be made in the two space dimensions of the surface and in time, components would be found over a wide range of wave-numbers and frequencies. These components of the pressure fluctuations acting upon the surface generate small forced oscillations, and the amplitude of any Fourier component of the surface displacement depends upon the amplitude of the corresponding component of the forcing pressure fluctuations. But the response of the water surface to the various Fourier components of the pressure field is not uniform, since certain combinations of wave-number and frequency in the components of the surface displacement are excited more readily than others. In particular, if the pressure distribution contains components whose wave-numbers and frequencies coincide with possible modes of *free* surface waves, then a type of resonance occurs, and the continued presence of these components in the pressure distribution (although their amplitudes may not be large) generates surface waves whose amplitude continually increases.

The nature of this resonance can be seen most clearly by considering the motion in a frame of reference moving with the convection velocity of the surface pressure distribution. Suppose we can, for the moment, neglect the evolution of the pattern of stress fluctuations so that the distribution is stationary in the convected frame of reference. The various components generate wavelets of small amplitude which propagate along the surface in all directions; but for a given convection velocity (provided it is not too small) there are two particular wave modes that propagate in the direction of the wind at the convection velocity. These particular wavelets remain stationary with respect to the pressure distribution which produced them. The phase difference between these particular wavelets and the Fourier component of the pressure field with the same wave-number remains fixed, so that the conditions which gave them birth remain to ensure their continued growth.

But this is an over-simplification, because the evolution of the stress pattern usually cannot be ignored. If we make a two-dimensional spatial Fourier analysis of the surface pressure distribution with respect to axes moving with the convection velocity, the amplitude and phase of each component varies slowly in a random manner with time. The particular wavelet which is stationary with respect to the convected reference frame is still subject to a pressure component of the same wave-number, but one whose phase now wanders and whose amplitude varies. However, the average amplitude of the wavelet continues to increase, although we should expect the variation of mean square amplitude at this wave-number to be slower than it would be if the phase were constant. This process of

statistical development through a random influence is already familiar in the contexts of diffusion and random-walk problems.

The mathematical problem in which this process appears has already been formulated in the previous section, and certain assumptions will now be made to facilitate the analysis. We should like to be able to assume that the statistical properties of the applied pressure fluctuations are independent of the waves already generated. We will therefore endeavour to determine the conditions under which this is likely to be true. Initially the water is at rest, so that in the very early stages of wave growth (i.e. the 'initial stage' of § 3) this assumption can clearly be made as a first approximation, since the initial pattern of ripples has not yet grown large enough in amplitude to have a significant effect on the wind. Presumably, however, the pattern of ripples soon reaches some sort of statistical equilibrium, and there is evidence (see Ursell 1956, p. 240) that the roughness length z_0 of the surface is determined by these short steep ripples rather than by the height of the longer waves that subsequently develop. It seems, then, that after quite a short duration these ripples begin to exercise a profound influence upon the mean velocity profile and the other mean properties of the turbulent wind. However, a much greater time is taken for the development of the longer gravity waves in which we are more interested. It seems, therefore, that when the duration is sufficiently long, the components of the pressure distribution generating the longer *gravity* waves are independent of the waves of this kind already present. To summarize, this assumption seems justified under two sets of conditions: (i) when the duration of the wind is very small, and (ii) for gravity waves when the duration is large. In both cases, this assumption must be expected to fail when the wave steepness becomes too great, since, for example, sheltering effects may then become important.

As a further simplification, the viscosity of the water will be neglected, since it is probably unimportant for all but the shortest waves over moderate intervals of time. The motion, which is envisaged as starting from rest, is then irrotational. Consideration is restricted to waves whose mean-square slope is small, so that the surface boundary condition can be linearized. Finally, for definiteness and convenience, the surface pressure fluctuations are assumed to be statistically homogeneous over regions of the surface whose extent is comparable with the correlation areas of the atmospheric turbulence, and, after the initial instant, to be statistically steady.

2.2. *The equations of motion*

In this problem it is convenient to express the surface pressure fluctuations and surface displacements in terms of their Fourier components. The pressure fluctuation p and displacement ξ are stationary random functions of position $\mathbf{x} = (x_1, x_2)$ in the surface plane, so that simple Fourier transforms do not exist. However, we can invoke a more effective technique, used widely in the theory of random functions (see, for example, its application

to turbulence theory in Batchelor (1953)), by defining the Fourier–Stieltjes transform

$$\xi(\mathbf{x}, t) = \int dA(\mathbf{x}, t) e^{i\mathbf{x}\cdot\mathbf{x}}, \tag{2.2}$$

where the integration is over all wave-numbers $\mathbf{x}$ in the plane. The two-dimensional instantaneous spectrum of the surface displacement is the Fourier transform of the covariance

$$\Xi(\mathbf{r}) = \overline{\xi(\mathbf{x})\xi(\mathbf{x}+\mathbf{r})},$$

which decreases to zero rapidly as $\mathbf{r} \to \infty$, so that its Fourier transform

$$\Phi(\mathbf{x}) = (2\pi)^{-2} \int \Xi(\mathbf{r}) e^{-i\mathbf{x}\cdot\mathbf{r}}\, d\mathbf{r},$$

where $d\mathbf{r}$ represents $dr_1\, dr_2$ and the integration is over the entire surface with $\mathbf{x}$ fixed, does exist in the ordinary sense. From the inverse of this relation, it can be shown that the spectrum is given in terms of the Fourier–Stieltjes transform by

$$\Phi(\mathbf{x}, t) = \frac{\overline{dA(\mathbf{x}, t)\, dA^*(\mathbf{x}, t)}}{d\kappa_1\, d\kappa_2}, \tag{2.3}$$

where the asterisk indicates the complex conjugate. Similar expressions can be written down to specify the pressure fluctuations on the surface. The two-dimensional Fourier–Stieltjes transform

$$p(\mathbf{x}, t) = \int d\varpi(\mathbf{x}, t) e^{i\mathbf{x}\cdot\mathbf{x}} \tag{2.4}$$

is related to the spectrum function $\Pi(\mathbf{x}, t)$ of the surface pressure fluctuations by the expression

$$\Pi(\mathbf{x}, t) = (2\pi)^{-2} \int \overline{p(\mathbf{x}, t')p(\mathbf{x}+\mathbf{r}, t'+t)}\, e^{-i\mathbf{x}\cdot\mathbf{r}}\, d\mathbf{r},$$

$$= \frac{\overline{d\varpi(\mathbf{x}, t')\, d\varpi^*(\mathbf{x}, t'+t)}}{d\kappa_1\, d\kappa_2}, \tag{2.5}$$

which is a function of the wave-number $\mathbf{x}$ and time separation t.

The motion in the water has been assumed to be irrotational, so that a potential ϕ can be defined such that

$$\mathbf{u} = \nabla\phi \quad \text{and} \quad \nabla^2\phi = 0, \tag{2.6}$$

where $\mathbf{u}$ is the velocity vector. The surface boundary condition for waves of infinitesimal height is

$$\frac{1}{\rho}\left\{p - T\left(\frac{\partial^2\xi}{\partial x_1^2} + \frac{\partial^2\xi}{\partial x_2^2}\right)\right\} = \left[\frac{\partial\phi}{\partial t}\right]_{z=0} - g\xi, \tag{2.7}$$

where ρ is the density of the water, T the surface tension at the interface, g the gravitational acceleration, ξ the surface displacement, and z is the vertical position coordinate to be measured downwards from the undisturbed

surface level. It is convenient to express this equation in a frame of reference moving with an arbitrary velocity U, and it becomes

$$\frac{p}{\rho} = \left[\frac{\partial\phi}{\partial t} - U_i\frac{\partial\phi}{\partial x_i}\right]_{z=0} - g\xi + \frac{T}{\rho}\left(\frac{\partial^2\xi}{\partial x_1^2} + \frac{\partial^2\xi}{\partial x_2^2}\right). \tag{2.8}$$

The normal velocity of the surface is $d\xi/dt$, or in the moving frame of reference,

$$\left(\frac{\partial}{\partial t} - U_i\frac{\partial}{\partial x_i}\right)\xi = \left[\frac{\partial\phi}{\partial z}\right]_{z=0} = \int (dA' - i\mathbf{x}\,.\,\mathbf{U}\,dA)e^{i\mathbf{x}\,.\,\mathbf{x}}, \tag{2.9}$$

where the representation (2.1) is used, and where the accent represents time differentiation in the convected frame of reference. The irrotational motion in the water is specified by the solution of $\nabla^2\phi = 0$ with the boundary conditions that $\phi \to 0$ as $z \to \infty$, and that at $z = 0$, $\partial\phi/\partial z$ is as given by (2.9). This solution is (see Phillips 1955)

$$\phi = -\int \frac{dA' - i\mathbf{x}\,.\,\mathbf{U}\,dA}{\kappa}\,e^{-\kappa z}e^{i\mathbf{x}\,.\,\mathbf{x}}, \tag{2.10}$$

where $\kappa = |\mathbf{x}|$. The equation (2.8) can now be expressed in terms of the Fourier–Stieltjes transforms as

$$\frac{d\varpi}{\rho} = -\left[\frac{\partial}{\partial t} - i\mathbf{x}\,.\,\mathbf{U}\right]^2\frac{dA}{\kappa} - g\,dA - \frac{T}{\rho}\kappa^2\,dA, \tag{2.11}$$

or

$$dA'' - 2in_1\,dA' - (n_1^2 - n_2^2)\,dA = -\frac{\kappa}{\rho}d\varpi(t), \tag{2.12}$$

where

$$n_1 = \mathbf{x}\,.\,\mathbf{U} = \kappa U\cos\alpha, \qquad n_2 = (g\kappa + T\kappa^3/\rho)^{1/2}. \tag{2.13}$$

Equation (2.12) describes the growth of each component of the surface displacement in terms of the corresponding component of the pressure distribution. If we now specify U as the convection velocity of the component of the pressure field of wave-number $\mathbf{x}$, the quantity n_1 represents the frequency, in radians per second, of a wave with wave-number κ and speed $\mathbf{U}\,.\,\mathbf{x}/\kappa = U_c\cos\alpha$ in a direction at an angle α to that of the wind, and n_2 is the frequency of free surface waves of wavelength $2\pi/\kappa$.

The fundamental equation (2.12) specifies the development with time of the Fourier–Stieltjes transform $dA(\mathbf{x}, t)$ of the surface displacement in terms of the transform $d\varpi(\mathbf{x}, t)$ of the pressure fluctuations, which is, after the initial instant, a stationary random function of time. Its solution, subject to the initial conditions appropriate to an undisturbed surface at rest, namely $dA = dA' = 0$ at $t = 0$, can be expressed as

$$dA(\mathbf{x}, t) = \frac{e^{i(n_1+n_2)t}}{2in_2}\int_0^t \frac{\kappa}{\rho}d\varpi(\tau)\exp\{-i(n_1+n_2)\tau\}\,d\tau - \\ - \frac{e^{i(n_1-n_2)t}}{2in_2}\int_0^t \frac{\kappa}{\rho}d\varpi(\tau)\exp\{-i(n_1-n_2)\tau\}\,d\tau,$$

or

$$dA(\mathbf{x}, t) = \frac{i\kappa}{2\rho n_2}\int_0^t d\varpi(\tau)[\exp\{-i(n_1-n_2)(\tau-t)\} - \\ - \exp\{-i(n_1+n_2)(\tau-t)\}]\,d\tau. \tag{2.14}$$

This solution provides the common starting point for the investigations of the next two parts of this paper. It illustrates how the amplitude of each Fourier–Stieltjes component of the wave pattern is dependent upon the history of the applied pressure distribution from the initial instant $t = 0$. The development of each component of the wave field falls naturally into two stages: the intial stage over values of time $t \ll \Theta(\mathbf{x})$ (i.e. the development time of the fluctuations in pressure of wave-number $\mathbf{x}$, or the time scale of $d\varpi(\mathbf{x}, t)$ in the convected frame of reference), and the second or principal stage of development for which $t \gg \Theta$ and during which most of the growth of gravity waves takes place. The properties of the waves in each of these stages will be discussed in turn.

3. The initial stage of wave development

3.1. *The initial response of the water surface*

We define the initial stage of development as the period of time for which $t \ll \Theta(\mathbf{x})$, so that over this range of t, $d\varpi(\mathbf{x}, t)$ in the convected frame of reference varies little from its value at the initial instant. In the integration of the general solution (2.14), $d\varpi(\mathbf{x})$ can be considered independent of time, and the solution becomes

$$dA(\mathbf{x}, t) \doteq \frac{i\kappa\, d\varpi(\mathbf{x})}{2\rho n_2}\int_0^t \{\exp\{-i(n_1-n_2)(\tau-t)\} - \exp\{-i(n_1+n_2)(\tau-t)\}\}\, d\tau,$$

$$= \frac{\kappa\, d\varpi(\mathbf{x})}{\rho(n_1^2-n_2^2)}\left\{1 - \frac{n_1+n_2}{2n_2}\exp\{-i(n_1-n_2)t\} + \right.$$

$$\left. + \frac{n_1-n_2}{2n_2}\exp\{-i(n_1+n_2)t\}\right\}. \quad (3.1)$$

From this, there follows a relation between the wave spectral function $\Phi(\mathbf{x})$ and the two-dimensional, simultaneous pressure spectrum $\Pi(\mathbf{x}) \equiv \Pi(\mathbf{x}, 0)$; for

$$dA^*(\mathbf{x}, t) \doteq \frac{\kappa\, d\varpi^*(\mathbf{x})}{\rho(n_1^2-n_2^2)}\left\{1 - \frac{n_1+n_2}{2n_2}\exp\{i(n_1-n_2)t\} + \frac{n_1-n_2}{2n_2}\exp\{i(n_1+n_2)t\}\right\},$$

and since

$$\Phi(\mathbf{x}) = \frac{\overline{dA(\mathbf{x})\, dA^*(\mathbf{x})}}{d\kappa_1\, d\kappa_2}, \qquad \Pi(\mathbf{x}) = \frac{\overline{d\varpi(\mathbf{x})\, d\varpi^*(\mathbf{x})}}{d\kappa_1\, d\kappa_2},$$

we have

$$\Phi(\mathbf{x}, t) \doteq \frac{\kappa^2\Pi(\mathbf{x})}{\rho^2(n_1^2-n_2^2)^2}\left\{\frac{3}{2} + \frac{n_1^2}{2n_2^2} - \frac{n_1+n_2}{n_2}\cos(n_1-n_2)t + \frac{n_1-n_2}{n_2}\cos(n_1+n_2)t - \right.$$

$$\left. - \frac{n_1^2-n_2^2}{2n_2^2}\cos 2n_2 t\right\}. \quad (3.2)$$

If we write

$$\nu_1 = n_1 t = \kappa t U_c \cos\alpha, \qquad \nu_2 = n_2 t = (g\kappa + T\kappa^3/\rho)^{1/2} t, \quad (3.3)$$

a dimensionless response factor can be defined as

$$\Gamma = (\nu_1^2 - \nu_2^2)^{-2}\left\{\frac{3}{2} + \frac{\nu_1^2}{2\nu_2^2} - \frac{\nu_1+\nu_2}{\nu_2}\cos(\nu_1-\nu_2) + \frac{\nu_1-\nu_2}{\nu_2}\cos(\nu_1+\nu_2) - \right.$$
$$\left. - \frac{\nu_1^2-\nu_2^2}{2\nu_2^2}\cos 2\nu_2\right\}, \quad (3.4)$$

so that the wave spectrum can be expressed in the form

$$\Phi(\mathbf{\kappa}, t) \doteqdot \Gamma\kappa^2\Pi(\mathbf{\kappa})t^4/\rho^2. \quad (3.5)$$

The function $\Phi(\mathbf{\kappa}, t)$ is therefore determined, when $t \ll \Theta(\mathbf{\kappa})$, jointly by the spectrum of the imposed pressure fluctuations $\Pi(\mathbf{\kappa})$ and by the response factor Γ, itself a function of κ through ν_1 and ν_2, and of t; the balance between these two factors must always be taken into account in considering the wave generation in the initial stage. The function $\kappa^2\Pi(\mathbf{\kappa})$ has its maximum when κ is large, of the same order as the wave-numbers associated with the dissipating eddies in the atmospheric turbulence. A brief examination of (3.4) suffices to show that in the (ν_1, ν_2)-plane, Γ is large near the line $\nu_1 = \nu_2$ and in regions where ν_1/ν_2 is large.

Wave-numbers of the first class, for which $\nu_1 \doteqdot \nu_2$, are such that the convection velocity of the pressure distribution is equal to the velocity of free waves with these wave-numbers in the direction of convection; for, from (3.3),

$$U_c \cos\alpha = (g/\kappa + T\kappa/\rho)^{1/2} = c(\kappa). \quad (3.6)$$

Because of the factor $\kappa^2\Pi(\mathbf{\kappa})$, the amplitude of these waves is significant only when κ is large (i.e. the wavelength λ is small), which in turn implies, from (3.6), that $U_c \cos\alpha$ should also be small. Waves, or perhaps more properly ripples, of this type are generated immediately after the onset of a gust of sufficient strength. Their direction and speed is such that they remain in phase with the applied pressure distribution during this initial period, developing by the simple resonance mechanism described in § 2.1. These waves can conveniently be called 'resonance waves'. Wave-numbers of the second class, for which $\nu_1 \gg \nu_2$, are associated with the *forced* oscillations of the water surface produced by the pressure fluctuations, and it will be shown later that their amplitude does not increase with time t beyond a small upper bound.

3.2. *Resonance waves*

A simple approximation to the response factor (3.4) when $\nu_1 \doteqdot \nu_2$ can be found in the following manner. Let

$$\chi = \nu_1 - \nu_2; \quad (3.7)$$

and, on substituting this into (3.4), we have

$$\Gamma = (2\nu_2+\chi)^{-2}\chi^{-2}\left\{\frac{3}{2} + \frac{\nu_2^2+2\nu_2\chi+\chi^2}{2\nu_2^2} - \frac{2\nu_2+\chi}{\nu_2}\cos\chi + \frac{\chi}{\nu_2}\cos(2\nu_2+\chi) - \right.$$
$$\left. - \frac{\chi(2\nu_2+\chi)}{2\nu_2^2}\cos 2\nu_2\right\}.$$

$$= \frac{1}{2\nu_2^2}\left\{\frac{1-\cos\chi}{\chi^2} + O\left(\frac{\chi}{\nu_2}\right)\right\}.$$

If $\nu_2 \gg 1$, that is, if $t \gg n_2^{-1}$ or $(2\pi)^{-1}$ times the period of free waves of wave-number κ, the second term is negligible and the wave spectrum is given approximately by

$$\Phi(\mathbf{x}, t) \doteq \frac{\kappa^2 \Pi(\mathbf{x}) t^2}{2\rho^2 n_2^2} \frac{1-\cos\chi}{\chi^2} \tag{3.8}$$

when $n_2^{-1} \ll t \ll \Theta$ and $n_1 \doteq n_2$.

The existence of a range of values of t satisfying this condition clearly requires that n_2^{-1} is less by one or two orders of magnitude than Θ. Since $n_1 \doteq n_2$ for resonance waves, an equivalent statement is that the wavelength λ of the surface disturbance is very much less than the distance travelled by the convected pressure distribution in the time Θ. This condition is likely to be satisfied best when λ is small, in the range corresponding to ripples and short gravity waves. (If, for example, $\Theta(\mathbf{x})$ is of the same order as the time scale of the eddies of wave-number κ in the equilibrium range, then the condition can be expressed as

$$\lambda = 2\pi/\kappa \ll U_c \Theta \sim U_c \epsilon^{-1/3} \kappa^{-2/3}$$

(where ϵ is the rate of energy dissipation) or $\kappa \gg 8\pi^3 \epsilon / U_c^3$.)

The wave-number κ in any direction α for which $\Phi(\mathbf{x})$ is a maximum is determined by the equation $\chi = 0$, or, from (3.3),

$$T\kappa^2/\rho - \kappa U_c^2 \cos^2\alpha + g = 0, \tag{3.9}$$

which, for each value of $U_c \cos\alpha$ above a certain minimum, gives two resonant wave-numbers, one corresponding to a gravity wave and one to a capillary wave. This is illustrated in figure 1. The solid curve $c(\kappa)$ gives the speed of free surface waves as a function of wave-number κ and the broken line $U_c(\kappa)$ a typical convection speed of the components of the pressure field of wave-number κ, which, as we have seen earlier, is a function which may decrease slowly as κ increases. The exact shape of $U_c(\kappa)$ depends upon the surface roughness, and the curve in figure 1 is for illustrative purposes only. In the direction $\alpha = 0$, that of the convection velocity, resonance waves occur near the wave-numbers such that $U_c(\kappa) = c(\kappa)$, given in figure 1 by the points A and B. As α increases, since the condition for resonance waves is that $U_c(\kappa)\cos\alpha = c(\kappa)$, the resonance wave-numbers are found by translating the dashed curve downwards, and the intersections of the two curves approach each other until at a certain critical angle α_{cr} they coincide. For values of α greater than α_{cr}, no resonance waves are possible. If, as one might expect under normal atmospheric conditions and with an 'aerodynamically-smooth surface' appropriate to the initial period of development, the dependence of U_c upon κ is not very rapid except when κ is large (of order unity), the coincidence point will occur near or a little to the right of G in this diagram, which marks the minimum velocity of free waves under the influence of both gravity and surface tension. It can readily be established from (3.6) that this minimum velocity is given by

$$c_{\min} = (4gT/\rho)^{1/4}, \tag{3.10}$$

so that the wavelength of the critical waves is approximately

$$\lambda_{cr} \doteqdot 2\pi(T/\rho g)^{1/2}. \tag{3.11}$$

The critical angle α_{cr}, i.e. the maximum angle from the direction of the wind at which resonance waves are generated, is given by

$$\alpha_{cr} \doteqdot \cos^{-1}(c_{min}/U_c) = \cos^{-1}(4gT/\rho U_c^4)^{1/4}, \tag{3.12}$$

where U_c is the convection velocity of the wave-numbers κ, i.e. the mean wind velocity at a height of approximately κ^{-1}. Taking the values for water: $\rho = 1\,\mathrm{gm\,cm^{-3}}$, $T = 73\,\mathrm{gm\,sec^2}$, and taking $g = 980\,\mathrm{cm\,sec^{-2}}$, we have $c_{min} = 23\,\mathrm{cm\,sec^{-1}}$ and the critical wavelength $\lambda_{cr} = 2\pi/\kappa_{cr} = 1{\cdot}7$ cm.

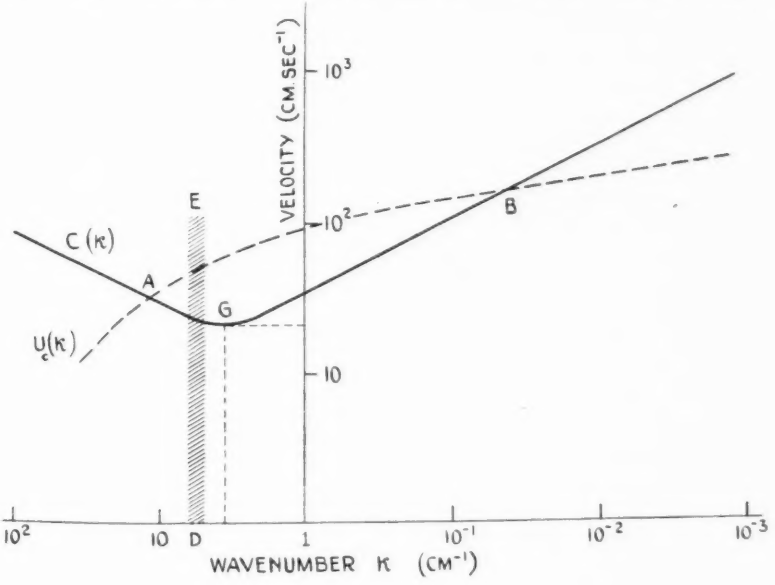

Figure 1.

Of these possible resonance waves, not all may be excited, since for some wave-numbers $\kappa^2\Pi(\mathbf{\kappa})$ may be negligible. It is well known that in turbulent flow there is a certain maximum wave-number κ_{max} of the velocity fluctuations, or minimum eddy size, which depends upon the rate of kinetic energy dissipation per unit volume in the flow near the surface and upon the kinematic viscosity ν of the fluid. If the mean velocity gradient is not too large, $\kappa_{max} \sim (\epsilon/\nu^3)^{1/4}$. The surface pressure fluctuations will also have a minimum scale, or maximum wave-number, of the same order of magnitude, so that for values of κ greater than κ_{max}, $\Pi(\mathbf{\kappa})$ is negligible. Not a great deal of relevant experimental information is available concerning the magnitude of ϵ under the conditions with which we are concerned, but for a mean wind speed of order $1\,\mathrm{m\,sec^{-1}}$ at a height of

1 metre, a rough estimate guided by experiments such as those of Taylor (1952) suggests that the maximum value of κ is of the order of 10 cm^{-1} or less. Thus, in figure 1, only those wave-numbers below a band such as DE are excited. In the direction $\alpha = 0$, running before the wind, the only resonance waves that occur are the gravity waves corresponding to the point B; the wavelength of the capillary waves given by the point A is too small for excitation to occur. Even if the turbulence were more vigorous, with a smaller minimum eddy size, the growth of the very short capillary waves is hindered by direct viscous dissipation which becomes important for very short wavelengths. Under the conditions illustrated in this figure, no true capillary waves at all would be generated, the smallest wavelengths being little less than λ_{cr}.

It will now be shown that the angle α_{cr} is associated with limiting behaviour in yet another respect. Not only does it represent the maximum angle from the wind direction at which resonance waves can be generated, but also it is found that the amplitude of waves moving in this direction is greater than those in other directions with $\alpha < \alpha_{cr}$. The curve $\chi = 0$ gives the locus of the points in the wave-number plane for which the maximum amplification of resonance waves can occur, and for a given value of U_c is of the form shown in figure 2, where the 1-direction is taken as that of the wind. For angles $\alpha > \alpha_{cr}$ there are no resonance waves, and for angles $\alpha < \alpha_{cr}$ there are two *possible* values of κ for which resonance may occur, although one may not be excited if the minimum scale of the turbulence is too large. The maximum wave-numbers that occur in the surface pressure distribution can be represented by the arc AB, and only the wave-numbers near the curve $\chi(\mathbf{\kappa}) = 0$ and within the sector OAB (and its mirror image in OA) will be excited as resonance waves. The width of the resonance band is, as (3.8) shows, determined by the range of values of χ for which $(1 - \cos\chi)/\chi^2$ is significant. The limits of this range can conveniently be taken as $\chi(\mathbf{\kappa}) = \pm 2\pi$, where, from (3.7),

$$\chi(\mathbf{\kappa}) = t\{\kappa U_c \cos\alpha - (g\kappa + T\kappa^3/\rho)^{1/2}\}, \tag{3.13}$$

and these limits, when $n_2 t \gg 1$, are illustrated by the dotted lines in figure 2. It can be shown from (3.13) that the thickness $\Delta\kappa$ of the resonance band at the wave-number κ is such that $|\Delta\mathbf{\kappa}| \ll \kappa$ when $t \gg n_2^{-1}$ and decreases as t^{-1}. As time goes on, the range of excited wave-numbers near the curve $\chi(\mathbf{\kappa}) = 0$ becomes narrower and narrower while the magnitude of the wave spectral function $\Phi(\mathbf{\kappa})$ along this curve rapidly increases.

Now the mean-square surface displacement is given by

$$\overline{\xi^2} = \int \Phi(\mathbf{\kappa})\, d\mathbf{\kappa}, \tag{3.14}$$

the integration being over the whole $\mathbf{\kappa}$-plane. But the integrand is significant only in the part of the strip near the curve $\chi(\mathbf{\kappa}) = 0$ lying within the quadrant OAB. A simple and useful approximation to the integral can be obtained by taking locally orthogonal coordinates s, being the distance along the curve $\chi(\mathbf{\kappa}) = 0$ from the point D, and χ specifying the

distance normal to the curve. Since the effective width of the resonance band is small, the Jacobian in the expression

$$\xi^2 = \iint \Phi(\mathbf{\kappa})\kappa \, d\kappa d\alpha = \iint \Phi(\mathbf{\kappa})\kappa \frac{\partial(\kappa, \alpha)}{\partial(\chi, s)} \, d\chi ds \tag{3.15}$$

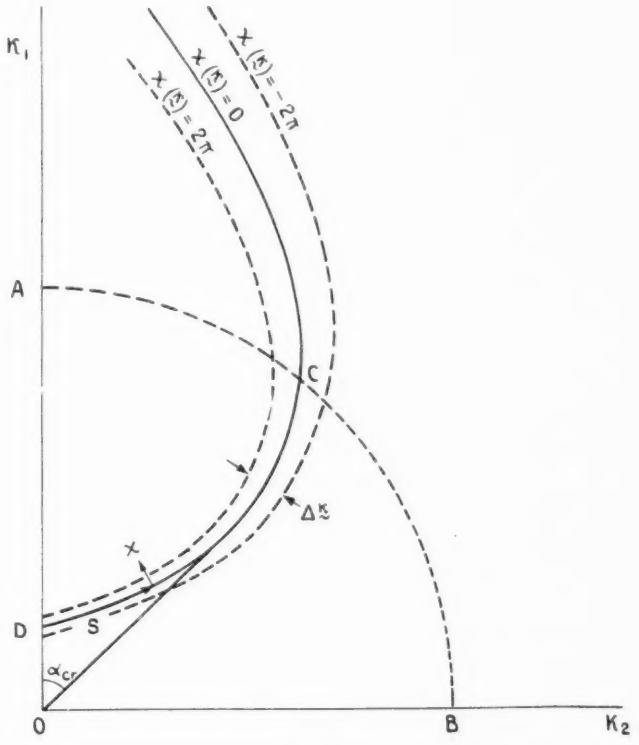

Figure 2.

can be evaluated along $\chi = 0$. The limits of integration of χ can be taken as $\pm \infty$. From (3.13), it can be shown that, when $\chi = 0$,

$$\left.\begin{aligned} \frac{\partial \kappa}{\partial \chi} &= \frac{2\kappa U_c \cos\alpha}{t(g - T\kappa^2/\rho)}, & \frac{\partial \alpha}{\partial \chi} &= -\frac{1}{t\kappa U_c \sin\alpha}, \\ \frac{\partial \kappa}{\partial s} &= \frac{\kappa U_c^2 \sin 2\alpha}{\mathscr{D}}, & \frac{\partial \kappa}{\partial s} &= \frac{g - T\kappa^2/\rho}{\kappa \mathscr{D}}, \end{aligned}\right\} \tag{3.16}$$

where $\mathscr{D}^2 = (\kappa U_c^2 \sin 2\alpha)^2 + (g - T\kappa^2/\rho)^2$, so that

$$\left[\frac{\partial(\kappa, \alpha)}{\partial(\chi, s)}\right]_{\chi = 0} = \frac{4U_c \cos\alpha}{t\mathscr{D}}.$$

The contribution to the mean-square surface displacement per unit length of the resonance band is simply

$$\int_{-\pi}^{\pi} \Phi(\mathbf{x})\kappa\left[\frac{\partial(\kappa,\alpha)}{\partial(\chi,s)}\right]_{\chi=0} d\chi \doteq \frac{2\kappa\Pi(\mathbf{x})t}{\rho^2 U_c \mathscr{S}\cos\alpha}\int_{-\infty}^{\infty}\frac{1-\cos\chi}{\chi^2}\,d\chi,$$
$$= \frac{2\pi\,.\,\kappa\Pi(\mathbf{x})\,.\,t}{\rho^2 U_c \mathscr{S}\cos\alpha},$$

and the contribution per unit angle in the wave-number plane, or the directional distribution of wave amplitude in the physical plane, is found by multiplying this expression by $\partial s/\partial\alpha$. With the aid of (3.16), this gives

$$\Psi(\alpha) = \frac{2\pi\,.\,\kappa^2\Pi(\mathbf{x})\,.\,t}{\rho^2 U_c\cos\alpha(g - T\kappa^2/\rho)}, \tag{3.17}$$

where κ and α are related by $\kappa U_c\cos\alpha = (g\kappa + T\kappa^3/\rho)^{1/2}$.

From this result, (3.17), most of the important properties of resonance waves in the initial stage can be found immediately. In directions $\alpha \ll \alpha_{cr}$ the resonant wave-number $\kappa \ll \kappa_{cr} = (\rho g/T)^{1/2}$, so that (3.17) becomes approximately

$$\Psi(\alpha) = \frac{2\pi\kappa^2\Pi(\mathbf{x})t}{\rho^2 g U_c\cos\alpha}. \tag{3.18}$$

However, as $\kappa \to \kappa_{cr}$, $T\kappa^2/\rho \to g$, and from (3.17), the directional distribution function $\Psi(\alpha)$ becomes infinite at α_{cr}. When $(\kappa_{cr} - \kappa)$ is small, (3.17) gives

$$\Psi(\alpha) \doteq \frac{\pi\kappa^2\Pi(\mathbf{x})t}{\rho^2 U_c\cos\alpha}\left(\frac{\rho}{gT}\right)^{1/2}(\kappa_{cr}-\kappa)^{-1}.$$

But from (3.13), on the curve $\chi = 0$ near α_{cr},

$$\alpha_{cr} - \alpha = \frac{1}{\sin 2\alpha_{cr}}\left(\frac{T^3}{\rho^3 U_c^4 g}\right)^{1/2}(\kappa_{cr}-\kappa)^2 + O(\kappa_{cr}-\kappa)^3,$$

so that near the critical direction α_{cr}, the directional distribution function of the wave motion is given approximately by

$$\Psi(\alpha) \doteq \frac{\pi\kappa^2\Pi(\mathbf{x})t}{\rho^2 U_c^2\cos\alpha}\left(\frac{T}{g^3\rho\sin^2 2\alpha_{cr}}\right)^{1/4}(\alpha_{cr}-\alpha)^{-1/2}. \tag{3.19}$$

The form of $\Psi(\alpha)$ is shown in figure 3. As α increases from zero towards α_{cr}, $\Psi(\alpha)$ increases towards its (integrable) infinity; and when $\alpha > \alpha_{cr}$, $\Psi(\alpha)$ is zero to this approximation.

The mean-square surface displacement is obtained by integrating $\Psi(\alpha)$ over all possible propagation angles α and wave-numbers κ subject to the condition $\chi = 0$. Near $\alpha = \alpha_{cr}$ the directional density of the wave distribution is large and should produce wave patterns more pronounced in this direction than in others. The reason for this accumulation of waves in the direction α_{cr} is, of course, that the range of wave-numbers that propagate at speeds within, say, δc of the minimum speed of surface waves is proportional to $(\delta c)^{1/2}$ only; within an angle $\delta\alpha$ of α_{cr} the range of wave-numbers propagated is proportional to $(\delta\alpha)^{1/2}$, so that the directional density of the wave pattern is proportional to $(\delta\alpha)^{-1/2}$.

The angle between the direction of propagation of these waves and that of the wind, i.e. $\alpha_{cr} = \cos^{-1}(c_{min}/U_c)$, will be small only for light airs. It is doubtful whether a wind of, say, 30 or 40 cm sec^{-1} would contain turbulent components whose scale is as small as the 1·7 cm necessary to excite such waves, and unlikely that they would be observed at small angles α_{cr} under natural conditions. As the wind velocity becomes larger and contains smaller-scale turbulent components, α_{cr} also increases, and these critical angle waves may travel almost at right angles to the wind! Under the conditions visualized in this paper, with a large fetch and sudden onset of the wind, this wave pattern would be a transient one, and would disappear as the waves developed beyond the initial period.

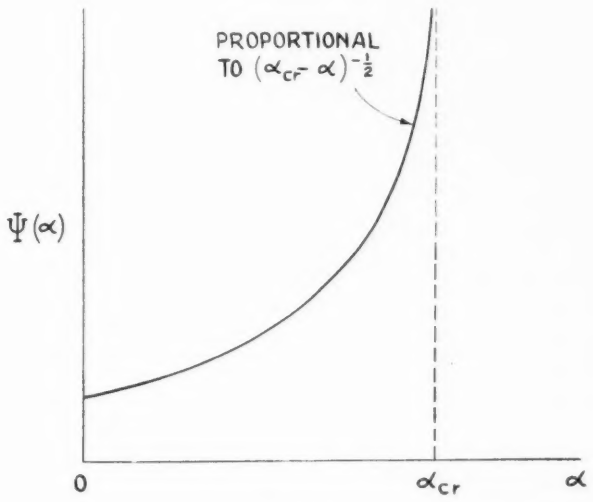

Figure 3.

However, it is likely that the waves are similar to those generated in steady winds at a small fetch, since the time of development of each wave is small, and the growth would be analogous to that discussed here. Assuming a correspondence between the two cases of short wind duration and short fetch, an explanation of some of Roll's (1951) observations can be given. These experiments were made under natural conditions on pools left in tidal mud flats at Neuwerk. On one occasion, when the wind velocity at a height of 35 cm was 195 cm sec^{-1}, Roll observed a rhombic wave pattern of wavelength about 1·7 cm. Unfortunately he does not record the shape of the rhombic pattern, but this observation seems consistent with the establishment of the two trains of resonance waves at angles α_c to the wind direction, as predicted by the theory. On two other occasions, when the wind velocity was approximately 400 cm sec^{-1}, waves

with $\lambda = 1{\cdot}7$ cm were observed with their crests nearly parallel to the direction of the wind, which again is consistent with the theoretical predictions. However, many more careful experiments will have to be made before quantitative comparison with this part of the theory will be possible.

3.3. *The question of* $U_{\min}$

It is perhaps appropriate at this point to offer some remarks concerning the idea that there exists a minimum wind speed capable of raising waves. It is natural that this concept should arise if the problem is considered as one of stability and many attempts to determine $U_{\min}$ experimentally have been made in the past. Ursell (1956), however, discounts the idea, pointing out that any turbulent air motion will necessarily generate some surface displacements, however minute, and that there seems to be no reason why this should not be described as a wave motion. He quotes a table of 'measured values of $U_{\min}$' ranging from 40 cm sec^{-1} (Roll 1951) to above 1200 cm sec^{-1} (Keulegan 1951).

According to the present theory, the minimum wind velocity capable of raising *resonance* waves is 23 cm sec^{-1}, but waves will actually be generated only if there exist near the surface turbulent fluctuations of sufficiently small scale. But, as Ursell points out, turbulent motion in the air will generate surface displacements irrespective of the mean wind velocity. For example, if $U_c = 0$, then in (3.4) $\nu_1 = 0$ and

$$\Gamma = \left(\frac{1-\cos\nu_2}{\nu_2^2}\right)^2, \tag{3.20}$$

so that, when $t < \Theta$,

$$\Phi(\mathbf{x}, t) = \frac{\kappa^2 \Pi(\mathbf{x})}{\rho^2 n_2^4}(1-\cos n_2 t)^2$$

and

$$\overline{\xi^2} = \frac{1}{\rho^2}\int \frac{\kappa^2\Pi(\mathbf{x})}{n_2^4}(1-\cos n_2 t)^2\, d\mathbf{x}$$

$$\leqslant \frac{4}{\rho^2}\int \frac{\kappa^2\Pi(\mathbf{x})}{n_2^4}\, d\mathbf{x} = \text{const.} \tag{3.21}$$

The mean-square displacement of these forced waves is therefore bounded and unlike the resonance waves they do not continue to develop in time. To the eye they may appear as a shimmer or ruffle on an otherwise glassy surface. When $\nu_1 \gg \nu_2$, a similar system of forced oscillations can also be found.

4. The principal stage of development

4.1. *The wave spectral function*

The principal stage of development for a wave-number $\mathbf{x}$ is defined as the period during which the time elapsed from the initial instant is greater than $\Theta(\mathbf{x})$, the development time of $d\varpi(\mathbf{x}, t)$, but not so great that the

amplitude of the wave at this wave-number has increased to such an extent that the infinitesimal wave theory ceases to apply.

We return to the fundamental solution (2.14), namely

$$dA(\mathbf{\kappa}, t) = \frac{i\kappa}{2\rho n_2} \int_0^t d\varpi(\mathbf{\kappa}, \tau)[\exp\{-i(n_1 - n_2)(\tau - t)\} - \\ - \exp\{-i(n_1 + n_2)(\tau - t)\}]\, d\tau. \quad (4.1)$$

The wave spectral function $\Phi(\mathbf{\kappa}, t)$ is given by

$$\Phi(\mathbf{\kappa}, t) = \frac{\overline{dA(\mathbf{\kappa}, t)\, dA^*(\mathbf{\kappa}, t)}}{d\kappa_1\, d\kappa_2}$$

$$= \frac{\kappa^2}{4\rho^2 n_2^2} \int_0^t \int_0^t \Pi(\mathbf{\kappa}, \tau - \tau')\{\exp\{-i(n_1 + n_2)(\tau - \tau')\} + \\ + \exp\{-i(n_1 - n_2)(\tau - \tau')\} - 2\exp\{-in_1(\tau - \tau')\}\exp\{-in_2(\tau + \tau')\} \times \\ \times \cos 2n_2 t\}\, d\tau d\tau'. \quad (4.2)$$

If the variables of integration are changed from τ, τ' to τ_1, τ_2, where $\tau_1 = \tau - \tau'$, $\tau_2 = \tau + \tau'$, it is found that the asymptotic form, as $t \to \infty$, of the expression (4.2) is

$$\Phi(\mathbf{\kappa}, t) \sim \frac{\kappa^2 t}{4\sqrt{2}\rho^2 n_2^2} \int_{-\infty} \Pi(\mathbf{\kappa}, \tau)\{\exp\{-i(n_1 + n_2)\tau\} + \exp\{-i(n_1 - n_2)\tau\}\}\, d\tau, \quad (4.3)$$

where the suffix has now been dropped from τ_1. This asymptotic form can be written in a simpler manner if we interpret the integral in terms of time scales in frames of reference themselves moving with respect to the convected frame in which the analysis has been made. If a spatial Fourier transform $F(\mathbf{\kappa}, \tau)$ of some covariance $f(\mathbf{r}, \tau)$, a function of space separation $\mathbf{r}$ and time interval τ, is defined as

$$f(\mathbf{r}, \tau) = \int F(\mathbf{\kappa}, \tau) e^{i\mathbf{\kappa} \cdot \mathbf{r}}\, d\mathbf{\kappa},$$

then, in a reference frame moving with a relative velocity $\mathbf{V}$, such that $\mathbf{r} = \mathbf{q} + \mathbf{V}\tau$, we have

$$f(\mathbf{q}, \tau) = \int F(\mathbf{\kappa}, \tau) e^{i(\mathbf{\kappa} \cdot \mathbf{q} + \mathbf{\kappa} \cdot \mathbf{V}\tau)}\, d\mathbf{\kappa},$$

so that

$$e^{i\mathbf{\kappa} \cdot \mathbf{V}\tau} F(\mathbf{\kappa}, \tau) = (2\pi)^{-2} \int f(\mathbf{q}, \tau) e^{-i\mathbf{\kappa} \cdot \mathbf{q}}\, d\mathbf{q},$$

the $\mathbf{q}$-coordinates being in the moving frame of reference. Thus the spectral function in the moving frame is

$$e^{i\mathbf{\kappa} \cdot \mathbf{V}\tau} F(\mathbf{\kappa}, \tau),$$

where $F(\mathbf{\kappa}, \tau)$ is the spectral function in the original frame. The integral time scale, for the wave-number $\mathbf{\kappa}$, in the moving frame, is therefore given by $\theta(\mathbf{\kappa}, \mathbf{V})$, where

$$\int_{-\infty}^{\infty} e^{i\mathbf{\kappa} \cdot \mathbf{V}\tau} F(\mathbf{\kappa}, \tau)\, d\tau = 2F(\mathbf{\kappa}, 0)\theta(\mathbf{\kappa}, \mathbf{V}). \quad (4.4)$$

Equation (4.3) can therefore be expressed as

$$\Phi(\mathbf{x}, t) \sim \frac{\kappa^2 \Pi(\mathbf{x}, 0) t}{2\sqrt{2}\rho^2 n_z^2} \{\theta(\mathbf{x}, V_1) + \theta(\mathbf{x}, V_2)\}, \tag{4.5}$$

where, from (4.4), V_1 and V_2 are given by

$$\left.\begin{aligned} -\mathbf{x}.\mathbf{V}_1 &= n_1 + n_2 = \mathbf{x}.\mathbf{U}_c + (g\kappa + T\kappa^3/\rho)^{1/2}, \\ -\mathbf{x}.\mathbf{V}_2 &= n_1 - n_2 = \mathbf{x}.\mathbf{U}_c - (g\kappa + T\kappa^3/\rho)^{1/2}, \end{aligned}\right\} \tag{4.6}$$

so that

$$\mathbf{x}.(\mathbf{U}_c + \mathbf{V}_1) = -\kappa c(\kappa), \qquad \mathbf{x}.(\mathbf{U}_c + \mathbf{V}_2) = \kappa c(\kappa), \tag{4.7}$$

$c(\kappa)$ being, as before, the speed of free surface waves of wave-number κ. Notice that the velocities $\mathbf{V}$ (relative to the convected frame) of the frames of reference in which the time scales are to be measured are each specified by only one scalar equation, so that either the speed V of this frame, or its direction of motion can be chosen arbitrarily. For convenience the direction of $\mathbf{V}$ can be chosen to coincide with that of $\mathbf{U}$, and so

$$(U_c + V_1)\cos\alpha = -c(\kappa), \qquad (U_c + V_2)\cos\alpha = c(\kappa).$$

Hence $$V_1 = -U_c - c(\kappa)/\cos\alpha, \qquad V_2 = -U_c + c(\kappa)/\cos\alpha. \tag{4.8}$$

The absolute speeds of the frames of reference in which the scales θ are to be measured are $c(\kappa)/\cos\alpha$ and $-c(\kappa)/\cos\alpha$, the negative sign implying motion in the direction against the wind. It is evident that the time scale of the pressure fluctuations observed in a reference frame moving against the wind is less than that moving with the wind at the same speed, so that $\theta(\mathbf{x}, V_1) \ll \theta(\mathbf{x}, V_2)$, and the expression (4.5) can be approximated by

$$\Phi(\mathbf{x}, t) \sim \frac{\kappa^2 \Pi(\mathbf{x}) t}{2\sqrt{2}\rho^2 n_z^2}\, \theta(\mathbf{x}, V). \tag{4.9}$$

The speed $V = c(\kappa)\cos\alpha$ is just equal to that of the waves of wave-number κ propagating in the direction α, observed along a line parallel to the wind, so that the integral time scale represents the time scale of the variations in phase difference between the pressure fluctuations and the wave pattern.

The expression (4.9) is the basic result of this part of the paper, and from it several important deductions can be made immediately. Since the only way in which the elapsed time t enters the right-hand side is in the explicit linear factor, the mean-square wave height is directly proportional to time in the principal stage of development. Furthermore, the shape of the wave spectrum is independent of time, at any rate until the development is such that the mean-square slope (governing the importance of non-linearities in the equation of motion) associated with any group of wave-numbers becomes too large. It will be seen later that this occurs first at the shorter wavelengths excited, and the contribution from these to the total mean-square surface displacement is small. Thus the direct proportionality of $\overline{\xi^2}$ to t should continue until the mean-square slope of the largest waves attains a limiting value, after which time an equilibrium structure is presumably attained.

However, a direct application of (4.9) is hindered by the presence of the factor $\theta(\mathbf{x}, V)$ about which little is known. When $V = U_c$, so that the wave pattern moves with the convection velocity of the pressure fluctuations, we have the true resonance waves which figured in § 3.2, and the time scale $\theta(\mathbf{x}, V)$ is equal to the convected or natural time scale Θ. The use of the capital letter in this latter case emphasizes the particular significance of this time scale. However, when $V \neq U_c$, and usually $V < U_c$, the time scale in the reference frame moving with speed V is less than Θ, since it is governed by the rate at which the convected fluctuations are swept past the point of observation. A rough approximation to $\theta(\mathbf{x}, V)$, but one which is probably satisfactory, is to take it as the length scale κ^{-1} divided by the relative speed of the convected pressure fluctuations and the waves; thus

$$\theta(\mathbf{x}, V) \doteq \frac{1}{\kappa(U_c - c(\kappa)/\cos\alpha)}, \tag{4.10}$$

when U_c is greater by about a factor of about two than $c(\kappa)/\cos\alpha$. More properly, the time scale represented by the expression on the right is a differential scale, whereas $\theta(\mathbf{x}, V)$ is defined as an integral scale. However, the two scales should be proportional, and probably of the same order of magnitude, so that the approximation (4.10) can be used in the absence of better information, provided the results are interpreted as being valid only to orders of magnitude.

For gravity waves, $n_2^2 = g\kappa$, so that, from (4.9) and (4.10), we have

$$\Phi(\mathbf{x}, t) \sim \frac{\Pi(\mathbf{x})t}{2\sqrt{2}\rho^2 g(U_c - c(\kappa)/\cos\alpha)}. \tag{4.11}$$

When U is greater than $c(\kappa)/\cos\alpha$ by a factor of about three or four, this expression can be further simplified to

$$\Phi(\mathbf{x}, t) \sim \frac{\Pi(\mathbf{x})t}{2\sqrt{2}\rho^2 U_c g}, \tag{4.12}$$

so that we have immediately

$$\boxed{\overline{\xi^2} \sim \frac{\overline{p^2}t}{2\sqrt{2}\rho^2 U_c g}}, \tag{4.13}$$

and, for the mean-square slope,

$$\overline{(\nabla\xi)^2} \sim \frac{\overline{(\nabla p)^2}t}{2\sqrt{2}\rho^2 U_c g}. \tag{4.14}$$

Further reference will be made presently to these particularly simple and important results. At this stage we must consider the conditions under which the assumption that $U_c \gg c(\kappa)/\cos\alpha$ is likely to be valid for most of the range of wave-numbers over which the spectral function $\Phi(\mathbf{x})$ is significant. Support is given to the approximation (4.10) by the observation that for moderate winds over all but the longest durations, the wave spectrum is appreciable only over wave-numbers for which the condition $U_c \gg c(\kappa)$ is satisfied. It is instructive, however, to see why this

is so by examining the relevant meteorological and other evidence on the surface pressure fluctuations. The dependence of this function on $\boldsymbol{\kappa}$ is determined, as (4.9) shows, jointly by $\theta(\boldsymbol{\kappa}, V)$ and the pressure term, which for gravity waves where $n_2^2 = g\kappa$ is of the form $\kappa\Pi(\boldsymbol{\kappa})$. It is unfortunate that the properties of the spectral function $\Pi(\boldsymbol{\kappa})$ of the imposed surface pressure distribution are at present almost unknown, though by using the results of some recent atmospheric measurements of the turbulent velocities (made over land, alas, not over the sea), some of its qualitative properties can be surmised. But one important property that can be established without recourse to these experiments is that when $\boldsymbol{\kappa} = 0$, $\Pi(\boldsymbol{\kappa}) = 0$; this is proved

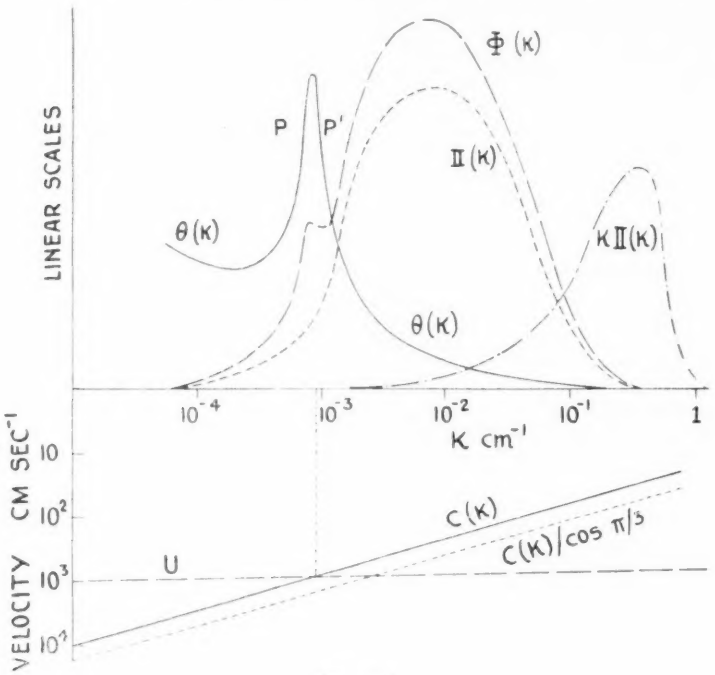

Figure 4.

in the Appendix to this paper. Thus in any direction α in the κ-plane, $\Pi(\boldsymbol{\kappa})$ rises from zero at the origin to a maximum and then decreases again to zero as κ approaches its value for the dissipating eddies. We are now faced with the question of deciding the order of magnitude of the values of κ for which $\Pi(\boldsymbol{\kappa})$ is a maximum. The only guide we have at present are experiments such as those of MacCready (1953 a, b), Taylor (1955) and Ellison (1956) on velocity autocorrelations over land in winds within the range 1 to 5 m sec^{-1}. These point to a longitudinal scale of the energy-containing eddies in the lowest few metres of the order 10 m (the lateral

scales are considerably smaller), that is to say, the peak value of the velocity spectrum under these conditions occurs at wave-numbers of order $2\pi/10^3 = 6 \times 10^{-3}\,\mathrm{cm}^{-1}$. Apparently this scale does not depend greatly upon wind velocity or distance from the ground. In isotropic turbulence, Batchelor (1951) has shown that the scale of the pressure fluctuations is rather less, about half, of that of the velocity fluctuations; and if a similar situation exists in the atmosphere, the maximum value of $\Pi(\mathbf{x})$ may occur for values of κ of about $10^{-2}\,\mathrm{cm}^{-1}$. Furthermore, atmospheric turbulence generally contains a large range of eddy sizes, so that the spectra tend to be fairly broad. These considerations make it likely that $\Pi(\mathbf{x})$, in a given direction α in the κ-plane, is a function of κ of the shape illustrated in the top portion of figure 4, with a broad maximum near $\kappa = 10^{-2}\,\mathrm{cm}^{-1}$, decreasing to zero for both large and small values of κ. The function $\kappa\Pi(\mathbf{x})$, being weighted towards the larger values of κ, has its maximum at a larger κ, and would be expected to be of the form also illustrated in figure 4.

The time scale $\theta(\mathbf{x})$ has its maximum when κ has such a value that the waves of this wave-number move with the convection velocity U_c; then $\theta(\mathbf{x}) = \Theta$, the development time of the pressure fluctuations. For a wind speed of, say, $10^3\,\mathrm{cm\,sec}^{-1}$, a fresh sailing breeze, the maximum for angles α in the range $-\frac{1}{3}\pi$ to $\frac{1}{3}\pi$ (containing most of the wave energy) occurs when $\kappa \sim 10^{-3}\,\mathrm{cm}^{-1}$. For larger and smaller values of κ away from this maximum, $\theta(\mathbf{x})$ is given by (4.10), so that the function has the form of the solid curve in the upper part of figure 4.

The wave spectrum is given by the product of the functions $\theta(\kappa)$ and $\kappa\Pi(\mathbf{x})$ represented by the curves in this diagram, and it is clear that for a wind speed of $10\,\mathrm{m\,sec}^{-1}$ the range of wave-numbers PP', over which the approximation (4.10) is insufficient, contributes little to the integral $\int \Phi(\mathbf{x})\,d\mathbf{x}$. The result (4.12), therefore, would be expected to give a good approximation to the wave spectrum except for the smallest values of κ, whose contribution to the mean-square wave height is small. For wind speeds greater than the value $10^3\,\mathrm{cm\,sec}^{-1}$ chosen for purposes of illustration in figure 4, the wave-number for which $U_c = c(\kappa)$ decreases as U^{-2}, so that the curve $\theta(\mathbf{x})$ is translated to the left. It is unlikely that the reciprocal of the scale of the pressure-generating eddies should decrease with wind speed as rapidly as this, so that the range of wave-numbers PP' contributes even less to the integrated wave spectrum, and the approximations inherent in (4.12) and (4.13) become more accurate. However, when the wind speed and associated convection velocity is small, say $1\,\mathrm{m\,sec}^{-1}$, it is probable that the range PP' will occur at a point where the value of $\kappa\Pi(\mathbf{x})$ is no longer negligible. These circumstances are illustrated in figure 5, and the wave spectrum calculated from the curves $\theta(\mathbf{x})$ and $\kappa\Pi(\mathbf{x})$ is clearly no longer similar in shape to $\Pi(\mathbf{x})$ but possesses a more pronounced peak. In light winds, therefore, the wave spectrum is narrower, and presumably the wave pattern more regular, a deduction which would appear to be substantiated by visual observations. A similar situation exists for higher wind velocities when α is very nearly $\pm\frac{1}{2}\pi$, and the curve $\theta(\mathbf{x})$ is displaced considerably to the right, but the

range of angles over which the approximation (4.10) fails is small and again contributes little to the integrated wave spectrum, or to $\overline{\xi^2}$.

4.2. *Termination of the principal stage of development*

There is another effect which limits the validity of (4.12) and (4.13) and which we have not yet considered. As the wave pattern develops, the mean-square slope of the waves increases linearly with time. After a certain interval, the mean-square slope associated with some band of wave-numbers becomes so large that the waves can no longer be described by a linear

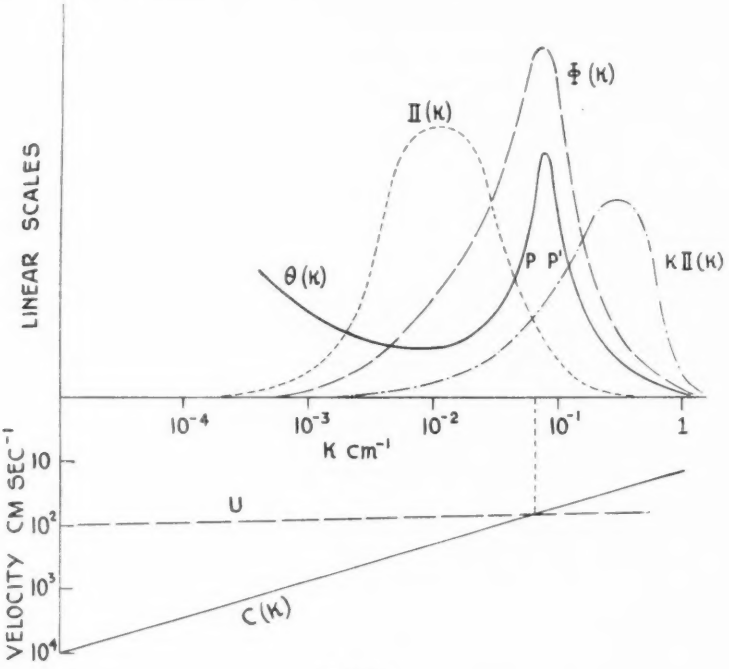

Figure 5.

theory. The non-linear processes which then become important tend, among other things, to limit the maximum surface slope that can be attained. Without a detailed examination of the role of the non-linearities in modifying the wave spectrum, it is not immediately clear exactly what criterion determines the importance of the non-linearities, although it is very reasonable to suppose that it concerns the value of the slope spectrum $\kappa^2\Pi(\mathbf{\kappa})$ in some manner. There is some evidence (Danel 1956) that the effect is appreciable when the mean-square surface slope $\overline{(\nabla\xi)^2} = \int \kappa^2\Phi(\mathbf{\kappa})\,d\mathbf{\kappa}$ attains a certain value. But whatever the exact criterion might be, provided only that it involves a limitation on the slope spectrum, which is largest when the wave-number κ is large or the wavelength λ small, its effect will

clearly be felt first in this range of κ; the actual wave spectrum will for these wave-numbers be smaller than that predicted by the linear theory, and instead of continuing to grow will presumably attain some sort of equilibrium. As time goes on and the wave amplitudes at other wave-numbers increase, the wave-numbers contributing significantly to the slope spectrum extend to smaller and smaller values; so that the effects of the non-linearity gradually spread to the wave-numbers for which the wave spectrum $\Phi(\mathbf{x})$ itself is appreciable. This process whereby the principal stage of development of each wave-number is ended in turn implies that the value of λ for which $\Phi(\mathbf{x})$ is a maximum increases with time, since the longer waves continue to grow while the amplitude of the shorter waves is limited. A detailed analytical description of this process has not yet been attempted, but it seems likely to provide part of the explanation of the observed increase with time in the dominant wavelength of the surface displacement.

An important consequence of these remarks is that the result (4.13) remains valid until the wave-numbers near the maximum of the linear spectrum $\Phi(\mathbf{x})$ become affected by the non-linearity, although over a large range of larger wave-numbers, or smaller wavelengths, the principal stage of development has terminated, and the expression (4.14) for the mean-square slope has become seriously inadequate. The reason is, of course, that the wave-numbers contributing greatly to the slope spectrum make little contribution to the wave spectrum.

4.3. *Comparison with observations on the wave field*

The most important result of § 4.2 from the practical point of view is (4.13). In order to compare this result with the oceanographic measurements that are available for conditions of finite duration, we must obtain an estimate for $\overline{p^2}$ in terms of the quantities that determine the mean velocity profile of the wind. It has already been pointed out that these relevant parameters are the friction velocity u_* and (for aerodynamically rough flow) the length z_0, so that the mean-square pressure fluctuations at the surface should be expressed as

$$\overline{p^2} = A\rho_a^2 u_*^4, \tag{4.15}$$

where A is a numerical constant to be estimated and ρ_a is the density of the air.

In shear-flow turbulence in general, $\overline{p^2}$ is of the order of $\frac{1}{4}\rho_a^2 \overline{\mathbf{v}^2} V^2$, where $\mathbf{v}$ and V are turbulent and mean velocities representative of the region concerned. The atmospheric measurements of MacCready (1953 b) are helpful in applying this expression and obtaining an estimate for A. Under conditions of almost neutral thermal stability over land with z_0 of the order 0·1 cm, he found that in the lowest few metres $\overline{\mathbf{v}^2} = \overline{v_1^2} + \overline{v_2^2} + \overline{v_3^2} \doteq \frac{1}{4}V^2$. In view of the fact that under these conditions, the maximum of the pressure spectrum occurs at wave-numbers corresponding to length scales of order 10 m, it seems likely that the velocity fluctuations at heights of the order of 1 m contribute most to $\overline{p^2}$, and by relating MacCready's measured

values of $\overline{\mathbf{v}^2}$, V and u_*, we obtain the result that, to the correct order of magnitude at least,

$$\overline{p^2} \doteq 9 \times 10^3 \rho_a^2 u_*^4. \tag{4.16}$$

In most published oceanographic measurements, the wave heights observed have been expressed in terms of wind velocities U measured at some level, usually several metres, from the surface. In order to compare our theory with these observations, it is necessary to relate the friction velocity to the measured 'wind velocity' for conditions similar to those under which the observations were made. For the sea surface with moderate winds, a typical value of z_0 is of the order of 0·15 cm, and if the height z at which U is observed is of the order of 5 m, we have from (2.1) that approximately

$$U \doteq 18 u_*.$$

The factor 18 is not critically dependent upon z or z_0, so that it can reasonably be taken as representative of the conditions under which measurements, such as those reported by Sverdrup & Munk (1947), were made. From (4.16), therefore

$$\overline{p^2} \doteq 9 \times 10^{-2} \rho_a^2 U^4.$$

This relation can be substituted into (4.13), and since for pressure components of the scale of gravity waves the convection velocity U_c is equal to the velocity several metres from the surface, it is approximately equal to the 'wind velocity' U. We therefore have, from (4.13),

$$\overline{\xi^2} \sim 0{\cdot}035 \left(\frac{\rho_a}{\rho_w}\right)^2 \frac{U^3 t}{g}.$$

where ρ_w is the density of the water.

In oceanographic practice, wave heights are usually measured from trough to crest, and a widely used measure is H, the mean height of the third highest waves. Longuet-Higgins (1952) has shown that $H^2 = 8\,\overline{\xi^2}$ approximately, so that the previous equation can be written

$$\frac{gH}{U^2} \sim 6 \times 10^{-4} \left(\frac{gt}{U}\right)^{1/2}, \tag{4.17}$$

taking the value 10^{-3} for ρ_a/ρ_w. The accuracy of the constant in this expression is quite low, mainly as a result of the uncertainties in the value of $\overline{p^2}$ to be expected upon the surface. (Some reliable measurements of this would be very valuable.) It might be pointed out, however, that the factor $2^{-3/2}$ in (4.13) represents an underestimate in consequence of the neglect of $\theta(\mathbf{\kappa}, V_1)$ and of the term $c(\kappa)/\cos\alpha$ in (4.11) leading to (4.12).

When the result (4.17) is compared with some of the wave heights observed under conditions of finite duration as in figure 6, we find quite good agreement over the rather restricted range of durations for which measurements have been made. The observations are those given by Sverdrup & Munk in their figure 7. The ratios of the speed C of the highest waves to the wind speed U are also plotted in figure 6, and in these

observations the ratio C/U is of the order of unity. Under these circumstances, other wave-generating processes such as sheltering and the effects of variations in shear stresses may have become important, and, in any case, this theory would be expected to give an appreciable underestimate of the wave heights for the reasons mentioned above. In spite of this, it seems that the approximations used are sufficiently accurate to account for the order of magnitude of the wave heights observed.

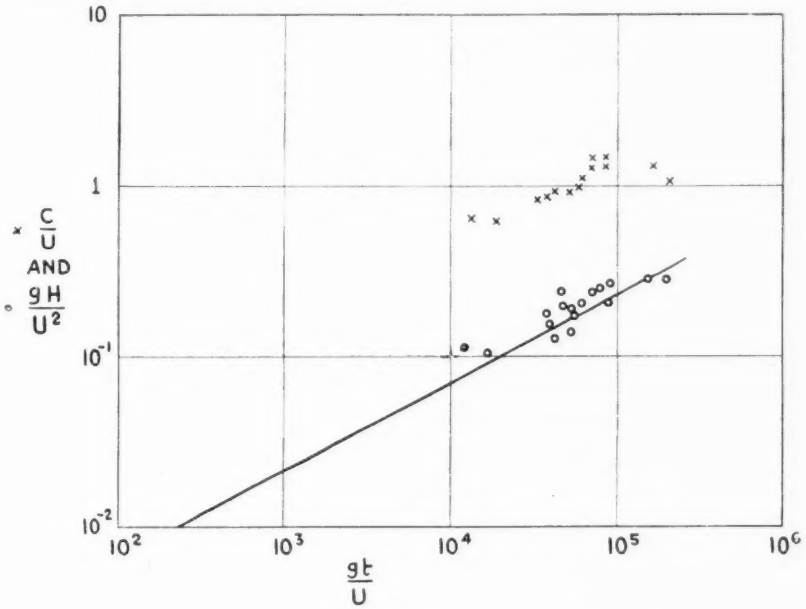

Figure 6.

We are now in a position to see rather more clearly the probable reason for the failure of Eckart's theory to predict the magnitude of the wave heights generated by the wind. His less precise specification of the pressure distribution has 'smoothed off' the resonance peak of the response of the water surface, and it is the wave-numbers near this peak that can contribute largely to the wave spectrum at large durations.

Appendix

We wish to show that $\Pi(\mathbf{x}) = 0$ when $\mathbf{x} = 0$, or equivalently that

$$\int \overline{p(\mathbf{x})p(\mathbf{x}+\mathbf{r})}\, d\mathbf{r} = 0,$$

the integration being over the whole surface with $\mathbf{x}$ fixed. This result is established by joint consideration of the surface boundary condition (2.12)

relating the surface displacements to the surface pressure distribution, and the dynamics of the mass of air above. If (2.12) is multiplied in turn by $dA''(\mathbf{\varkappa}, t)$ and $d\varpi(\mathbf{\varkappa}, t)$, and the probability average taken to find the spectral functions in the manner of (2.3), we can put $\mathbf{\varkappa} = 0$ (and so $n_1 = n_2 = 0$) in the resulting equations. The result of these operations can be expressed as

$$\int \overline{\ddot{\xi}(\mathbf{x})\ddot{\xi}(\mathbf{x}+\mathbf{r})}\, d\mathbf{r} = 0,$$

$$\int \overline{p(\mathbf{x})\ddot{\xi}(\mathbf{x}+\mathbf{r})}\, d\mathbf{r} = 0,$$

or if v_3 is the velocity of the fluid normal to the surface Σ, say,

$$\left.\begin{aligned} \int \overline{\dot{v}_3(\mathbf{x})\dot{v}_3(\mathbf{x}+\mathbf{r})}\, d\Sigma(\mathbf{r}) = 0, \\ \int \overline{p(\mathbf{x})\dot{v}_3(\mathbf{x}+\mathbf{r})}\, d\Sigma(\mathbf{r}) = 0. \end{aligned}\right\} \tag{A.1}$$

We now turn to the dynamics of the fluid above the liquid surface. It has been proved formally by the author in another context (Phillips 1956) that the integrated surface pressure covariances are related to the acceleration covariances, integrated throughout the fluid, by an expression of the form

$$\int \overline{g(\mathbf{x})p(\mathbf{x}+\mathbf{r})}\, d\Sigma(\mathbf{r}) = \rho_a \int \overline{g(\mathbf{x})\dot{v}_3(\mathbf{x}+\mathbf{r}')}\, d\mathbf{r}', \tag{A.2}$$

where $\mathbf{r}' = r_1', r_2', r_3'$ is a point in the interior of the fluid, and the integration on the right is throughout the volume occupied by the fluid. $g(\mathbf{x})$ is a fluctuating quantity of zero mean whose precise nature is, in this expression, immaterial; it is introduced simply to provide integrable covariances with $p(\mathbf{x}+\mathbf{r})$ and $\dot{v}_3(\mathbf{x}+\mathbf{r})$. Taking $g(\mathbf{x}) = p(\mathbf{x})$, the surface pressure at the point $\mathbf{x}$, it can be shown to be a consequence of continuity that

$$\iint \overline{p(\mathbf{x})\dot{v}_3(\mathbf{x}+\mathbf{r}')}\, dr_1'\, dr_2'$$

is independent of r_3'. But when $r_3' = 0$, i.e. at the surface, the integral vanishes according to (A.1) so that the integral

$$\iiint \overline{p(\mathbf{x})\dot{v}_3(\mathbf{x}+\mathbf{r}')}\, dr_1'\, dr_2'\, dr_3'$$

vanishes throughout any layer of large finite thickness above the surface. Hence, from (A.2),

$$\int \overline{p(\mathbf{x})p(\mathbf{x}+\mathbf{r})}\, d\Sigma(\mathbf{r}) = 0, \tag{A.3}$$

which is the result that we set out to establish.

References

Batchelor, G. K. 1951 *Proc. Camb. Phil. Soc.* **47,** 359.

Batchelor, G. K. 1953 *The Theory of Homogeneous Turbulence.* Cambridge University Press.

Danel, P. 1956 *Proc. IV Journées de l'Hydraulique* (Paris).

Eckart, C. 1953 *J. Appl. Phys.* **24,** 1458.

Ellison, T. H. 1956 *Surveys in Mechanics,* p. 400. Cambridge University Press.

Jeffreys, H. 1924 *Proc. Roy. Soc.* A, **107,** 189.

Jeffreys, H. 1925 *Proc. Roy. Soc.* A, **110,** 341.

Keulegan, G. H. 1951 *J. Res. Nat. Bur. Stand., Wash.,* **50,** 99.

Longuet-Higgins, M. S. 1952 *J. Mar. Res.* **11,** 245.

MacCready, P. B. 1953 a *J. Met.* **10,** 325.

MacCready, P. B. 1953 b *J. Met.* **10,** 434.

Phillips, O. M. 1955 *Proc. Camb. Phil. Soc.* **51,** 220.

Phillips, O. M. 1956 *Proc. Roy. Soc.* A, **234,** 327.

Roll, H. U. 1951 *Ann. Met.* (*Hamburg*) **4,** 269.

Sverdrup, H. U. & Munk, W. 1947 *Wind, Sea and Swell. Theory of Relations for Forecasting. Publ. Hydrog. Off., Wash.,* no. 601.

Taylor, R. J. 1952 *Quart. J. Roy. Met. Soc.* **78,** 179.

Taylor, R. J. 1955 *Aust. J. Phys.* **8,** 535.

Ursell, F. 1956 *Surveys in Mechanics,* p. 216. Cambridge University Press.

A cross-flow theory for the normal force on inclined bodies of revolution of large thickness ratio

By R. N. COX

Armament Research and Development Establishment, Fort Halstead, Kent

(*Received* 28 *February* 1957)

In the Munk–Jones cross-flow theory for slender bodies of revolution (Munk 1924; Jones 1946), the cross force on an inclined body is obtained by replacing the three-dimensional flow by a non-steady two-dimensional flow, and by equating the cross-force to the rate of change of cross-flow momentum on a transverse lamina moving past the body with the free stream velocity U_0. The result obtained for the lift force L on an element of the body is, for small angles of attack α,

$$dL/dx = \tfrac{1}{2}\rho U_0^2 (dA/dx)\, 2\alpha, \tag{1}$$

where A is the cross-sectional area of the body, and, by integration

$$L = \tfrac{1}{2}\rho U_0^2 A_B\, 2\alpha, \tag{1 a}$$

where A_B is the base area of the body.

Although the fact is not generally recognized, this result is in poor agreement with exact calculations and with experimental data for finite bodies of revolution, and in order to develop a cross-flow theory for bodies of large thickness ratio, it is necessary to examine the assumptions of the simple theory.

The main assumption is that the flow in the cross-plane is approximately two-dimensional. Thus, in the three-dimensional incompressible potential equation (using wind axes)

$$\phi_{xx} + \phi_{yy} + \phi_{zz} = 0, \tag{2}$$

the first term must be small compared with the other two. By writing $x = lX$, $y = sY$, $z = sZ$, where s is a typical width and l a typical length of the body, and $\phi(x, y, z) = U_0\, l\Phi(X, Y, Z)$, we may re-write (2) as

$$\frac{s^2}{l^2}\Phi_{XX} + \Phi_{YY} + \Phi_{ZZ} = 0. \tag{3}$$

It is evident that the condition that the first term is small is that $s^2/l^2 \ll 1$. For compressible flows satisfying the Prandtl–Glauert differential equation for the perturbation potential:

$$\beta^2\phi_{xx} + \phi_{yy} + \phi_{zz} = 0 \tag{4}$$

where $\beta = (1 - M^2)^{1/2}$, the compressible flow is related to the incompressible flow past a body of revolution elongated in the x-direction by a factor β, and the condition for two-dimensional flow in the cross-plane becomes, for the compressible flow, $\beta^2 s^2/l^2 \ll 1$. For moderate values of β, this condition will hold for surprisingly large values of the body thickness ratio. (For a 20° cone, for instance, $s^2/l^2 \doteqdot 0{\cdot}1$.)

In order to calculate the cross-flow, it is necessary to solve the two-dimensional equation

$$\phi_{yy} + \phi_{zz} = 0 \tag{5}$$

with ϕ_n specified on the boundary. In the Munk–Jones approximation, this boundary condition becomes (using cylindrical coordinates (x, r, ω) with the body shape defined by $R(x)$)

$$\phi_r(x, R, \omega) = U_0 \cos\alpha \frac{d}{dx} R(x) + U_0 \sin\alpha \cos\omega, \tag{6}$$

or, by superposition for the cross-flow, writing $\phi_r = \phi_{1r} + \phi_{2r}$,

$$\phi_{2r}(x, R, \omega) = U_0 \alpha \cos\omega \tag{7}$$

for small angles of attack.

This approximate tangency condition amounts to an assumption that the longitudinal component of the velocity on the body, which is the velocity with which the transverse lamina moves along the body, is approximately equal to the main stream velocity U_0. This is manifestly untrue for thick bodies of revolution. For a 20° cone with a free stream Mach number of 1·3, for instance, the surface velocity is $0{\cdot}8U_0$, and the longitudinal component is $0{\cdot}75U_0$. This suggests that an improvement to the cross-flow theory may be made by employing a more exact tangency condition in which the main stream velocity is replaced by the longitudinal component of the surface velocity $U_s(x)$. The lamina then moves along the body with a velocity $U_s \cos\theta$, where θ is the inclination of the surface to the body axis.

Thus (7) becomes

$$\phi_{2r}(x, R, \omega) = U_s \cos\omega\, \alpha. \tag{8}$$

The lift force on an element of the body is then

$$dL/dx = \tfrac{1}{2}\rho U_s^2 \cos^2\theta (dA/dx) 2\alpha. \tag{9}$$

In order to illustrate the use of this result, a comparison is made in figure 1 with the exact calculation by Kopal (1947) of the supersonic flow past yawed cones of semi-angle θ_0. Since, for such flows, the surface velocity U_s is constant, equation (9) may be integrated to yield

$$L = \tfrac{1}{2}\rho U_0^2 \left(\frac{U_s \cos\theta_0}{U_0}\right)^2 A_B 2\alpha. \tag{10}$$

The lift coefficient slope is then

$$[C_{L_\alpha}]_{\alpha=0} = \frac{L}{\tfrac{1}{2}\rho U_0^2 A_B \alpha} = 2\left(\frac{U_s \cos\theta_0}{U_0}\right)^2,$$

where U_s is obtained from Kopal's calculations. To convert the quantities tabulated by Kopal to the notation used here, the following relationships were employed:

$$U_s = \bar{U}_s\{\tau^2 + 2a_1^2/(\gamma - 1)\}^{1/2}, \quad \text{and} \quad C_{L_\alpha} = C_{N_\alpha} - C_D,$$

where $$C_{N_\alpha} = 8K_N/\pi, \qquad C_D = 8K_D/\pi.$$

The results given in figure 1 for cones of semi-angle 10°, 20° and 30° show that the present method gives good agreement with the exact results for cones up to 30° semi-angle, and correctly predicts the variation of C_{L_z} with Mach number for quite large Mach numbers. This implies that the cross-flow close to the body remains approximately two-dimensional even for cases in which the parameter $\beta^2 s^2/l^2$ becomes large. The Munk–Jones value $C_{L_z} = 2(\text{radian})^{-1}$ is also shown on the figure.

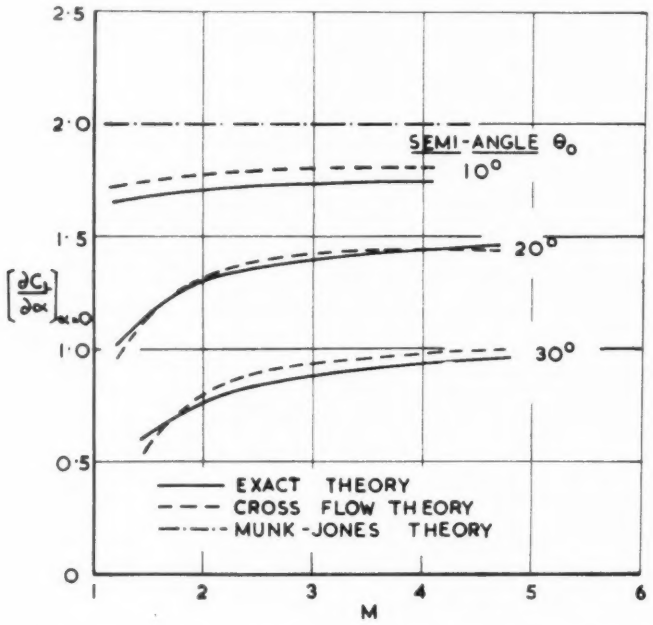

Figure 1. Variation of lift force slope with Mach number for supersonic flow past inclined cones.

The method has also been employed by the author (Cox & Maccoll 1956) for calculating the cross-force on yawed cones in fully developed cavitating flow.

References

Cox, R. N. & Maccoll, J. W. 1956 Recent contributions to basic hydrodynamics. Paper presented at Symposium on Naval Hydrodynamics, Washington.

Jones, R. T. 1946 Properties of low-aspect-ratio pointed wings at speeds below and above the speed of sound, *Nat. Adv. Comm. Aero., Wash., Tech. Note* no. 1032.

Kopal, Z. & Staff of the Computing Section, Center of Analysis, M.I.T. 1947 Tables of supersonic flow around yawing cones, *Massachusetts Institute of Technology, Tech. Rep.* no. 3.

Munk, M. M. 1924 Elements of wing section theory and of the wing theory, *Nat. Adv. Comm. Aero., Wash., Rep.* no. 191.

The laminar and turbulent mixing of jets of compressible fluid. Part I Flow far from the orifice

By L. J. CRANE and D. C. PACK
Department of Mathematics, The Royal College of Science and Technology, Glasgow

(*Received* 18 *January* 1957)

SUMMARY

For flows of jet type, the assumption of a coefficient of eddy kinematic viscosity in turbulent flow leads to the possibility of combining in one the equations for laminar and turbulent motion. An approximation to the solution of these equations is found for the flow of compressible fluid issuing from a narrow slit, far from the slit. The stream function is expanded in a power series in squares of the Mach number. Bickley's solution (1937) for the corresponding problem in incompressible flow is used to start the iterative process by which successive terms of the power series are obtained. In order to find an analytical form for the second term of the series, it has been assumed that the Prandtl number is unity, that the viscosity varies as the nth power of the absolute temperature, and that the stagnation temperature of the jet is the same as that of the surrounding gas. The solution found differs only slightly from that of Howarth (1948) and Illingworth (1949) when laminar flow is considered; only the 'change of scale' effect (arising from a distortion of the coordinates in Bickley's solution) is of importance. In turbulent flow the effect of the second term of the series is as important as the 'change of scale' effect. The effect of compressibility on the width of the mixing region is discussed for both laminar and turbulent jet flow far from the orifice.

INTRODUCTION

The problem of the mixing of streams has received a good deal of attention, both theoretically and experimentally, in recent years. The interest has been in the extension to compressible fluid flow of the problems investigated for incompressible fluid during the years before the war. For jet flows there are two main simplifications of the real problem; one is to suppose that the jet issues from a narrow slit, in which case the field at some distance from the orifice may be examined on the basis of a similarity of velocity profiles in sections normal to the axis of the jet, and the other is to treat only the so-called 'half-jet' mixing, being the case when the two streams in relative motion are both semi-infinite laterally. Each of these problems is itself divisible into two further problems, according as the flow is supposed to be laminar or turbulent.

In this paper it is first shown that the assumption of the existence of an eddy kinematic viscosity coefficient in turbulent flow, which is known to

be reasonably satisfactory for jet flows, leads to the possibility of combining in one the equations for laminar and turbulent motion. Next, an approximation to the solution of these equations is found for the flow of compressible fluid issuing from a narrow slit, far from the slit. The method used is that developed by Pack (1954) for the study of axially symmetric jets of compressible fluids far from the orifice. The stream function is expanded in a power series in squares of the Mach number. The solution of Bickley (1937), for the corresponding problem in incompressible flow, is used to start the iterative process by which successive terms of the power series are obtained. In order to obtain the second term of the series in an analytical form, it has been assumed that the Prandtl number is unity, that the viscosity varies as the nth power of the absolute temperature, and that the stagnation temperature of the jet is the same as that of the surrounding gas. The solutions for two-dimensional flow out of a slit obtained by Howarth (1948) and Illingworth (1949) are seen as particular cases of the solutions found here. The problem of the 'half-jet' mixing will be considered in a later paper.

Equations of motion

Let u, v be the velocity components (or mean velocity components in the case of turbulent flow) parallel either to Cartesian axes (x, y) in two-dimensional flow, or to cylindrical coordinates (x, y) with x measured along the axis of symmetry in axially symmetrical flow. Let the origin of coordinates be taken at the point at which the mixing begins. Let ρ be the density of the gas in the jet and T its absolute temperature.

When the Reynolds number of the flow is large, the approximate equation of motion for jet mixing is the same as for boundary-layer flow at constant pressure:

$$\rho\left(u\frac{\partial u}{\partial x}+v\frac{\partial u}{\partial y}\right)=\frac{1}{y^{\delta}}\frac{\partial}{\partial y}\left(\epsilon\rho y^{\delta}\frac{\partial u}{\partial y}\right), \tag{1}$$

where $\delta = 0$ for two-dimensional flow and $\delta = 1$ for flow with axial symmetry. In this equation $\epsilon = \mu/\rho$, the ordinary kinematic coefficient of viscosity, when the motion is laminar, while when the flow is turbulent $\epsilon = \epsilon(x)$, a coefficient of eddy kinematic viscosity which is assumed to be independent of the y-coordinate.

The equation of continuity is

$$\frac{\partial}{\partial x}(\rho u y^{\delta})+\frac{\partial}{\partial y}(\rho v y^{\delta})=0. \tag{2}$$

From this equation it follows that a stream function ψ exists such that

$$\rho u y^{\delta}=\frac{\partial\psi}{\partial y}, \qquad \rho v y^{\delta}=-\frac{\partial\psi}{\partial x}.$$

If the independent variables are changed to (x, z), where

$$\rho_1 z^{1+\delta}=(1+\delta)\int_0^{y}\rho y^{\delta}\,dy, \tag{3}$$

the equation of motion becomes

$$\frac{\partial\psi}{\partial z}\frac{\partial^2\psi}{\partial x\partial z}-\frac{\partial\psi}{\partial x}\frac{\partial^2\psi}{\partial z^2}+\frac{\delta}{z}\frac{\partial\psi}{\partial x}\frac{\partial\psi}{\partial z}=z^\delta\frac{\partial}{\partial z}\left\{\frac{\epsilon\rho^2y^{2\delta}}{\rho_1 z^\delta}\frac{\partial}{\partial z}\left(\frac{1}{z^\delta}\frac{\partial\psi}{\partial z}\right)\right\}. \tag{4}$$

To allow for the variation of viscosity with temperature, write

$$\frac{\mu}{\mu_1}=\mu^*=\left(\frac{T}{T_1}\right)^n=(T^*)^n. \tag{5}$$

The boundary-layer assumptions underlying the equations of motion imply that pressure is constant, to at least a first approximation, through the field, giving $\rho^*T^*=1$, where $\rho^*=\rho/\rho_1$.

Now write $\epsilon=\theta e(x)$, where (i) in a laminar jet, $\theta=\mu/\rho$ and $e(x)=1$, and (ii) in a turbulent jet, $\theta=\epsilon_0$, Reichardt's constant exchange coefficient, with $e(x)$ an experimentally determined function of x. Introduce also the new independent variable

$$\zeta=\int_0^x e(x)\,dx.$$

Then the equation of motion reduces to

$$\frac{\partial\psi}{\partial z}\frac{\partial^2\psi}{\partial\zeta\partial z}-\frac{\partial\psi}{\partial\zeta}\frac{\partial^2\psi}{\partial z^2}+\frac{\delta}{z}\frac{\partial\psi}{\partial z}\frac{\partial\psi}{\partial\zeta}=\alpha z^\delta\frac{\partial}{\partial z}\left\{\frac{T^*\theta y^{2\delta}}{z^\delta}\frac{\partial^2\psi}{\partial z^2}\right\}, \tag{6}$$

where $\alpha=\mu_1$ and $\beta=n-1$ for laminar flow, and $\alpha=\epsilon_0\rho_1$ and $\beta=-2$ for turbulent flow.

The energy equation is

$$\rho\left(u\frac{\partial i}{\partial x}+v\frac{\partial i}{\partial y}\right)=\frac{1}{y^\delta}\frac{\partial}{\partial y}\left(\frac{y^\delta\rho\epsilon_T}{C_p}\frac{\partial i}{\partial y}\right)+\rho\epsilon\left(\frac{\partial u}{\partial y}\right)^2, \tag{7}$$

where $\epsilon_T=\kappa/\rho$ for laminar flow, κ being the coefficient of heat conduction, and when the flow is turbulent ϵ_T is the eddy coefficient of heat transfer, and where $i=C_p T$ (the enthalpy per unit mass), C_p being the (supposed constant) specific heat at constant pressure.

When it is assumed that the Prandtl number σ, which is equal to $C_p\epsilon/\epsilon_T$, has the value unity, a particular integral satisfying equations (1), (2) and (7) is the Crocco relation

$$\tfrac{1}{2}u^2+i=A+Bu, \tag{8}$$

where A and B are constants, the values of which depend upon the boundary conditions in the problem considered.

Two-dimensional motion

For two-dimensional flow, $\delta=0$ in (6). In the first place it is of interest to note the simplifications of the equation of motion which are then possible.

When $T^*=1$, it follows that $z=y$, $\rho=\rho_1$ and the equation is that of incompressible flow in a boundary layer. The same equation results when $\beta=0$, this corresponding to laminar flow of a compressible fluid with viscosity proportional to temperature ($n=1$); for a two-dimensional jet, this case was treated by Howarth (1948) and Illingworth (1949).

FLOW FAR FROM THE ORIFICE IN A TWO-DIMENSIONAL JET OF COMPRESSIBLE FLUID

The solution for the flow far from the orifice in a two-dimensional laminar jet of incompressible fluid was given by Bickley (1937). It is

$$\psi = 6a\varkappa\zeta^{1/3}\tanh a\eta, \tag{9}$$

where $\eta = z/\zeta^{2/3}$ and a is a scale factor related to the momentum flux out of the orifice. It is not difficult to show that, if F is the momentum flux per unit time out of unit length of the slit, then $a^3 = \rho_1 F/48\varkappa^2$.

The same solution may clearly be used for the turbulent incompressible jet with the proper interpretation of the symbols. When $\eta = y/x$, $\zeta = x^{3/2}$, the kinematic eddy viscosity coefficient is proportional to $x^{1/2}$, and the solution is identical with that given by Görtler (1942); in this case the jet spreads linearly with x, in accordance with the experimental results of Förthmann (1934). Görtler's results were in excellent agreement with experiment except near the edges of the jet.

For the jet of compressible fluid, the boundary conditions far downstream may be expressed as follows:

$$\left.\begin{aligned} &\text{on } y = 0, \quad v = 0, \quad \text{and} \quad \frac{\partial u}{\partial y} = 0; \\ &\text{on } y = \pm\infty, \quad u = 0, \quad \frac{\partial u}{\partial y} = 0, \quad T = T_1 \quad \text{and} \quad \rho = \rho_1, \end{aligned}\right\} \tag{10}$$

where T_1 and ρ_1 are respectively the undisturbed temperature and density in the outer medium into which the jet spreads.

When it is assumed that the stagnation temperature of the jet and the temperature of the surrounding fluid are the same, Crocco's relation (8) takes the form

$$\tfrac{1}{2}u^2 + i = i_1, \tag{11}$$

where i_1 is the stagnation enthalpy in the jet.

The solution (9) is the starting-point for the solution of the equations of compressible flow in jets. It is treated as a first approximation to the required solution. First it is seen that, from (9),

$$\rho_1 u = \frac{6a^2\varkappa}{\zeta^{1/3}}\operatorname{sech}^2 a\eta.$$

Insertion of this value into the Crocco relation (11) gives for the temperature

$$T^* = 1 - \frac{k^2}{\zeta^{2/3}}\operatorname{sech}^4 a\eta,$$

where $k^2 = 18a^4\varkappa^2 C_p \rho_1^2 T_1$. When $\epsilon \propto x^{1/2}$ and T_1 is room temperature, T^* differs from unity by less than 1% for jets of air with Mach numbers on the axis $M_A < 0{\cdot}22$. For higher Mach numbers it will not be sufficiently accurate to use the solution for the incompressible jet flow to yield quantities in the compressible jet flow. In this case the technique used by Pack (1954) for axially symmetrical laminar jets may be employed. This requires the setting-up of an iterative process similar to that of Jansen (1913) and

Rayleigh (1916) by which the approximate solution at any stage is used to obtain a better approximation

The stream function ψ is to be expanded in a series of the form

$$\psi = 6a\nu\zeta^{1/3}\left[\tanh a\eta + \frac{k^2}{\zeta^{2/3}}F_1(a\eta) + \frac{k^4}{\zeta^{4/3}}F_2(a\eta) + \ldots\right].$$

This, substituted into equation (6), leads to the following equation for F_1, on equating coefficients of k^2:

$$F_1''' + 2\tanh\xi F_1'' + 8\,\mathrm{sech}^2\xi F_1' + 4\tanh\xi\,\mathrm{sech}^2\xi F_1 = 2\beta\,\mathrm{sech}^6\xi(7\tanh^2\xi - 1),$$

where the accents denote differentiations with respect to $\xi = a\eta$. With $t = \tanh\xi$, $F_1 = (1-t^2)G$ and $(1-t^2)^2\,dG/dt = H(t)$, the above equation simplifies to

$$(1-t^2)\frac{d^2H}{dt^2} - 2t\frac{dH}{dt} + 4H = 2\beta(1-t^2)^2(7t^2-1).$$

A particular integral of this equation is the following polynomial of the sixth degree in t:

$$H = \tfrac{1}{28}\beta(17 - 72t^2 + 45t^4 - 14t^6).$$

The complementary function is a linear combination of Legendre functions:

$$H = AP_n(t) + BQ_n(t),$$

where $$P_n(t) = F(-n_1, -n_2;\ 1;\ \tfrac{1}{2}(1-t))$$

and $$Q_n(t) = F(-n_1, -n_2;\ 1;\ \tfrac{1}{2}(1+t)),$$

with n_1 and n_2 the roots of the quadratic equation $n(n+1) = 4$, the notation being the usual one for hypergeometric functions. The boundary conditions to be satisfied are:

$$\left.\begin{aligned} &\text{on } t = 0, \quad F_1''(0) = 0 \quad \text{and } F_1'(0) \text{ is finite;} \\ &\text{on } t = 1, \quad \lim_{t\to 1}(1-t^2)F_1'(t) = 0, \qquad \text{i.e. } \lim_{t\to 1}(1-t)F_1'(t) = 0, \\ &\qquad\qquad \text{and } \lim_{t\to 1}\{(1-t)^2F_1''(t) - (1-t)F_1'(t)\} = 0. \end{aligned}\right\}$$

When the singularities of the Legendre functions near $t = 1$ are taken into account, it follows after some analysis that $A = B = 0$. Thus, finally, in the second approximation, when F_1 is calculated from the value obtained for H

$$\psi = 6a\nu\zeta^{1/3}\left[\tanh\xi - \frac{\beta k^2}{38\zeta^{2/3}}\left\{12\tanh\xi - \mathrm{sech}^2\xi\left(12\xi + \right.\right.\right.$$
$$\left.\left.\left. + 17\tanh\xi - \frac{14}{3}\tanh^3\xi\right)\right\}\right].$$

A check on the error involved in the use of the second approximation shows that it is likely to be less than 1% for $M_A < 0{\cdot}52$. In the neighbourhood of $M_A = 1$ the maximum error would be about 2% for laminar flow and 14% for turblent flow. These estimates are based on the assumption that F_2' is of the same order of magnitude as F_1' on the axis of the jet.

Thus the second approximation will express the effect of compressibility with fair accuracy up to sonic speed on the axis. For values of M_A greater than unity the solution still formally applies, but the possibility of the occurrence of shock-waves may render it invalid.

The values of F_1, F_1' for various values of t are given in table 1.

The correspondence between y and z (or ξ), to the first order in k^2, requires only the solution for incompressible flow. In fact,

$$ay = \zeta^{2/3}\left[\xi - \frac{k^2}{\zeta^{2/3}}\tanh\xi\left(1 - \frac{1}{3}\tanh^2\xi\right)\right].$$

Thus

$$ay \to \zeta^{2/3}\left(\xi - \frac{2}{3}\frac{k^2}{\zeta^{2/3}}\right) \quad \text{as } \xi \to \infty.$$

This relation is naturally the same as that obtained by Illingworth for the two-dimensional laminar jet, his solution corresponding to the first term alone in the expansion of ψ, for reasons already explained above.

t	$\xi = \tanh^{-1}t$	$57(-2/\beta)F_1(\xi)$	$57(-2/\beta)F_1'(\xi)$
0	0	0	−51·000
0·1	0·100	−5·012	−47·852
0·2	0·203	−9·490	−38·777
0·3	0·310	−12·919	−24·871
0·4	0·424	−14·794	−7·888
0·5	0·549	−14·643	9·863
0·6	0·693	−12·019	25·646
0·7	0·867	−6·482	36·437
0·8	1·099	2·454	39·027
0·9	1·472	15·548	29·720
1·0	∞	36·000	0

Table 1.

The difference between the velocity profile obtained from the *first term* in the expansion of ψ, when z is expressed in terms of the physical ordinate y, and the velocity profile in incompressible flow (which comes from the same term with $z = y$) will be called the 'change of scale' effect. The above expression for y in terms of ξ and ζ shows that this effect tends to sharpen the jet, i.e. to decrease the width of the mixing region for both laminar and turbulent jets; e.g. when $M_A = 1{\cdot}0$ the 'change of scale' effect diminishes the width of the mixing region by about 20%—the width of the jet being defined as $2\zeta^{2/3}/a$. The numerical value of F_1' is at most about 0·107 for a laminar jet. Since $k^2/\zeta^{2/3} \doteqdot 0{\cdot}4M_A^2$ for a perfect gas with $\gamma = C_p/C_v = 1{\cdot}4$, the effect of the term F_1' on the velocity profile of a subsonic laminar jet is negligible. This is not true for the turbulent jet because the value of F_1' on the axis is $-17/19$. Since F_1' is negative, then changes sign and decreases to zero with increasing ξ, this term tends to make the profile of the compressible turbulent jet broader than an incompressible turbulent jet with the same axial velocity. For laminar and turbulent flow far from the orifice, the net effect of compressibility is respectively to decrease and increase the width of the mixing region.

The analysis shows that the second approximation found in this paper will be useful for flows at any subsonic velocity. Higher approximations

would require attention to the terms neglected in deriving the boundary-layer equations from the full Navier–Stokes equations. The neglected terms are of a higher order than those retained in deriving the second approximation under the limitation imposed on the solution for the incompressible jet, namely $\rho_1 M_A \zeta^{2/3} \gg a^2$.

Motion with axial symmetry

When $\delta = 1$ it is possible to carry out an iterative process just as above which obtains a solution for a jet with axial symmetry. This was done by Pack (1954) for a laminar jet. The equation (6) shows that the same solution, correctly interpreted, may also be used for a turbulent jet. The solution is

$$\psi = a\zeta \left\{ \frac{b^2\eta^2}{(1+\frac{1}{4}b^2\eta^2)} + F_1(\eta)\frac{k^2}{\zeta^2} + F_2(\eta)\frac{k^4}{\zeta^4} + \ldots \right\},$$

where $k^2 = 2b^4/C_\mu T_1 \rho_1^2$, $\eta = z/\zeta a^{1/2}$, and the relation between b and the momentum flux F across a section of the jet is given by $b^2 = 3\rho_1 F/16\pi a$. The function $F_1(\eta)$ is defined by means of a new variable $t = 1/(1+\frac{1}{4}b^2\eta^2)$:

$$F_1(t) = \frac{(6+13n)}{494}(135 - 30t^3 - 8t^4) - \left(\frac{325}{76}n + \frac{519}{494}\right)t + \left(\frac{505}{228}n - \frac{917}{1482}\right)t^2 + \\ + \frac{28}{57}(1-n)t^5 - \frac{45}{247}(6+13n)(t^2-3t)\log t.$$

A table of values of F_1 and F_1' when $n = 0{\cdot}76$ is given in Pack's paper (1954).

The same general conclusions as were found for the two-dimensional laminar jet for the effects of 'change of scale' and compressibility apply equally to the laminar axially symmetric jet. It is found, for axially symmetric turbulent jets, that both of the above effects are of the same order of magnitude, but just as with the two-dimensional turbulent jet the sign of $\eta^{-1}F_1'(\eta)$ on the axis is negative; as η increases $\eta^{-1}F_1'(\eta)$ changes sign and then tends to zero as $\eta \to \infty$. This behaviour of $\eta^{-1}F_1'(\eta)$ tends to broaden the velocity profile of the jet, but the 'change of scale' is more significant and the net result is that the velocity profile of the jet is narrowed as the speed rises, in contrast with two-dimensional flow.

One of us (L. J. C.) is indebted to the Sir James Caird Trust for a Travelling Scholarship which enabled him to take part in this work.

References

Bickley, W. G. 1937 *Phil. Mag.* (7), **23,** 727.

Förthmann, E. 1934 *Ingen.-Arch.* **5,** 42. Translated as *Nat. Adv. Comm. Aero., Wash., Tech. Mem.* no. 789 (1936).

Görtler, H. 1942 *Z. angew. Math. Mech.* **22,** 244.

Howarth, L. 1948 *Proc. Roy. Soc.* A, **194,** 16.

Illingworth, C. R. 1949 *Proc. Roy. Soc.* A, **199,** 533.

Jansen, O. 1913 *Phys. Zeits.* **14,** 639,

Pack, D. C. 1954 *Proc. Camb. Phil. Soc.* **50,** 98.

Rayleigh, Lord 1916 *Phil. Mag.* (6), **32,** 1.

Turbulent transport of heat and momentum from an infinite rough plane

By T. H. ELLISON
Sidegarth, Heswall, Cheshire

(*Received* 22 *January* 1957)

SUMMARY

In the first part of the paper the dimensional laws governing the processes of heat and momentum transport from an infinite rough plane are assembled and their consequences set out. In the second part, the detailed equations for the turbulent energy, the mean square temperature fluctuation and the covariance of temperature and vertical velocity are used, together with some speculative assumptions concerning the dissipative action of the turbulence, to derive a series of relations between the turbulent intensities and the *Austausch* coefficients. One of these relations indicates that the flux form of the Richardson number cannot exceed a critical value which is about 0·15. It follows that in highly stable conditions the buoyancy forces have little direct effect on the turbulent energy balance, their action being primarily to cause a reduction in the scale of the motion and some change in its structure.

1. INTRODUCTION

The theory of turbulent flow near a heated or cooled horizontal rough surface is notoriously difficult, but in the past few years some progress has been made. This has largely been a result of an increased understanding of the role of the various physical quantities in the problem and the more precise formulation of a theoretical model, which have enabled certain relationships to be put forward on dimensional grounds. These restrict the possible forms of certain functions (e.g. the velocity profiles) and show that some of the empirical formulae hitherto used to describe them (e.g. Deacon's (1949) law) cannot be correct. It is the aim of the first part of this paper (§ 2 to § 5) to collect together these dimensional arguments and display the correct form of the physical laws. Nearly all of the steps in this demonstration have been described by earlier writers or are implicit in their work: but individual papers have presented only fragments of the argument and these have frequently been associated with assumptions which are very unlikely to be correct (e.g. that the *Austausch* coefficients for heat and momentum are equal). Thus, since it is only after the dimensional arguments have been completed that it is profitable to examine the mechanism of the flow in detail, the author hopes that any readers who are familiar with these arguments will excuse their repetition.

The character of the second part of the paper (§ 6) is different. In it an attempt is made to learn more about the physical processes controlling the transfer of heat and momentum from the equations of motion. In order to do this, the detailed equations for the turbulent energy, the mean square density fluctuation and the covariance between density and vertical velocity are written down. These alone are not sufficient to solve the problem, and to make further progress it is found necessary to resort to some speculation and guess-work; thus the results that are obtained, although based on assumptions which the author finds plausible, cannot be regarded as having any established validity. These assumptions concern the dissipative action of the turbulence on the turbulent energy, the density fluctuations and the covariance of the density and vertical velocity. It is suggested that the rates at which the turbulence would begin to destroy these quantities, if the simple processes continually creating them were to cease to operate, vary with the stability in such a way that their ratios remain constant. It is shown on the basis of this assertion that the ratio of the *Austausch* coefficient for heat to that for momentum approaches zero when the flux form of the Richardson number approaches a critical value which is considerably less than unity. It follows that in very stable conditions it is not through the energy balance that the buoyancy forces exercise their great influence on the properties of the turbulence. The intensity of the density fluctuations is shown to be an important quantity, and that further investigation of the way in which it is controlled is desirable.

2. The theoretical model

The boundary layers of meteorology commonly differ from those of aerodynamics in that their thickness is great and the region that is of primary interest and accesible for measurement is relatively small and close to the surface. The actual thickness and possible growth of these layers is often assumed to be of little importance, and it is customary to treat them theoretically as if the properties near the surface were independent of the state of the flow at great heights. Moreover, the turbulent shear-stress and heat flux are considered to be independent of height. This corresponds closely to the actual conditions near the ground so far as the shear-stress is concerned, but unfortunately the complex effects of radiation do in practice lead to some change with height in the turbulent heat flux. These are of dominant importance in stable conditions when the turbulent *Austausch* coefficient is very small, and possibly also very near the surface. In addition, it is seldom that the ground or sea is sufficiently uniform horizontally for advection to be negligible and a steady and homogeneous state to be established. For the present, theory must ignore these complications and consider a steady state in which the turbulent fluxes are both independent of height.

It is now possible to specify a theoretical model. We consider an infinite uniform rough plane ($z = 0$) which supports a fluid of great depth.

A stress ρu_*^2 is applied to the plane tangentially causing it to move in the negative x-direction, and heat is supplied to (or extracted from) the plane at a constant rate. We take our frame of reference to be fixed relative to the plane and confine our attention to the steady state which the flow in the vicinity of the plane is supposed to attain ultimately. In this model the mean velocity of the fluid (relative to the plane) increases indefinitely with height in an unknown way; and because of this, the indirect and rather unnatural specification of the flow is needed. The unproved assumption that the flow near the surface attains a steady state is important as it implies that the flow there is not influenced by that at great heights. If it is false and the flow near the surface does depend on the thickness of the boundary layer, the great complexity of the meteorological problem would indicate little prospect of deriving any theory at present.

We shall consider the fluid to be incompressible, but the known equivalence (subject to certain restrictions) between the motion of an incompressible fluid and that of a gas, enables the results to be applied to the atmosphere as required. Moreover, we shall assume that the fractional changes in density are so small that their effect on the inertia of the fluid can be neglected, so that they need only be taken into account in the gravitational terms. In other words, the fluid is treated as having *uniform density but variable weight*, as is commonly done in problems of this type.

3. The role of z_0

In conditions of neutral stability* (that is, when there is no heat flux) it is known that the mean velocity U at height z is given by the equation

$$\frac{dU}{dz} = \frac{u_*}{kz}, \tag{1}$$

where k is a constant with an observed value of about 0·4. The integral of (1) is

$$\frac{kU}{u_*} = \log(z/z_0), \tag{2}$$

where z_0 is a length characterizing the roughness of the surface; z_0 enters (2) only through the boundary condition determining the constant of integration of (1), and so a change in z_0 merely adds a constant velocity to the flow. It would seem reasonable to suppose that such a change would not affect the turbulence in any way (except at heights of the order of z_0). Even in stable and unstable conditions, (1) still holds near the surface and we are able to state quite generally that *the only effect of a change in the value of z_0 is to superpose a uniform translation on the whole flow without modifying its internal mechanism.*

* The word ' stability ' is used in this paper to indicate the static stability of an inviscid fluid with the same vertical distribution of potential density as that in the flow considered; it does not refer to the growth of small disturbances in the moving fluid.

This statement is so obvious and elementary that at first sight it seems strange that it has received little attention from meteorologists. The explanation of this probably lies in uncertainty concerning the assertion that the flow near the surface is independent of that at great heights. When the theory of the whole depth of the boundary layer (Ekman spiral) is considered, even in its simplest form (see Ellison 1956), it is found that z_0 is involved in determining its thickness. Thus, unless the assertion is correct, z_0 is likely to affect the whole structure of the flow.

4. Dimensional arguments

The statement of the last section has some immediate and far-reaching consequences. It implies that the only variables determining the internal structure of the flow are $g\overline{\rho' w}/\bar{\rho}$ (where ρ' is the density fluctuation and $\bar{\rho}$ the mean density), ν (the molecular kinematic viscosity), κ (the thermometric conductivity), u_* and z. At the very high Reynolds numbers of the atmosphere the molecular quantities may be omitted where they occur separately, but it is debatable whether or not the Prandtl number ν/κ ought to be considered in relation to heat transfer (Batchelor & Townsend 1956). It is omitted here, but since it is a dimensionless constant the omission has little importance at this stage. Hence, in neutral conditions all dimensionless groups such as $\overline{u^2}/u_*^2$, $\overline{v^2}/u_*^2$, $\overline{w^2}/u_*^2$, $(z/u_*)dU/dz$, $z^2\overline{(\partial p/\partial x)^2}/u_*^4$, etc., (where u, v and w are the components of the velocity fluctuation and p is the pressure fluctuation) must be constant and independent of height. Covariances such as $u(x_1, y_1, z_1)u(x_2, y_2, z_2)$ must be functions of only $(x_1-x_2)/z_1$, $(y_1-y_2)/z_1$, and $(z_1-z_2)/z_1$*.

When there is a heat flux, an additional length $L = -\bar{\rho}u_*^3/g\overline{\rho' w}$ is available and all the dimensionless groups will depend on the dimensionless height variable, $Z = z/L$ (Obukhov 1946; Charnock 1956). Thus, using the hypothesis that even in non-neutral conditions the effect of a change in z_0 is merely to superpose a uniform translation on the whole flow, we have

$$\frac{1}{u_*}\frac{dU}{d(\log|Z|)} = f'(\log|Z|, \operatorname{sgn} Z). \tag{3}$$

For small values of Z the buoyancy forces are negligible and f' must approach the constant value $1/k$ which it takes in neutral conditions. Thus, the integral of (3) is

$$\frac{kU}{u_*} + \log|S_n| = kf(\log|Z|, \operatorname{sgn} Z), \tag{4}$$

where S_n is Businger's (1955) stability index defined by

$$S_n = z_0/L = Zz_0/z, \tag{5}$$

* These variables can, of course, be combined in various ways, e.g. to give $(x_1-x_2)/(z_1+z_2)$, etc. The choice of the most convenient form is a matter of some delicacy.

and $f(\log|Z|, \operatorname{sgn} Z)$ tends to $\log|Z|$ for small Z. It will be seen from (4) that the velocity profile can take only two forms, one for stable and one for unstable condition; the logarithmic law is the limit of these for small heights.

The determination of the function $f(\log|Z|, \operatorname{sgn} Z)$ in (4) is, of course, a major task for theory, but not one that can yet be accomplished. However physical reasoning can take us a little farther. In 1920 Richardson showed that the quantity which is now known as the flux form of the Richardson number (Deacon 1955) (and denoted here by Rf) is equal to the ratio of the rate at which buoyancy forces extract energy from the turbulence to the rate at which it is supplied by the shear-stress. This result is a direct consequence of the energy equation for the turbulence, (13). Rf may be expressed in the following equivalent ways:

$$Rf = Ri\frac{K_H}{K_M} = -\frac{K_H g d\bar{\rho}/dz}{K_M(dU/dz)^2} = \frac{g\overline{\rho' w}}{\bar{\rho}u_*^2\, dU/dz} = \frac{g\overline{\rho' w}K_M^* z}{\bar{\rho}u_*^3} = ZK_M^*, \quad (6)$$

where $$K_M^* = \frac{K_M}{u_* z} = \frac{u_*}{z(dU/dz)} \text{ and } K_H = -\frac{\overline{\rho' w}}{d\bar{\rho}/dz}.$$

Richardson's arguments make it clear that Rf cannot exceed unity over any substantial depth of fluid, so it must have a maximum value (critical value) not greater than this. It will be suggested shortly that Rf_{crit} is in fact considerably less than one, but some deductions can be made from its mere existence. Rf and K_M^* are functions of Z, and physical intuition urges that they are monotonic functions. In that case, Rf must approach its critical value when Z becomes large and positive. We have in the limit:

$$Rf_{\text{crit}} = RiK_H/K_M = g\overline{\rho' w}K_M/\bar{\rho}u_*^4. \quad (7)$$

Hence in very stable conditions K_M is independent of height and determined by the heat and momentum fluxes. Linear velocity profiles such as are predicted by (7) have been observed in the atmosphere (e.g. by Rider & Robinson 1951), but the agreement is probably fortuitous since it is likely that in the conditions of the measurements the temperature profiles were controlled by radiation and that the turbulent heat flux was not independent of height.

If Ri, as well as Rf, has a maximum value, (7) determines K_M in terms of it; but there is no reason to think that this is the case. It seems more likely (especially in view of (20)) that turbulence can be maintained at large values of Ri. Proudman (1953), following earlier work of Sir Geoffrey Taylor, has analysed measurements of currents and salinity in the *Kattegat* and found appreciable transport of momentum by turbulence associated with values of Ri up to 10. As Ri increases, the ratio K_H/K_M must decrease in proportion; so, in our model, K_H decreases indefinitely with height and is not determined uniquely by the fluxes alone in the same way as K_M. In order to find K_H, and hence the density profile, it is necessary to know how the limit is approached. That is, one must know how K_H/K_M approaches zero as Rf approaches Rf_{crit}, and how Rf varies with Z.

At the other extreme, in very unstable conditions (large negative Z), a state of free convection may be assumed to exist, so that K_H is independent of u_*. It follows that the quantity H^* defined by,

$$H^{*2} = -\frac{\overline{\rho' w^2} \bar{\rho}}{g z^4 (d\bar{\rho}/dz)^3}, \tag{8}$$

is constant. Measurements made by workers in Australia (Taylor 1956) suggest that it has a value of about 0·8. An alternative expression for H^*, which brings out the dependence of K_H^* on Z in these conditions, is

$$H^{*2} = -K_H^{*3} Z^{-1}. \tag{9}$$

Any sort of mixing length theory would seem to suggest that K_M is also independent of u_* in free convection, and this is generally assumed to be the case. It follows that K_H/K_M must approach a constant value for large negative Z.

Our knowledge of K_M^* as a function of Rf can now be summarized as follows. When $Rf = 0$, $K_M^* = k$ (see (1)); when Rf approaches Rf_{crit} at large positive Z, K_M^* vanishes (see (7)); when Rf is large and negative, K_M^* is proportional to $Rf^{1/4}$ (see (9) and (6)). Hence the well known and useful semi-empirical formula of Holzman (1943),

$$(K_M^*/k)^2 = 1 - sRi, \tag{10}$$

where s is a constant, cannot be correct except for very small values of Ri. However, it is very convenient to have a semi-empirical formula like this, and so the following may be suggested:

$$(K_M^*/k)^4 = 1 - Rf/Rf_{\text{crit}}. \tag{11}$$

Note that the right hand side of(11) contains Rf in place of Ri. It can be written as a relation between K_M^* and Z, since by (6) we have

$$(K_M^*/k)^4 = 1 - ZK_M^*/Rf_{\text{crit}}.$$

(11) has no theoretical basis beyond having the correct form in limiting conditions and presumably a more elaborate formula with more empirical constants will be needed as soon as precise observations become available.

In the case of free convection (11) implies

$$K_H/K_M = Rf_{\text{crit}}^{1/3} H^{*2/3} k^{-4/3}. \tag{12}$$

When one inserts the numerical values already mentioned for K^* and k and the value 0·15 for Rf_{crit} as is suggested below, this gives $K_H/K_M = 1{\cdot}6$, which seems quite reasonable.

5. The (log + linear)-law

Presumably K_M^* can be expanded in a power series in Z:

$$K_M^*/k = 1 + a_1 Z + a_2 Z^2 + \ldots,$$

so

$$kU/u_* = \log(z/z_0) - a_1 Z + \ldots. \tag{13}$$

Businger (1955) has shown from an analysis of Rider's (1954) velocity profiles that a_1 is about 0·8, while Monin (undated) gives $a_1 = 0{\cdot}6$.

The semi-empirical equation (11) yields $a_1 = k/4Rf_{\text{crit}}$, which implies that $Rf_{\text{crit}} = 0{\cdot}14$ if $a_1 = 0{\cdot}7$. This value has no more authority that (11) itself, but it does strongly indicate that Rf_{crit} is small. It also turns out that this value is virtually identical with that suggested by a quite separate argument in the next section.

6. The transport mechanism

In this section an attempt is made to approach the subject from a new angle and to derive useful information from the equations of motions together with some relatively weak and general assumptions. The suggestion already made that Rf has a small critical value is confirmed, and it is shown that the assumptions lead to a reasonably consistent physical picture of the processes governing the flow. It is not claimed that the validity of the assumptions is established; but, whether they are correct or not, the theory does indicate subjects which are likely to repay further investigation.

From the Navier–Stokes equations, the equation of continuity and the equation of heat conduction, it is elementary to deduce the following equations for the mean square density fluctuation, the turbulent energy and the density flux:

$$\frac{1}{2}\frac{\partial\overline{\rho'^2}}{\partial t} + \frac{1}{2}\frac{\partial\overline{w'^2\rho}}{\partial z} + \overline{w\rho'}\frac{d\bar{\rho}}{dz} - \kappa\overline{\rho'\nabla^2\rho'} = 0, \tag{14}$$

$$\frac{1}{2}\frac{\partial}{\partial t}(\overline{u^2}+\overline{v^2}+\overline{w^2}) + \frac{1}{2}\frac{\partial}{\partial z}(\overline{u^2w}+\overline{v^2w}+\overline{w^3}) + \overline{uw}\frac{dU}{dz} + \\ + \frac{1}{\bar{\rho}}\frac{\partial\overline{wp'}}{\partial z} + \frac{\overline{w\rho'}g}{\bar{\rho}} - \nu(\overline{u\nabla^2u}+\overline{v\nabla^2v}+\overline{w\nabla^2w}) = 0, \tag{15}$$

$$\frac{\partial\overline{w\rho'}}{\partial t} + \frac{\partial\overline{w^2\rho'}}{\partial z} + \overline{w^2}\frac{d\rho}{dz} + \frac{1}{\bar{\rho}}\overline{\rho'\frac{\partial p}{\partial z}} + \frac{\overline{\rho'^2}g}{\bar{\rho}} - \kappa\overline{w\nabla^2\rho'} - \nu\overline{\rho'\nabla^2w} = 0. \tag{16}$$

In our model conditions are steady and so the first terms in these equations vanish; they have been written down merely to aid understanding. The 'diffusion' terms like $\partial(\overline{w\rho'^2})/\partial z$, etc., are probably always negligible since $\overline{\rho'^2}$, $\overline{u^2}$, etc., vary only slowly, if at all, with height. The 'pressure-flow' term $\partial(\overline{pw})/\partial z$ in (15) is zero in neutral conditions, and there seems no reason to think that it ever becomes significant. There remain the dissipation terms, the term $\overline{\rho'\partial p/\partial z}$ in (16), and the simple terms of obvious interpretation among which we wish to discover new relations.

Now it is well known that at high Reynolds numbers the rates of dissipation are very largely determined by typical length and velocity scales of the turbulence and not by molecular quantities such as viscosity. Let us therefore formally introduce decay times T_1, T_2, and T_3, for $\overline{\rho'^2}$, $\overline{u^2}+\overline{v^2}+\overline{w^2}$, and $\overline{w\rho'}$, such that, in the (imagined) absence of the producing terms, the mixing action of the turbulence would begin to destroy these

quantities at rates equal to $1/T_1$, etc. In other words, let us *define* T_1, T_2 and T_3 by the following equations:

$$\frac{\overline{\rho'^2}}{2T_1} + \overline{w\rho'}\frac{d\bar{\rho}}{dz} = 0, \tag{17}$$

$$\frac{\overline{u^2}+\overline{v^2}+\overline{w^2}}{2T_2} + \overline{uw}\frac{dU}{dz} + \overline{w\rho'}g = 0, \tag{18}$$

$$\frac{\overline{w\rho'}}{T_3} + \overline{w^2}\frac{d\bar{\rho}}{dz} + \frac{\overline{\rho'^2}g}{\bar{\rho}} = 0. \tag{19}$$

Since the mixing action of the turbulence tends to destroy the correlation between w and ρ', as well as $\overline{w^2}$ and $\overline{\rho'^2}$, T_3 may be expected to be substantially smaller than T_1 and T_2, which may well be roughly equal. While T_1, T_2 and T_3 certainly vary with stability, we may reasonably guess that they are all dominantly determined by the same typical length and velocity scales and that the relation between the processes responsible for the destruction of the turbulent energy, the density fluctuations, and the density flux, change only little with stability. If so, T_1, T_2 and T_3 must remain in roughly fixed ratios. Such an assertion is admittedly speculative, but seems to lead to a consistent physical theory.

In (19), the term $\overline{\rho'\partial p/\partial z}$ has been incorporated in $\overline{w\rho'}/T_3$. This is plausible if the term is considered to represent the drag on a rising blob of hot fluid in unstable conditions; in stable conditions the term turns out to be negligible and so the interpretation is unimportant.

It may be noted at once that (17) alone implies that K_H is always positive and that no selective action of the buoyancy forces, such as was once suggested by Priestley & Swinbank (1947), can cause a transfer of density against the gradient in stable conditions.

After a little algebra, the equations (17) to (19) can be rearranged to give K_H/K_M, T_2 (say), and $\overline{\rho'^2}$ in terms of the known fluxes, the ratios of T_1, T_2 and T_3, and the components of the turbulent energy. Let us first examine the equation for K_H/K_M:

$$\frac{K_H}{K_M} = \frac{(\overline{u^2}+\overline{v^2}+\overline{w^2})\overline{w^2}[1 - Rf(1 + T_1(\overline{u^2}+\overline{v^2}+\overline{w^2})/T_2\overline{w^2})]}{2u_*^4(T_2/T_3)(1-Rf)^2}, \tag{20}$$

which is the basic result of this part of the paper. There can be little doubt that for small positive values of Rf the term in square brackets is the dominant one. If we take $T_1/T_2 = 1$ and $(\overline{u^2}+\overline{v^2}+\overline{w^2})/\overline{w^2}$ to have the same value as in neutral conditions, which is known to be roughly 5·5, we see that K_H/K_M falls to zero when $Rf = 0{\cdot}15$. This small critical value of Rf is most remarkable since it implies that in stable conditions the buoyancy forces do not have any great effect on the energy balance. In these circumstances it is difficult to believe that the assumption that $(\overline{u^2}+\overline{v^2}+\overline{w^2})/\overline{w^2}$ has the same value as in neutral conditions is far wrong; but, in any case, one would expect that in stable conditions horizontal motions would be favoured at the expense of vertical ones, thereby causing the quantity to increase rather than decrease. Such a change would lead to an even smaller value

of Rf_{crit}. It is, of course, conceivable that T_1/T_2 decreases in stable conditions, but there is no obvious reason why this should be expected, and it would require a very drastic change to affect the general conclusion that the critical value of Rf is small.

The author knows of no measurements which are nearly precise enough to enable the conclusion to be checked. The work of Proudman (1953), which was referred to earlier, indicates a value around 0·25; but the conditions of the measurements were very different from the ideal considered in the theory and the discrepancy is not disturbing.

Even in neutral conditions it is known only that K_H/K_M is roughly unity. The work of Rider (1954) suggests a value about 1·3, while that of Swinbank (1955) suggests about 0·7. Cramer & Record (1953) found that K_M was often less than K_H, in agreement with Rider, but their results were definitely affected by the trajectory of the air in which the measurements were made. If we take $T_2/T_3 = 6$, $\overline{w^2}/u_*^2 = 1{\cdot}6$, and again $(\overline{u^2}+\overline{v^2}+\overline{w^2})/\overline{w^2} = 5{\cdot}5$, in neutral conditions ($Rf = 0$), (20) gives $K_H/K_M = 1{\cdot}2$. That it should be necessary to take quite such a high value of T_2/T_3 is perhaps a little surprising, but quite unavoidable. It seems likely that with these values for the constants, (20) will give a good representation of K_H/K_M while Rf is small.

With increasing instability the ratios of the intensities will begin to change. At the extreme, in free convection, the scale of the motion is limited to be proportional to the height; but the turbulent energy is produced entirely by the buoyancy forces, and so, being independent of the shear-stress, must on dimensional grounds increase as $Z^{2/3}$. The equation for K_H/K_M now degenerates into one for K_H alone, namely,

$$K_H = -\frac{\bar{\rho}(\overline{u^2}+\overline{v^2}+\overline{w^2})\overline{w^2}[1+T_1(\overline{u^2}+\overline{v^2}+\overline{w^2})/T_2\overline{w^2}]}{2g\overline{\rho' w}T_2/T_3}. \tag{21}$$

But by (9),

$$K_H = H^{*2/3}Z^{1/3}u_* z = H^{*2/3}(\overline{g\rho' w}/\bar{\rho})^{1/3}z^{4/3},$$

so

$$(z\overline{g\rho' w}/\bar{\rho})^{1/3} = \frac{H^{*2/3}(\overline{u^2}+\overline{v^2}+\overline{w^2})\overline{w^2}[1+T_1(\overline{u^2}+\overline{v^2}+\overline{w^2})/T_2\overline{w^2}]}{2T_2/T_3}, \tag{22}$$

which connects the turbulent energy with the heat flux in free convection. We do not know the value of $(\overline{u^2}+\overline{v^2}+\overline{w^2})/\overline{w^2}$ and the ratio of the T's in these conditions. If (22) is considered as an equation for $\overline{u^2}+\overline{v^2}+\overline{w^2}$, it is not very sensitive to the former and we may take a value of 3 as being reasonable; in the absence of any evidence that the ratios of the T's differ from their values in neutral conditions, we can only make a provisional guess that they are the same. If so, we obtain

$$\overline{u^2}+\overline{v^2}+\overline{w^2} = 3(z\overline{g\rho' w}/\bar{\rho})^{2/3}. \tag{23}$$

Now let us turn to the second of the equations derived from (17) to (19), that for T_2, which is just a restatement of (18). T_2 has little direct interest since it is not measurable, but on account of our assertion that it is determined

by typical length and velocity scales of the turbulence, it can to a limited extent help us to form a physical picture. $(\overline{u^2}+\overline{v^2}+\overline{w^2})^{1/2}$ is the obvious choice for the velocity scale, and so the equation for T_2 can be used to determine a length L_M defined as $T_2(\overline{u^2}+\overline{v^2}+\overline{w^2})^{1/2}$. From (18) and (6) we obtain

$$L_M = (\overline{u^2}+\overline{v^2}+\overline{w^2})^{3/2}u_*^{-3}LRf/(1-Rf). \tag{24}$$

This implies that L_M is proportional to z in neutral and unstable conditions and to L in very stable conditions, as was perhaps to be expected. The approximate numerical values are as follows: when $Rf = 0$, $L_M = 10z$; in free convection, $L_M = 5z$; in very stable conditions, $L_M = 5L$. It is of course only the relative sizes of L_M in the three states that is significant. It is a little surprising that its value in free convection is only half that in neutral conditions. This result may be partly spurious and due to an incorrect numerical constant in (23), but it is hardly possible that that is the whole cause of the difference. It is more likely that the effect is in some way connected with the fact that in free convection the turbulent energy is more nearly isotropically distributed than in neutral conditions.

The remaining equation to be discussed is that for $\overline{\rho'^2}$,

$$\frac{(\overline{w\rho'})^2}{\overline{\rho'^2}\,\overline{w^2}} = \frac{1-Rf[1+T_1(\overline{u^2}+\overline{v^2}+\overline{w^2})/T_2\overline{w^2}]}{2(T_1/T_3)(1-Rf)}. \tag{25}$$

If we keep the same numerical values as previously, this predicts that the correlation coefficient, $\overline{w\rho'}/(\overline{\rho'^2})^{1/2}(\overline{w^2})^{1/2}$, is about 0·6 in free convection; 0·3 in (almost) neutral conditions; and vanishes in very stable conditions. In principle these predictions can be tested easily, but again adequate measurements are lacking. The values given by Swinbank (1955) are very scattered, but indicate a value of 0·4 rather than 0·3 in nearly neutral conditions. The measurements do not show the form of the variation with stability beyond the sign of the general trend.

The simple physical explanation of the relative inefficiency of heat transfer in stable conditions expressed by (20) and (25) is that then a displaced fluid particle tends to return to its equilibrium level before it has had time to mix with its surroundings. A particle can transfer momentum during a brief excursion without mixing with its surroundings through the agency of pressure fluctuations, but in order to transfer heat it must mix.

Some idea of the vertical distance travelled by particles before either returning towards their equilibrium level or mixing can be obtained from the length $L_H = (\overline{\rho'^2})^{1/2}/d\rho/dz$. It can easily be shown that

$$L_H^2 = L_M^2\frac{T_3T_1}{2T_2^2}\frac{\overline{w^2}}{\overline{u^2}+\overline{v^2}+\overline{w^2}}\frac{1-Rf/Rf_{\text{crit}}}{1-Rf}, \tag{26}$$

which shows that in stable conditions L_H becomes much smaller than L_M. No precise interpretation of this can be given since the two scales have a different nature, but it presumably means that in stable conditions scales measured in the vertical direction are liable to be much smaller than those measured horizontally.

One last point is worth mentioning. In very stable conditions the last two terms of (19) become much greater than the first, and balance. Thus

$$\overline{w^2} = \frac{\overline{\rho'^2} g}{\bar{\rho} d\bar{\rho}/dz}$$

$$= \frac{g L_H^2}{\bar{\rho}} \frac{d\bar{\rho}}{dz}. \tag{27}$$

In other words, the scale L_H is just such that the work required to lift a particle a distance L_H from its equilibrium level is equal to its average kinetic energy.

7. Transport of inert pollutant

If the theory of the previous section is applied in a similar way to the transport of an inert pollutant (i.e. one that does not affect the density of the fluid), it is found that the *Austausch* coefficient for it is necessarily equal to K_H. The reason for this is that no mechanism is included in the theory which would enable the turbulence to destroy the correlation between density fluctuation and pollutant concentration. Thus the conclusion is one which may be seriously upset as the role of molecular processes in turbulent flow becomes better understood. Observational evidence based on direct measurements of the *Austausch* coefficients is at present conflicting; and it is likely that measurements of the correlation between density fluctuation and pollutant concentration would provide a simpler and more sensitive test.

References

Batchelor, G. K. & Townsend, A. A. 1956 Turbulent diffusion. *Surveys in Mechanics*. Cambridge University Press.

Businger, J. A. 1955 *J. Met.* **12,** 553.

Charnock, H. 1956 *Quart. J. Roy. Met. Soc.* **82,** 242.

Cramer, H. E. & Record, F. A. 1953 *J. Met.* **10,** 219.

Deacon, E. L. 1949 *Quart. J. Roy. Met. Soc.* **75,** 89.

Deacon, E. L. 1955 *Counc. Sci. Ind. Res. Org., Div. Met. Phys.* (*Melbourne*), *Tech. Pap.* no. 4.

Ellison, T. H. 1956 Atmospheric turbulence. *Surveys in Mechanics*. Cambridge University Press.

Holzman, B. 1943 *Ann. N.Y. Acad. Sci.* **44,** 13.

Monin, A. S. (undated) *Ministry of Supply Translation* no. TIB/T4516. (O mekhanizme nagrevaniya vozdukha v otkrytoi stepi. *Sborn. Izv. Akad. Nauk. S.S.S.R.* 100.)

Obukhov, A. M. 1946 *Tr. Inst. Theoretich. Geofiziki, Akad. Nauk., S.S.S.R.* **1,** M-L. Cited by Monin (undated).

Priestley, C. H. B. & Swinbank, W. C. 1947 *Proc. Roy. Soc.* A, **189,** 543.

Proudman, J. 1953 *Dynamical Oceanography*, p. 102. London: Methuen.

Richardson, L. F. 1920 *Proc. Roy. Soc.* A, **97,** 354.

Rider, N. E. 1954 *Phil. Trans.* A, **246,** 481.

Rider, N. E. & Robinson, G. D. 1951 *Quart. J. Roy. Met. Soc.* **77,** 375.

Swinbank, W. C. 1955 *Counc. Sci. Ind. Res. Org., Div. Met. Phys.* (*Melbourne*), *Tech. Pap.* no 2.

Taylor, R. J. 1956 *Quart. J. Roy. Met. Soc.* **82,** 89.

An experimental investigation of a wall jet

By P. BAKKE
Department of the Mechanics of Fluids, University of Manchester

(*Received* 19 *February* 1957)

SUMMARY

This paper deals with an experimental investigation of a turbulent low-speed jet of air spreading out radially over a flat smooth plate: a flow which has been discussed by Glauert (1956) in his theory of the wall jet.

The aim of the experiments has been to determine the mean velocity distribution and rate of growth of the jet. It is found, within the experimental range and accuracy, that the velocity profiles are similar and that the rate of change of velocity and width of the jet can be expressed by simple power-laws.

1. INTRODUCTION

The term 'wall jet' was introduced by Glauert (1956) to describe the flow that develops when a jet, consisting of a fluid similar to that of its surroundings, impinges on a plane surface and spreads out over the surface. Glauert studied such a flow in two dimensions and in three dimensions with axial symmetry, and pointed out that it has features common to both the free jet and the ordinary boundary layer; thus, the spreading fluid is retarded by frictional resistance of the wall and the inner part of the flow may be expected to show a certain structural similarity to a boundary layer, whereas entrainment of quiet fluid occurs near the outer edge of the flow which accordingly is likely to resemble a free jet in character.

This idea of a hybrid structure led Glauert to a solution of the turbulent wall jet by introducing an eddy viscosity distribution near the wall consistent with the Blasius power-law velocity-profile, and a constant eddy viscosity in the outer part of the flow. From this solution, which involved one disposable constant, it was concluded that exact similarity of the flow at all distances x from the origin—the 'point' of impingement of the jet—could not exist, since the eddy viscosities in the inner and outer parts of the flow varied in a slightly different manner with x or, what amounts to the same thing, with Reynolds number. As a consequence, if the local rates of change with x of maximum velocity and jet width are expressed by simple power laws, the exponents of these laws will themselves vary slowly with x. However, it appears from the analysis that for any particular jet the variation is so slow that it would be undetectable experimentally.

The experiments described in this paper were made with a turbulent, round, low-speed jet which spread radially over a smooth, plane surface.

Velocity distributions were measured and, as foreshadowed by the theory, were found to be similar, within the limits of experimental accuracy; they were also consistent with the shape of profile predicted by the theory.

2. Arrangement of the experiment

The experiment arrangement is shown diagrammatically in figure 1. The wall was a flat plate of bakelite 125 cm × 125 cm, placed horizontally on a steel frame.

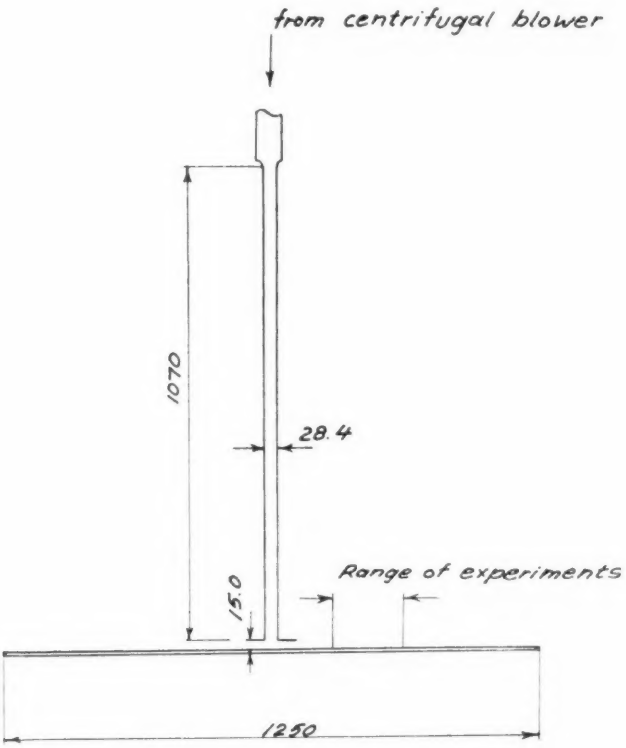

Figure 1. Arrangement of apparatus. All lengths in mm.

The air was supplied by a centrifugal blower connected to a rubber tube of internal diameter 56 mm and length 2·8 m, which terminated, by way of a smooth contraction, in a pipe of 28·4 mm diameter and 1·07 m length. A flange of 126 mm diameter was attached to the end of the pipe. The reason for installing this flange was partly to prevent the generation of large scale disturbances at the pipe exit, and partly to get a closer approximation to the form of source assumed by Glauert. During all

experiments the pipe was placed at right angles to the bakelite plate with the exit 15·0 mm above the plate. Preliminary measurements showed a fully developed turbulent velocity profile at the pipe exit with a peak velocity of 34 m/s. With a previous arrangement in which the rubber tube had a 90° bend the velocity profile at the pipe exit was not symmetrical. The deviation was consistent with a secondary flow due to the bending of the tube and disappeared when the rubber tube was straightened.

The velocity distribution along the plate was measured by means of a 1 mm external diameter total-pressure tube connected to a 'Casella' U-tube manometer, the measuring accuracy being 0·01 mm water. The time required to obtain a reading with this accuracy was about 15 minutes.

3. Experiments

The velocity distributions were measured at distances of 143 to 303 mm from the origin. At each station a Pitot traverse was made perpendicular to the plate and the velocities were computed by assuming the static pressure to be atmospheric everywhere. Each of the traverses consisted, on the average, of 20 readings at about 0·3 mm intervals near the wall and intervals of about 1·5 mm in the outer part of the flow. The accuracy of setting the Pitot tube was 0·05 mm.

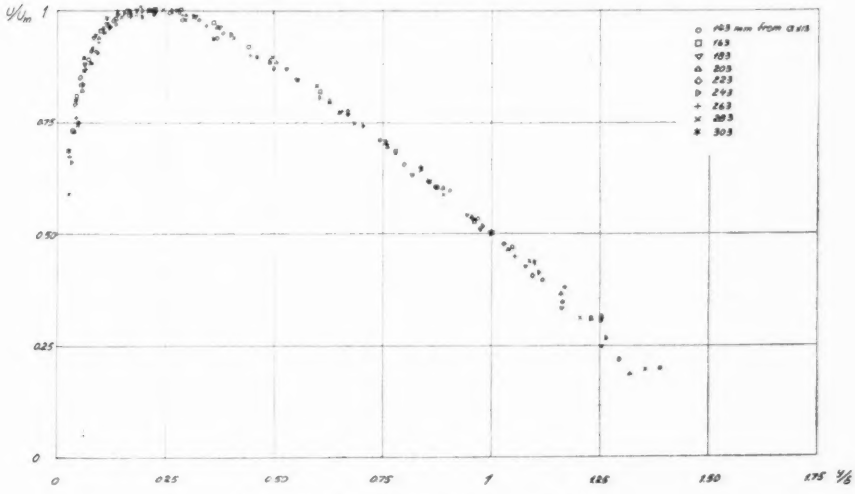

Figure 2. Experimental velocity profiles.

In the range mentioned the maximum velocity varied from 6·10 m/s to 2·60 m/s. The width of the jet, measured from the plate to the point where the velocity had decreased to half the maximum velocity, varied from 11 to 23 mm.

Figure 2 is a dimensionless plot of velocities obtained from nine traverses. The horizontal axis indicates the height y above the plate measured in terms

of δ, where $U(\delta)=\frac{1}{2}U_m$ and U_m is the maximum velocity. The vertical axis gives the measured velocities, U, in terms of U_m. Points corresponding to values of U/U_m below 0·2 in the outermost parts of the flow have been omitted. With the previously quoted estimate for the accuracy of a pressure measurement, the percentage velocity error is $7{\cdot}5/U^2$, where U is measured

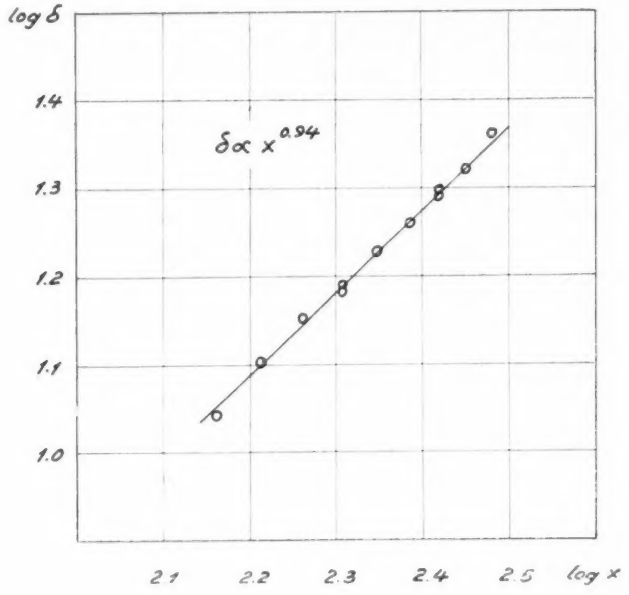

Figure 3. Variation of width of jet with distance from origin.

in m/s. For the largest velocity presented in figure 2, 6·10 m/s, the error is 0·2%; for the smallest velocity, which occurs at the outer edge of the flow at a point furthest from the origin, the accuracy of velocity measurement is 28%. Apart from errors in pressure measurement, there is a source of error at the outer edge where U tends to zero; the transverse inflow velocity tends to a finite value which results in a yawed flow relative to the Pitot tube. A rough estimate indicates that there is no yaw effect at $U/U_m=0{\cdot}5$, whereas at $U/U_m=0{\cdot}2$ the true values are of the order 20% less than the plotted ones. The points within a few Pitot-tube diameters from the wall are also subject to error.

Figures 3 and 4 respectively are plots of $\log U_m$ (U_m in m/s) and $\log\delta$ (δ in mm) *vs* $\log x$, where x is the distance from the origin in mm. The simple power laws quoted in the figures correspond to the least-square estimated inclination of a straight line through the points. The estimated accuracy is $\pm 0{\cdot}03$ for $-1{\cdot}12$ and $\pm 0{\cdot}02$ for 0·94.

Returning to figure 2, the experiments show no detectable departures from similarity of the velocity profile. Whether this observation holds for larger distances from the origin was not investigated due to the limitation set by the measuring accuracy of the apparatus.

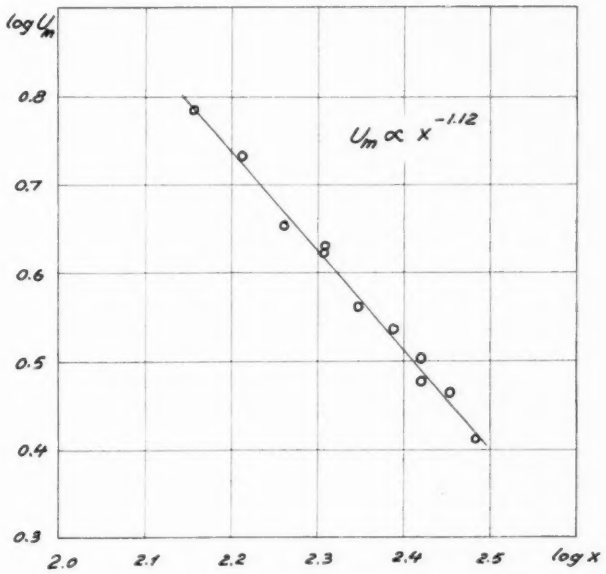

Figure 4. Variation of maximum velocity of jet with distance from origin.

4. Comparison with Glauert's theory

The shape of the velocity profile given by Glauert depends on a single parameter α, which is uniquely related to $\kappa R^{1/4}$. κ is an empirical constant related to the eddy viscosity in the outer layer, and R ($= U_m \delta_l/\nu$) is the jet Reynolds number, where δ_l, consistent with Glauert's definition, is the distance between the points at which $U = U_m$ and $U = \frac{1}{2}U_m$. The relation between α and $\kappa R^{1/4}$ is given in Glauert's table 1.

Figure 5 shows the experimental profile and Glauert's solution for $\alpha = 1{\cdot}3$ ($\kappa R^{1/4} = 0{\cdot}102$). This value of α was chosen to give the best agreement with experiment. The jet Reynolds number of the experiment was 3500. This corresponds to $\kappa = 0{\cdot}013$. This figure differs slightly from the value quoted by Glauert, $\kappa = 0{\cdot}012$, which was based on a preliminary experiment at $R = 5000$. The deviation between the experimental velocity profile and Glauert's solution is negligible except at the outer edge. However, this is analogous to the case of a free jet where the assumption of constant eddy viscosity leads to too large velocities in this region. The experimental points closest to the wall are certainly in error, and should be discounted.

Corresponding to $\alpha = 1{\cdot}3$, the predictions given by Glauert's table 1 are that $U_m \propto x^{-1{\cdot}14}$ and $\delta \propto x^{1{\cdot}02}$, whereas the present experiments give for these similarity exponents, $-1{\cdot}12 \pm 0{\cdot}03$ for U_m and $0{\cdot}94 \pm 0{\cdot}02$ for δ. The agreement in the case of U_m is reasonable. For δ on the other hand, Glauert gives values greater than unity for all values of α.

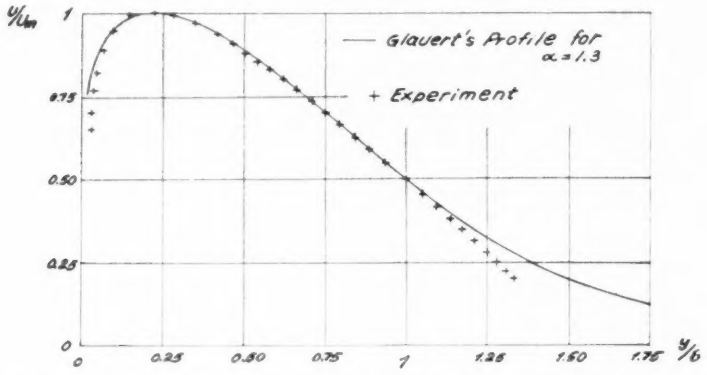

Figure 5. Comparison of M. B. Glauert's theoretical velocity profile and experiment.

In the present experiment the Reynolds number varies as $x^{-0{\cdot}18}$. By Glauert's theory this would increase the value of y/δ at the velocity maximum by 0·003 for x varying from 143 to 303 mm. Considering the experimental accuracy, one could not expect to detect such a small change of velocity profile.

The author is indebted to Mr M. B. Glauert, Mr H. K. Zienkiewicz and Professor P. R. Owen, for several discussions and suggestions. During the work the author was supported by a British Council Scholarship and a Research Fellowship from the Technical University of Denmark.

Reference

Glauert, M. B. 1956 *J. Fluid Mech.* **1**, 625.

Turbulent convection over a heated horizontal surface

By D. B. THOMAS and A. A. TOWNSEND
Cavendish Laboratory, Cambridge

(*Received* 11 *March* 1957)

SUMMARY

Detailed measurements have been made of the temperature field in natural convection above a heated horizontal surface in air, with and without a cold upper boundary. The object was to provide experimental material for the testing of existing theories of convection and the development of new ones. Using a variety of experimental techniques, it was possible to measure the heat transfer, the mean temperature profiles, mean squares of the temperature fluctuations and the autocorrelation functions of the temperature fluctuations. These results are considered in relation with the 'similarity' theory of Priestley and the 'neutral stability' theory of Malkus. Both these theories lead to the conclusion that, for convection between parallel planes at high Rayleigh numbers, nearly the whole of the mean temperature variation occurs in comparatively thin surface layers whose mutual interaction is small. The present experiments confirm this in some detail, but the exact form of the variation of mean temperature cannot be completely reconciled with either of the theories.

1. INTRODUCTION

The motion set up in a fluid which is enclosed by two plane horizontal boundaries and heated from below forms a very suitable subject for both theoretical and experimental study of heat convection, the boundary conditions being homogeneous in the horizontal directions. As the difference of temperature between the surfaces increases from zero, an ordered, cellular motion usually appears at a Rayleigh number about the predicted value of 1708, but this regular motion disappears and is replaced by a random 'turbulent' motion at some Rayleigh number around 50,000 (Jakob 1949; de Graaf & van der Held 1953). More recent work by Malkus (1954 a) has shown that there may be as many as five transitions between one flow regime and another before fully turbulent convection is established for Rayleigh numbers exceeding one million.

Apart from some observations of the motion of suspended particles (Malkus 1954 a), there have been few attempts to study any other aspects of the problem than the dependence of heat transfer coefficient on Rayleigh number, and the experimental work to be described was undertaken in the hope of providing more detailed information about conditions within the

fluid. Working with air, it has been possible to measure mean temperatures and temperature fluctuations at points between the surfaces and so to make a more stringent test of the several theoretical predictions than would be possible with heat transfer measurements alone. Similar measurements have been made in the convection field above a single heated plate. This last arrangement is an approximation to the convection over an infinite horizontal surface and may be compared with the predictions of the similarity theory (Priestley 1954). It may also resemble the convection near the lower of two parallel planes at very high Rayleigh numbers.

2. The equations of motion and of heat

Let us consider the convection in a perfect gas in the space above a rigid horizontal surface whose temperature is everywhere T_1, measured in the absolute gas scale. The coordinate system is chosen so that the origin is in the plane of the surface and Oz is vertically upwards. Sometimes the fluid is bounded above by a similar horizontal surface in the plane $z = D$, and with temperature T_2. If there is no such upper boundary, the temperature at a great distance from the surface is T_a. Then

u, v, w	are the velocity components parallel to Ox, Oy, Oz, $q^2 = u^2 + v^2 + w^2$,
P, p	are the mean pressure and the fluctuation about the mean,
T, θ	are the mean temperature and the fluctuation about the mean,
γ	is the ratio of the specific heats,
ν	is the kinematic viscosity,
κ	is the thermometric conductivity,
H	is the constant upward flux of total heat,
$Q = H/(\rho c_p T) = (\gamma - 1)H/\gamma P$	is a 'kinematic' measure of the heat flux,
$A = gD^3 \log(T_1/T_2)/\nu\kappa$	is the Rayleigh number (this definition is consistent with use of the logarithm of the absolute temperature and, for numerical purposes, is nearly identical with the ordinary definition).

For motions on the laboratory scale, and with fluid velocities small compared with the velocity of sound, the constant flux of total heat is given by

$$H = -\rho c_p \kappa \frac{\partial T}{\partial z} + \rho c_p \overline{\theta w}, \tag{2.1}$$

where the single bar denotes the mean value with respect to time. This may be written as

$$Q = -\frac{\kappa}{T}\frac{\partial T}{\partial z} + \frac{\overline{\theta w}}{T}, \tag{2.2}$$

where Q is also a constant.

To the customary approximation, the equation for the turbulent energy per unit mass is

$$\frac{\partial}{\partial z}\left(\frac{1}{2}\overline{q^2 w} + \frac{1}{\rho}\overline{pw}\right) = g\frac{\overline{\theta w}}{T} - \epsilon \tag{2.3}$$

where ϵ is the rate of dissipation of energy by viscous stresses. The terms on the left represent transport of energy from one part of the flow to another, the terms on the right represent generation of energy by buoyancy forces and the viscous dissipation.

Another mean value equation of some interest is the equation for the entropy associated with the temperature fluctuations, which is $-\frac{1}{2}c_p\overline{\theta^2}/T^2$. To this approximation it is

$$c_p\frac{\overline{\theta w}}{T}\frac{1}{T}\frac{\partial T}{\partial z} + c_p\frac{\partial}{\partial z}\left(\frac{\overline{\theta^2 w}}{2T^2}\right) = \kappa c_p\frac{\overline{\theta\nabla^2\theta}}{T^2}, \tag{2.4}$$

showing that entropy (or temperature fluctuations) is produced at a rate proportional to the mean temperature gradient.

It may be noticed that all three mean value equations (2.2 to 2.4) involve temperature variations only as fractions of the local mean temperature, which suggests that they would be more naturally expressed in terms of the logarithm of the temperature rather than the temperature. The distinction is of no importance if the total temperature variation is negligible compared with the absolute temperature, but this is far from true in most of the experiments to be described. In the following analysis of the experimental results, the logarithm of the temperature has been used consistently with a considerable improvement in the correlation with theoretical predictions.

3. Theories of the convection

A first step in the study of any problem of fluid motion is to use dimensional analysis to obtain the forms of the functional relations between the observables. For any convection between parallel, horizontal surfaces, the boundary conditions are geometrically similar and may be specified by the separation of the surfaces and the difference of the logarithms of the temperatures. If the equations of motion, heat, and conservation of mass, are put into non-dimensional form by use of scales of length, temperature and velocity derived from D, $\log(T_1/T_2)$ and the quantities g, ν, κ, it is immediately evident that the convection depends only on the Rayleigh number and the Prandtl number, ν/κ. For example, the heat transfer coefficient is

$$\frac{QD}{\kappa\log(T_1/T_2)} = F(A, \nu/\kappa), \tag{3.1}$$

and the distribution of mean temperature is

$$\log(T/T_1) = f\left(\frac{z}{D}, A, \frac{\nu}{\kappa}\right). \tag{3.2}$$

For very large separations of the surfaces (high Rayleigh numbers), it seems possible that the convection close to each surface may be nearly

independent of the presence of the other surface and so of D. The basic equations may still be made non-dimensional, and conveniently so by using the following scales of length, velocity and (logarithmic) temperature,

$$z_0 = \left(\frac{\kappa^3}{Qg}\right)^{1/4}, \qquad u_0 = (Qg\kappa)^{1/4}, \qquad \theta_0 = \left(\frac{Q^3}{\kappa g}\right)^{1/4},$$

and their solution depends only on the Prandtl number. It follows that

$$\log \frac{T_1}{T_a} = C\theta_0 = C\left(\frac{Q^3}{\kappa g}\right)^{1/4}, \tag{3.3}$$

that

$$\log \frac{T}{T_1} = \theta_0 f\left(\frac{z}{z_0}, \frac{\nu}{\kappa}\right), \tag{3.4}$$

and that

$$\frac{\overline{\theta^2}}{T^2} = \theta_0^2 g\left(\frac{z}{z_0}, \frac{\nu}{\kappa}\right), \tag{3.5}$$

where C is a function of Prandtl number, and T_a is the asymptotic temperature far from the lower surface but not so far as to be within the range of influence of the upper surface. If this temperature exists, equation (3.3) defines the variation of heat transfer coefficient with Rayleigh number as

$$\frac{QD}{\kappa \log(T_1/T_2)} = (2C)^{-1/3}\left(\frac{\nu}{\kappa}\right)^{1/3} A^{1/3} \tag{3.6}$$

for Rayleigh numbers so high that the temperature gradient is negligible except close to the surfaces. The proportionality between heat transfer coefficient and cube root of Rayleigh number is well confirmed by experiment for Rayleigh numbers above 10^6 (e.g. Malkus 1954 a), and this provides strong support for the concept of surface convection layers within which most of the temperature variation occurs.

The concept of a surface layer with a structure determined by the heat flux through it is very similar to the concept of a constant stress layer in turbulent flow near a wall, and this suggests that there may be a part of the surface layer within which the direct effects of conductivity and viscosity are negligible. If there is such a region, within it we have

$$\log \frac{T}{T_a} = B_t Q^{2/3} g^{-1/3} z^{-1/3} \tag{3.7}$$

and

$$\frac{\overline{\theta^2}}{T^2} = B_0 Q^{1/3} g^{-2/3} z^{-2/3}, \tag{3.8}$$

where the constants may depend on Prandtl number. The prediction (3.7) is supported by measurements of heat transfer in the lower atmosphere (Priestley 1954).

The only complete theory of the convection between parallel planes is that proposed by Malkus (1954 b) and suggested to him by his observations of successive transitions between the initial cellular convective flow and the final state of completely disordered turbulent motion. Malkus suggests that the flow adjusts itself to transfer the maximum amount of heat

compatible with the boundary conditions and subject to the additional restrictions,

(*a*) that the heat flux is everywhere down the gradient of mean temperature,

(*b*) that the variations of temperature and vertical velocity may be represented by Fourier series which terminate after a finite number of terms. (The number of terms in the two Fourier series is determined by requiring that the distribution of mean temperature, which is defined by these conditions, should be neutrally stable with respect to perturbations of the smallest wavelength occurring in the Fourier series.)

Unlike most current theories of turbulent motion, this theory is based on generalizations more like to those of thermodynamics than those of fluid mechanics, but it has the considerable virtue of making definite numerical predictions. For our purpose the most relevant are (i) that, not too close to the bounding surfaces,

$$\frac{1}{T}\frac{dT}{dz} = -\frac{1}{2}\frac{\kappa}{QD^2}\left(\frac{\log T_1/T_2}{\sin \pi z/D}\right)^2 \tag{3.9}$$

or, more usefully,

$$\log T/T_a = -\frac{\kappa}{2\pi QD}\left(\log\frac{T_1}{T_2}\right)^2 \cot\frac{\pi z}{D} \tag{3.10}$$

where $T_a^2 = T_1 T_2$, and (ii) that the mean square of the temperature fluctuations, averaged over the whole space, is

$$\frac{\overline{\overline{\theta^2}}}{T^2} = \frac{2}{3\pi^2}\left(\log\frac{T_1}{T_2}\right)^3 \frac{\kappa}{QD}\log\frac{QD}{\kappa}, \tag{3.11}$$

where the double bar signifies a double average, first over time at a point and then over all values of z in the field. It should be remarked that the Malkus theory is consistent with the assumption of independent surface layers at high Rayleigh numbers but not with the additional assumption that the direct effects of viscosity and conductivity are negligible. By using published measurements of the heat transfer coefficient, which may be represented by equation (6.2), equation (3.10) may be written as

$$\log\frac{T}{T_a} = \frac{(2000\nu/\kappa)^{1/2}}{2\pi^2}\theta_0\left(\frac{z}{z_0}\right)^{-1}, \tag{3.12}$$

valid for values of z/z_0 within the surface layer which are not too small. This is of the same functional form as equation (3.4).

4. Experimental arrangements

The source of heat in these experiments was an electrically heated rectangular duraluminium plate of dimensions 30 cm × 40 cm × 1 cm. In order to secure a uniform distribution of surface temperature and to allow direct measurements of heat transfer, this plate formed the upper side of a duraluminium-asbestos-duraluminium sandwich (figure 1), the lower plate being heated by a grid of resistance wire wound on an asbestos former

and placed against its lower side. Four copper-constantan thermocouples were inserted in each duraluminium plate, and from the mean temperature difference and the measured thermal conductivity of the asbestos thermal resistance the total heat loss from the top plate could be calculated. From this was subtracted the heat loss by radiation and by conduction along the pillars supporting the upper surface. The radiation correction was computed using the emissivity 0·24 appropriate to polished aluminium, and was found to form about 30% of the total heat loss. In the parallel plate experiments, the upper boundary was a similar aluminium plate forming part of a water jacket. The temperature of this plate could also be measured by thermocouples set in it. Both plates were ground flat after assembly and were kept at known distances apart by glass pillars ground to size. Vertical walls of rubber or asbestos were always fitted to prevent entry of air from the edges of the space. For the measurements over a single heated surface, vertical side walls, 60 cm high, were provided for the same purpose.

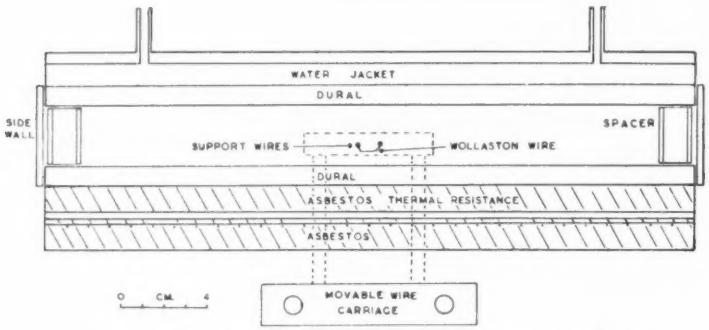

Figure 1. Experimental arrangement : diagrammatic section.

Temperature measurements in the air space were made using resistance thermometers of Wollaston wire, 0·00025 cm in diameter of measured temperature coefficient 0·00353 deg^{-1}, along which were passed measuring currents of about one milliampere. The length of the sensitive, etched portion of the wires was usually about 3 mm, giving a resistance of about 30 ohms. The response time of such a wire is of order one millisecond. The wires were soldered between two 30 s.w.g. copper wires stretched horizontally between supports on a movable carriage spanning the whole apparatus. This carriage could be moved either vertically or horizontally by micrometer screws.

The resistance of the Wollaston wires was measured with a Wheatstone bridge supplied with alternating current of 1000 c.p.s. The out-of-balance signal of the bridge was amplified and supplied to a phase-sensitive detector. The current output from such a detector is a linear function of the wire resistance and, passed through a reflecting galvanometer of period about one second, gave deflections of a light beam that could be recorded by a drum camera (see figure 2, plate 1 and figure 9, plate 2 for some sample records).

The whole system was calibrated by substituting known resistances for the thermometer element. From these records, the mean temperature was determined using a planimeter to measure the area under the trace, and the variance by measuring the deviation at intervals along the record. The duration of each record was about eight minutes.

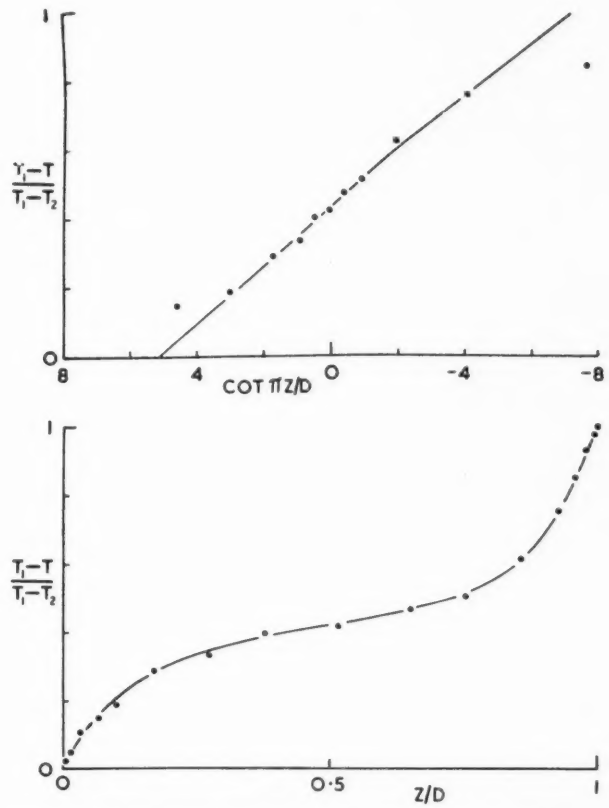

Figure 3. Distribution of mean temperature between parallel plates ($D = 2{\cdot}92$ cm, $T_1 = 52{\cdot}4^\circ$ C, $T_2 = 12{\cdot}3^\circ$ C, $A = 0{\cdot}85 \times 10^5$).

In general, the supports of the wire were not at the same height as the wire itself and so were not at the same temperature. An appreciable amount of heat may be conducted along the supports and lead to a systematic error in mean temperature. A correction for this was calculated and applied to the measured values.

Some measurements of the autocorrelation function of the temperature fluctuations were also made. For this, the rectified and smoothed output from the Wheatstone bridge was used to modulate the frequency of an

oscillator, and the oscillations recorded on magnetic tape. This record could be played back and the autocorrelation function determined by comparing frequencies at points on the tape separated by a known fixed distance, that is, the frequencies recorded at moments separated in time by the time necessary for the tape to travel the fixed distance. The actual comparison consists of the observation of the rate of coincidences between standard duration pulses constructed from each set of played-back oscillations, the rate being proportional to the product of the instantaneous pulse frequencies (Thomas 1956).

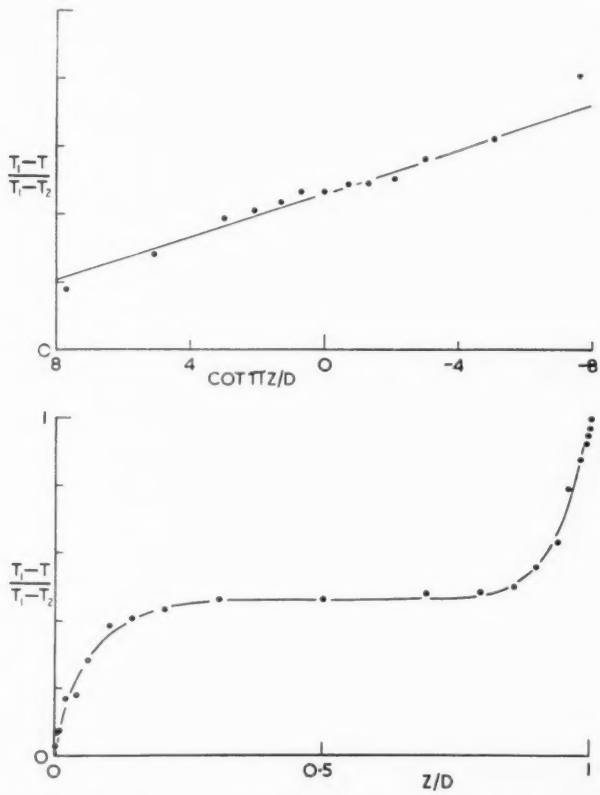

Figure 4. Distribution of mean temperature between parallel plates ($D = 4{\cdot}88$ cm, $T_1 = 46{\cdot}8^\circ$ C, $T_2 = 10{\cdot}6^\circ$ C, $A = 3{\cdot}77 \times 10^5$).

5. The convection between parallel horizontal planes

Three sets of measurements were made with very nearly the same temperature difference between the plates and three different spacings. Table 1 summarizes the experimental conditions and the measured heat

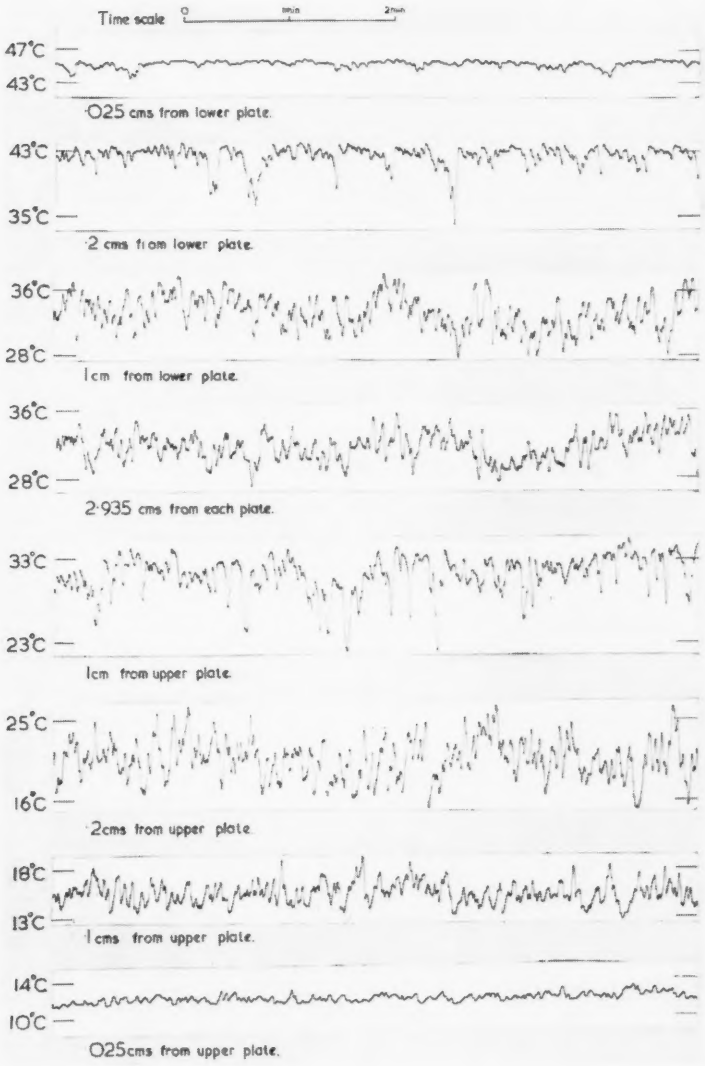

Figure 2. Temperature fluctuation records between parallel horizontal plates ($D = 5{\cdot}87$ cm, $T_1 = 46{\cdot}5°$ C, $T_2 = 9{\cdot}7°$ C).

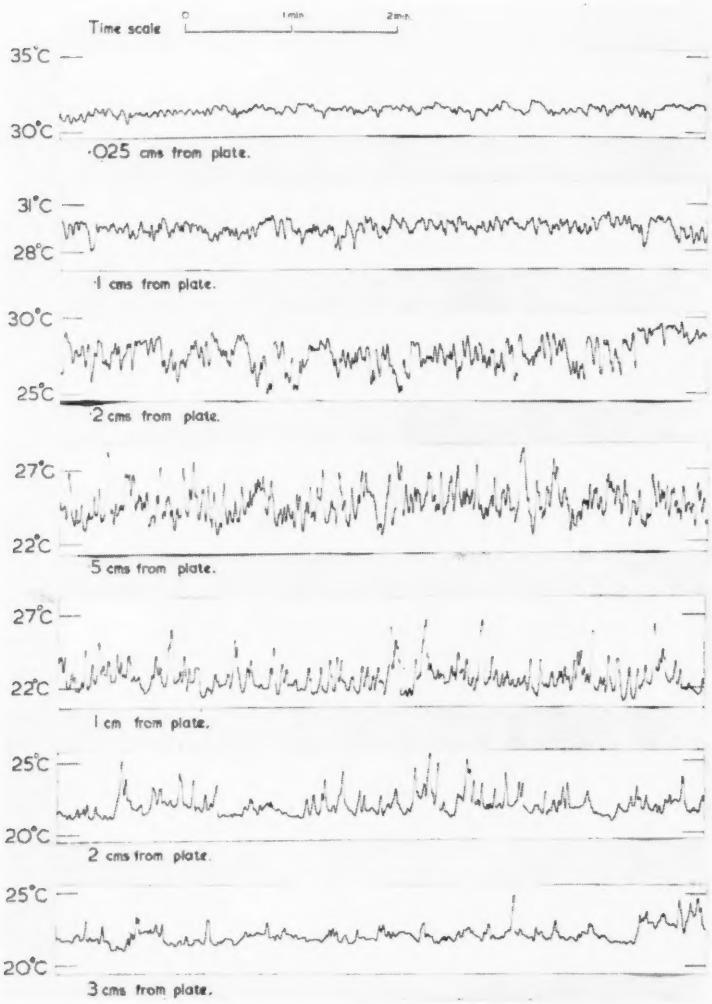

Figure 9. Temperature fluctuation records over a heated horizontal plate ($T_1 = 31{\cdot}6^\circ$ C, $T_R = 21{\cdot}6^\circ$ C).

fluxes. It will be noticed that the measured coefficients of heat transfer are rather less than those found by Malkus (1954 a) who used water and acetone, but that the difference seems to decrease with increasing Rayleigh number.

The measurements of mean temperature are shown in figures 3 to 5. It will be noticed that the profile at the highest Rayleigh number is markedly asymmetrical and even contains a section with reversed temperature gradient.

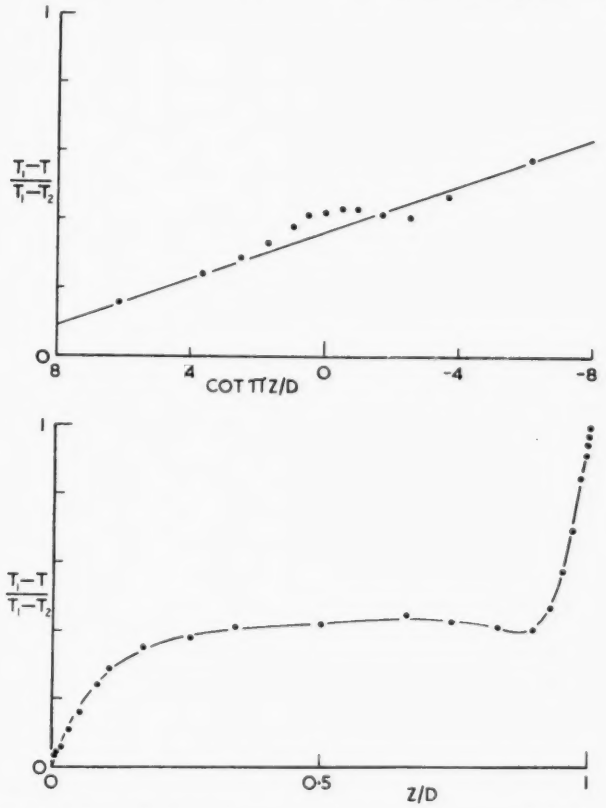

Figure 5. Distribution of mean temperature between parallel plates ($D = 5{\cdot}87$ cm, $T_1 = 46{\cdot}5°$ C, $T_2 = 9{\cdot}7°$ C, $A = 6{\cdot}75 \times 10^5$).

It is believed that this is due to the onset of a circulatory motion of dimensions similar to those of the whole apparatus, with air rising from the centre of the lower plate where the measurements were taken. This motion would cause a finite mean shearing stress at the boundaries and logarithmic distributions of mean velocity and temperature may be expected. If the mean temperature is plotted against the logarithms of the distances from the upper and lower surfaces (figure 6), substantial regions of logarithmic variation are found.

Measured quantities				Derived quantities							Malkus (1954 a)
D	T_1	T_2	$H \times 10^{-4}$	$(T_1\,T_2)^{1/2}$	$\log T_1/T_2$	ν	κ	$A \times 10^{-5}$	$Q \times 10^2$	$\frac{QD}{\kappa \log (T_1/T_2)}$	$\frac{QD}{\kappa \log (T_1/T_2)}$
2·92	52·4° C = 325·6° K	12·3° C = 285·5° K	8·5, 11·2, 8·3	304·9° K	0·132	0·164	0·230	0·85	2·65	2·58	3·6
4·88	46·8° C = 320·0° K	10·6° C = 283·8° K	10·2, 9·3, 9·2	301·4° K	0·121	0·161	0·226	3·77	2·73	4·91	5·3
5·87	46·5° C = 319·7° K	9·7° C = 282·9° K	10·5, 14·0, 5·6	300·7° K	0·123	0·160	0·225	6·75	2·90	6·11	6·1

Table 1. Heat transfer measurements (c.g.s units). The values of ν and κ at temperature $(T_1\,T_2)^{1/2}$ are taken from Montgomery (1947). The first column of heat transfers is obtained from the total heat loss by subtracting the computed losses by radiation and by conduction along the spacing pieces. The second column gives the two values of the transfer computed from the temperature gradients at the upper and lower surfaces respectively. The value used for the derived quantities is the mean of these three values.

If the other two profiles are plotted in like manner, there is no sign of a linear section on the curves. The onset of this circulation at a Rayleigh number around $5 \cdot 10^5$ is probably due to the side walls forcing the large eddies of the convection to remain relatively fixed in position. It is probable that,

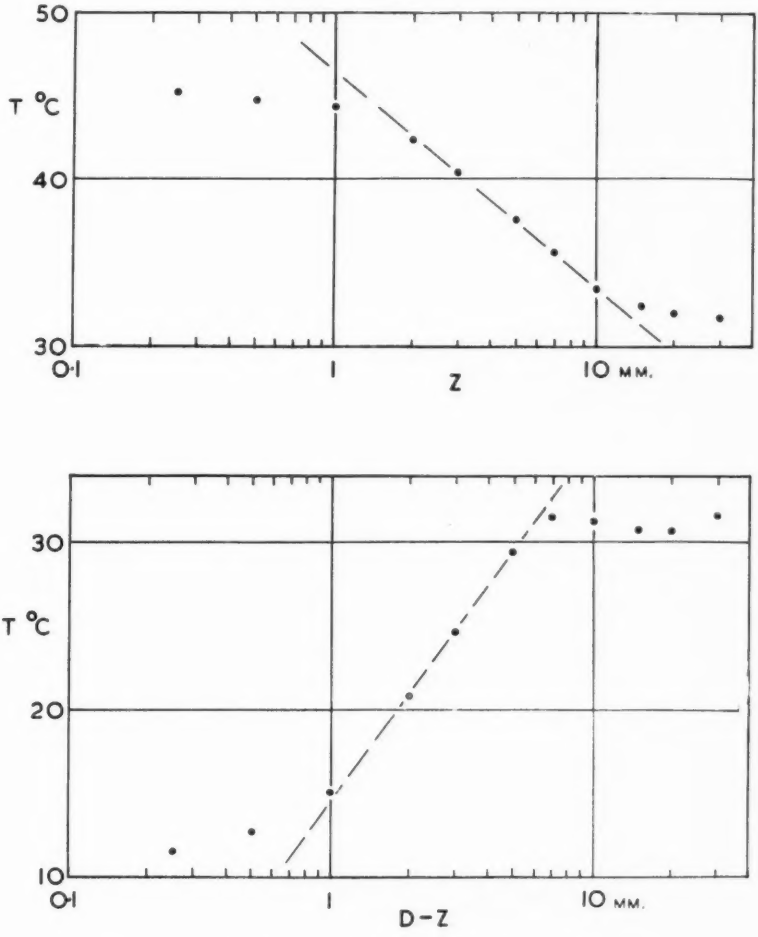

Figure 6. Logarithmic temperature profiles ($A = 6 \cdot 75 \times 10^5$).

for greater ratios of plate width to separation, these eddies could wander freely and then measurements at a fixed point would be identical with spatial means—which clearly they are not, for this particular profile.

For comparison with the Malkus theory, the three profiles have been plotted against $\cot(\pi z/D)$ and straight lines fitted to the central portion

(figure 3 to 5). At the lower Rayleigh number there is a substantial linear region but the slope is less than the predicted value. The slope of the second profile agrees more closely with the prediction, but substantial departures from linearity exist. As shown by this method of plotting, these departures are similar in kind to the gross distortion in the third profile and may be caused by a weak circulation of large scale.

Rayleigh Number	$\frac{2\pi QD}{\kappa \log(T_1/T_2)}$	(Measured slope)$^{-1}$
$0{\cdot}85 \times 10^5$	16·1	12·4
3·77	30·9	35
6·75	38·5	30

Table 2. Comparison of equation (3·10) with experiment.

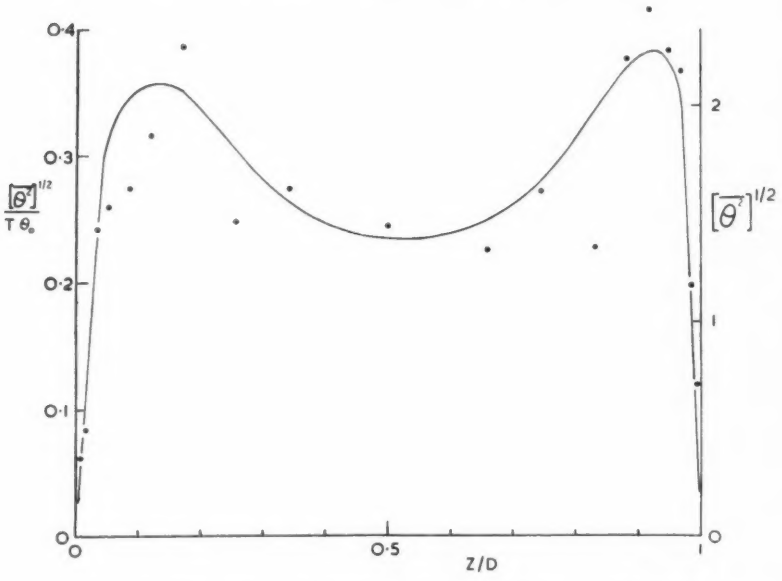

Figure 7. Temperature fluctuation intensities between parallel plates ($A = 6{\cdot}75 \times 10^5$).

Measurements of the root-mean-squares of the temperature fluctuations for the highest Rayleigh number are shown in figure 7. The average level is 1·9° C, compared with the value of 4·9° C given by equation (3.11). This discrepancy is probably too large to be explained by the finite time of response of the recording equipment. As would be expected from the shape of the mean temperature profile, the intensity of the temperature fluctuations reaches a peak just outside the conduction layer.

Figure 8 shows the autocorrelation function of the temperature fluctuations, defined as

$$R(\tau) = \overline{\theta(t)\theta(t+\tau)}/\overline{\theta^2} \tag{5.1}$$

at three values of z. It will be noticed that the time scale of the fluctuations decreases sharply as the lower surface is approached.

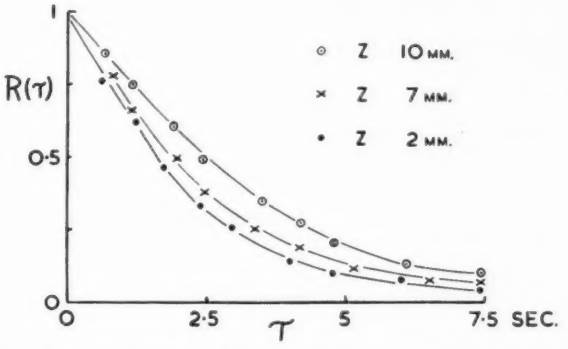

Figure 8. Autocorrelation functions of the temperature fluctuations ($D = 5{\cdot}87$ cm, $T_1 - T_2 = 38{\cdot}8°$ C).

6. The convection over a single horizontal plane

Before discussing these measurements, it is necessary to consider the relation of the experimental arrangement—a horizontal heated plane forming the bottom of an open box of roughly cubical form—to the infinite heated plane considered in the theory. Unless there is appreciable large-scale circulation, and subsidiary experiments showed that there were not, the conditions near the surface will approximate to those near an infinite plane if the distance from the surface is small compared with distance from the walls and distance from the top of the box. With the single exception of the autocorrelation measurements, no measurements were made more than three centimetres from the surface and the condition is satisfied.

Measured quantities					Derived quantities			
T_1	T_R	$H\times10^{-4}$	$H\times10^{-4}$	T_a	$\log T_1/T_a$	$Q\times10^2$	$\theta_0\times10^2$	z_0
31·6° C	21·6° C	0·535	0·503	21·6° C	0·0434	1·48	1·12	0·158
52·1° C	23·6° C	1·71	1·79	24·4° C	0·0917	4·99	2·80	0·116
72·1° C	22·1° C	3·38	3·09	28·5° C	0·1565	9·20	4·44	0·100

Table 3. Convection over a horizontal plane (c.g.s. units).

The boundary conditions of the theoretical flow are defined by the temperature of the plane and the temperature at infinity, the 'ambient temperature', which corresponds with the temperature at the base of the

convection plume that rises from the top of the box and carries away the heat convected from the plane. Unfortunately, measurements of this base temperature, which may differ from room temperature by as much as 8° C, were not made at the time of the experiments, and it is necessary to estimate it by extrapolation of the measured temperature profiles. In figure 10, the three measured temperature profiles are plotted non-dimensionally as $\theta_0^{-1}\log(T/T_R)$ *vs* z/z_0, using the room temperature as reference temperature. It is clear that vertical displacement of the curves, corresponding to changes in the effective ambient temperature, will bring

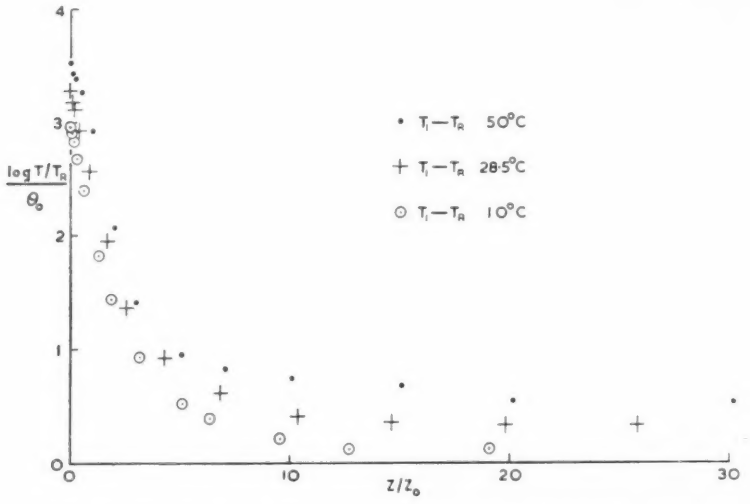

Figure 10. Distribution of mean temperature over a heated horizontal plate (similarity plot referred to room temperature).

them into near coincidence. The results plotted in figure 11 have been adjusted in this way, using the smallest possible positive differences of ambient temperature from room temperature, that is, zero for the first profile for which $T_1 - T_R = 10{\cdot}0$° C. The necessary adjustment increases rapidly with plate temperature, probably because air currents in the room are more effective in ventilating the top of the box when the convection plume is weak.

The universal non-dimensional profile so obtained may be represented within experimental error by

$$\theta_0^{-1}\log(T/T_a) = 3{\cdot}0(z/z_0)^{-1} \tag{6.1}$$

for all values of z/z_0 greater than two (see figures 11 and 12). It is not possible to represent the profile by a $z^{-1/3}$-law over a substantial range of z/z_0 without assuming ambient temperatures much less than room temperature and an upper limit to its validity at $z/z_0 = 12$. This upper

limit would imply that the influence of the distant boundaries becomes dominant at only 1 cm from the plate, which seems highly unlikely, and that the effective ambient temperature is less than room temperature, which is equally unlikely.

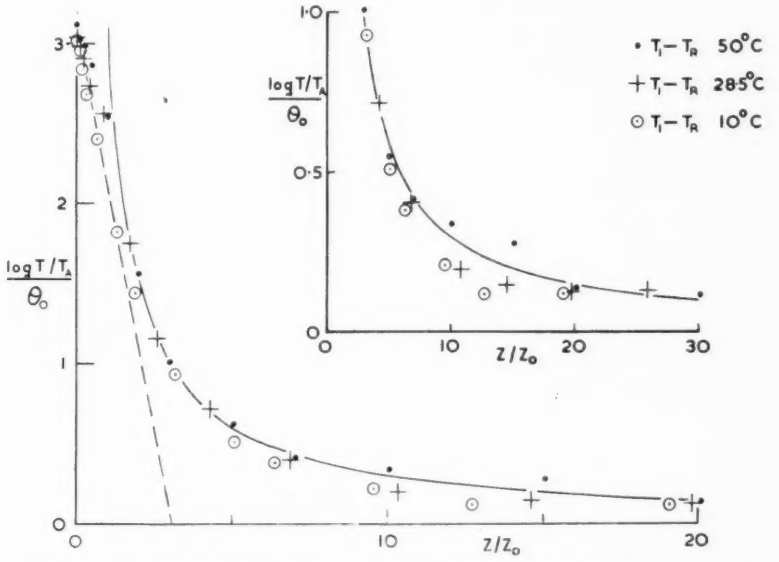

Figure 11. Distribution of mean temperature over a heated horizontal plate (similarity plot referred to a selected ambient temperature). The full line follows equation (6.1).

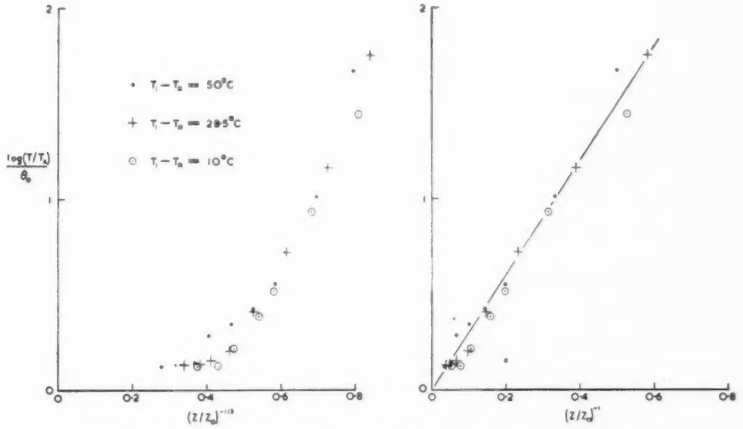

Figure 12. Mean temperatures plotted against $(z/z)^{-1}$ and $(z/z)^{-1/3}$ for $z/z_0 > 2$.

Direct measurements of heat transfer are shown by plotting first $\theta_0^{-1}\log(T_1/T_R)$ and $\theta_0^{-1}\log(T_1/T_a)$ against $\log(T_1/T_R)$ (figure 13). In the second graph, appropriate values of $T_a - T_R$ have been obtained by interpolating between the values used in figure 11. If the convection is really independent of the side walls and the distant boundaries, $\theta_0^{-1}\log(T_1/T_a)$ should be independent of temperature difference, as is implied by equation (3.3). With these values for the ambient temperature, these measurements indicate that

$$\log\frac{T_1}{T_a} = 3{\cdot}4\theta_0 = 3{\cdot}4\left(\frac{Q^3}{\kappa g}\right)^{1/4}, \tag{6.2}$$

nearly independent of temperature difference. The coefficient 3·4 may be compared with the value 3·1 obtained from the temperature profiles.

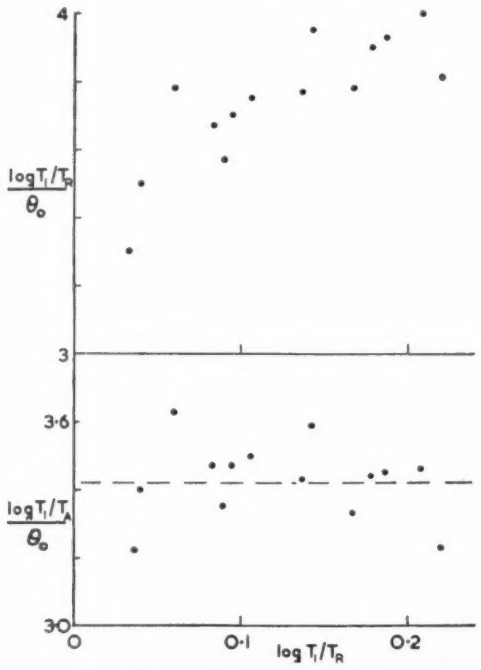

Figure 13. Measurements of heat transfer from a heated horizontal plate (plotted non-dimensionally).

It is also interesting to compare these values of heat transfer with measurements between parallel planes at large Rayleigh numbers. The measurements of Malkus (1954 a) and others are closely represented by

$$\frac{HD}{k(T_1 - T_2)} = \left(\frac{\lambda}{2000}\right)^{1/3}. \tag{6.3}$$

If the heat transfer at each surface were little affected by the presence of the other surface, we would expect the ratio

$$\frac{\log (T_1/T_a)}{(Q^3/\kappa g)^{1/4}}$$

to be a constant and the temperature midway between the surfaces to be the geometric mean of the surface temperatures. From equation (6.3) and inserting the value of the Prandtl number ν/κ for air, we find

$$\log \frac{T_a}{T_1} = 3{\cdot}12 \left(\frac{Q^3}{\kappa g}\right)^{1/4} \tag{6.4}$$

($T_a = (T_1 T_2)^{1/2}$), in good agreement with the previous values*. Even the measurements of heat transfer of the previous section give values of 4·0, 3·7 and 3·6 at Rayleigh numbers of $0{\cdot}85 \times 10^5$, $3{\cdot}77 \times 10^5$ and $6{\cdot}75 \times 10^5$, although these are too low for independence of the two surface layers.

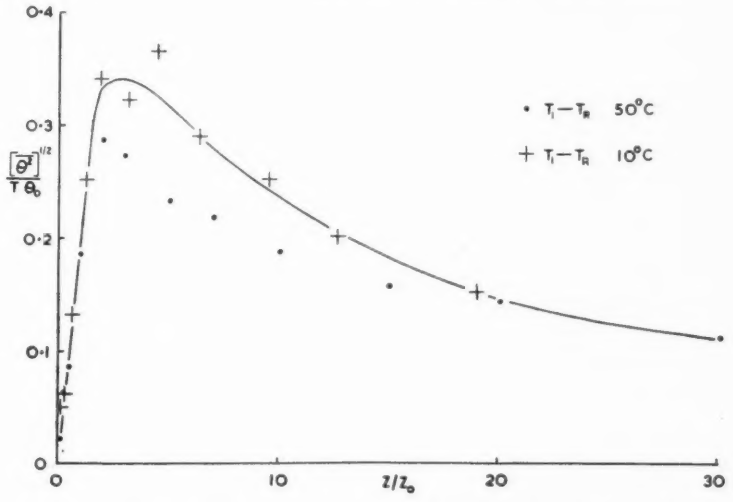

Figure 14. Temperature fluctuation intensities over a heated horizontal plate.

Measurements of root-mean-square temperature fluctuation, plotted non-dimensionally as $[\overline{\theta^2}]^{1/2}/[T(Q^3/\kappa g)^{1/4}]$ against $(gQ/\kappa^3)^{1/4}z$, are shown in figure 13. The measurements for the two heat transfers only agree at the larger values of $(gQ/\kappa^3)^{1/4}z$. It is very probable that the response time of the galvanometer prevented the complete recording of the rapid fluctuations occurring near the surface. The single measurement of the autocorrelation function (figure 14) shows that a substantial part of the intensity resides in

* These non-dimensional equations refer to air with $\nu/\kappa = 0{\cdot}77$. Accepting equation (6.3) as correct, the general form of equation (6.4) is

$$\log \frac{T_1}{T_a} = 3{\cdot}34 \left(\frac{Q^3}{\kappa g}\right)^{1/4} \left(\frac{\nu}{\kappa}\right)^{1/4}.$$

Fourier components of periods less than the period of the galvanometer, one second. It may be mentioned that more recent work using equipment with faster response has registered temperature fluctuations of much greater amplitude.

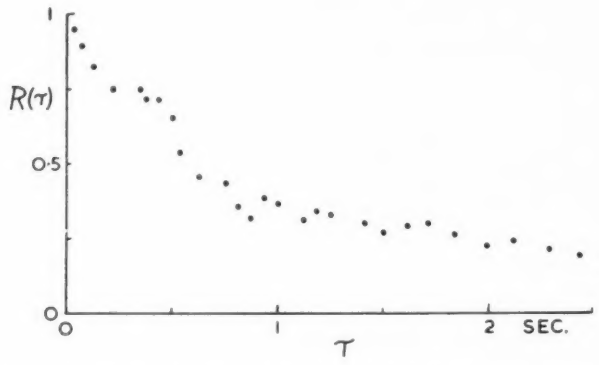

Figure 15. Autocorrelation function of the temperature fluctuations over a horizontal plate ($T_1 - T_R = 70{\cdot}9^\circ$ C, $z = 4$ cm).

7. Discussion of results

The most interesting feature of these measurements is the close correlation between heat transfer from a single surface and heat transfer between parallel planes. Even though the Rayleigh numbers of the parallel plane experiments were comparatively small, they tend to confirm the experimental finding of Malkus that, at high Rayleigh numbers, the heat transfer coefficient is nearly proportional to the cube root of the Rayleigh number and so is independent of the separation of the surfaces. This must mean that the conditions near each surface dictate the heat transfer and that the central region is a region of negligible temperature gradient, easily capable of transmitting the imposed heat flux. Nearly all the temperature drop occurs in the wall layers which have a temperature distribution determined by the heat transfer, the conductivity (and viscosity) and the gravitational field. Additional confirmation of this view is found in the observation of Malkus (1954 a) that the heat transfer between parallel planes is practically unaffected by the presence of vertical partitions even though they restrict greatly the motion of the central region.

Although both the existing theories of convection conform to this general pattern, neither is capable of describing accurately the measured profiles. The similarity theory (Priestley 1954) requires that $\log(T/T_a)$ should be proportional to $z^{-1/3}$ for *all* large values of z/z_0, where T_a, the temperature at large distances from the surface, is certainly not less than room temperature. It is impossible to fit any substantial part of the observations by such a power law without using a value of T_a less than room temperature.

The very interesting theory of Malkus (1954 b) is more successful in as much as its prediction that

$$\log \frac{T}{T_a} = C\theta_0 \frac{z_0}{z} \tag{7.1}$$

fits the observations well if $C = 3{\cdot}0$. However, consistency of the heat transfer measurements and the theory requires that $C = 2{\cdot}0$ (see equation (3.9)).

The failure of the similarity theory to describe the temperature variation within the range of measurement implies that the local temperature gradients and other local characteristics of the convection are affected either by the conductivity (or viscosity) of the fluid or by the convection near the distant boundary. This may appear surprising in view of the considerable success of the similarity treatment of flow in the constant stress region of turbulent wall flow, for which similar assumptions of independence of viscosity and presence of distant boundaries are made. The analogy fails in that the constant stress layer is a layer of substantially uniform turbulent intensity in which no appreciable net transport of turbulent energy is expected, while the surface layer, as described by the similarity theory, would have a turbulent intensity varying as $(Qgz)^{2/3}$ and substantial transport of turbulent energy towards the surface would be expected. Also, the intensity of the temperature fluctuations varies considerably and they will be transported through the surface layer. These considerations (and the present results) suggest that interaction between different parts of the surface layer may be more effective than the similarity theory supposes. It is possible that the conditions assumed may exist for values of z/z_0 beyond the range of measurement, where the difference from ambient temperature is very small compared with the temperature difference across the whole layer. If the meteorological evidence is accepted, it presumably means that these measurements were made in such a region.

The defects in the Malkus theory are difficult to diagnose, partly because the theory is based on general statements not easily related to the more common approach through the equations of motion and heat. The difference between the theoretical and observed distributions of temperature in the surface layer indicates that the convection has not attained the optimum condition specified in the theory. In fact, it seems to have settled down with a heat transport about 70% of the maximum set by the theory. Two possible causes are (*a*) that the requirement that the minimum temperature gradient is zero is insufficiently restrictive, and (*b*) that the Fourier series used to describe the convection does not satisfy all the boundary conditions. In the central region at the higher Rayleigh numbers, there is a systematic tendency to lower gradients, which is a departure in the opposite direction. Some of this may be due to the presence of a large-scale circulation, but measurements of the closely analogous flow between concentric rotating cylinders show an extensive region of constant angular momentum, the quantity analogous to temperature in convection (Taylor 1935). Pai (1943)

finds that the gradient of angular momentum is reversed in two small regions adjacent to each cylinder, and explains this as a result of large-scale circulations which are part of the general flow. It may well be that the large-scale circulation postulated to explain the form of the temperature profile at the largest Rayleigh number is typical of the flow as a whole, except in its position, which is determined by the presence of side walls. For the present, it may be concluded that the Malkus theory is in fair but not good agreement with experiment, which is a remarkable achievement for a theory of turbulence not containing any disposable constants.

The experimental work described above was done in the Cavendish Laboratory by the first author (D. B. T.), who is pleased to acknowledge the sponsorship of the work by the Meteorological Office. The second author has contributed some additional analysis of the results.

References

De Graaf, J. G. A. & van der Held, E. F. M. 1953 *Appl. Sci. Res.* A, **3,** 393.
Jakob, M. 1949 *Heat Transfer,* Vol. 1. New York : Wiley.
Malkus, W. V. R. 1954 a *Proc. Roy. Soc.* A, **225,** 185.
Malkus, W. V. R. 1954 b *Proc. Roy. Soc.* A, **225,** 196.
Montgomery, R. B. 1947 *J. Met.* **4,** 193.
Pai, S. I. 1943 *Nat. Adv. Comm. Aero., Wash., Tech. Note* no. 892.
Priestley, C. H. B. 1954 *Aust. J. Phys.* **7,** 176.
Taylor, G. I. 1935 *Proc. Roy. Soc.* A, **151,** 494.
Thomas, D. B. 1956 Ph.D. Dissertation, University of Cambridge.

Contributions to the theory of the Pitot-tube displacement effect

By M. J. LIGHTHILL

Department of Mathematics, University of Manchester

(*Received* 8 *April* 1957)

SUMMARY

In an earlier paper the uniform shear flow past a sphere was studied, by investigating how vortex lines are deformed by the 'primary flow' (flow in the absence of shear), and deducing the 'secondary' vorticity field (first approximation for small shear). In another paper the image system associated with each element of secondary vorticity was found, whence the Biot–Savart law can be used to determine the secondary flow field by integration. The integration is here carried out for the 'downwash' (secondary flow component perpendicular to the undisturbed flow, down the velocity gradient) on the dividing streamline. Difficulties due to the infinite domain of integration and singularities of the integrand are overcome by selecting variables of integration carefully and using known analytical properties of the secondary vorticity. From the computation of downwash is inferred the first approximation (for small shear A) to the 'displacement' δ (displacement of the dividing streamline, up the velocity gradient, far upstream of the sphere). If U is the upstream flow velocity and a the radius of the sphere, the computed value of $\lim_{A\to 0}(U\delta/Aa^2)$ is 0·9.

Details of the calculation show that the secondary trailing vorticity is not an important contributor to the displacement. The downwash is due almost entirely to vorticity upstream of the sphere (Hall's earlier simplified theory gave good results, e.g., 1·24 instead of 0·9, because it concentrated on the effect of local vorticity in producing downwash); further, this produces displacement principally through its image vorticity.

The relation between theories for a sphere and experimental results on Pitot tubes (beginning with Young & Maas 1936) is discussed. Theoretical evidence on tertiary- and quartary-flow effects is used here in the light of recent work which renders the successive-approximation sequence uniformly valid at infinity. The conclusion is that the theories, taken together, are not inconsistent with the experimental evidence that (i) at values of the 'shear parameter' Aa/U at which the displacement is measurable the ratio δ/a seems to have asymptoted to an approximately constant value, and (ii) displacement is greatly reduced in supersonic flow (Johannesen & Mair 1952) or when 'sharp-lipped' tubes are used (Livesey 1956).

finds that the gradient of angular momentum is reversed in two small regions adjacent to each cylinder, and explains this as a result of large-scale circulations which are part of the general flow. It may well be that the large-scale circulation postulated to explain the form of the temperature profile at the largest Rayleigh number is typical of the flow as a whole, except in its position, which is determined by the presence of side walls. For the present, it may be concluded that the Malkus theory is in fair but not good agreement with experiment, which is a remarkable achievement for a theory of turbulence not containing any disposable constants.

The experimental work described above was done in the Cavendish Laboratory by the first author (D. B. T.), who is pleased to acknowledge the sponsorship of the work by the Meteorological Office. The second author has contributed some additional analysis of the results.

References

De Graaf, J. G. A. & van der Held, E. F. M. 1953 *Appl. Sci. Res.* A, **3**, 393.
Jakob, M. 1949 *Heat Transfer*, Vol. 1. New York : Wiley.
Malkus, W. V. R. 1954 a *Proc. Roy. Soc.* A, **225**, 185.
Malkus, W. V. R. 1954 b *Proc. Roy. Soc.* A, **225**, 196.
Montgomery, R. B. 1947 *J. Met.* **4**, 193.
Pai, S. I. 1943 *Nat. Adv. Comm. Aero., Wash., Tech. Note* no. 892.
Priestley, C. H. B. 1954 *Aust. J. Phys.* **7**, 176.
Taylor, G. I. 1935 *Proc. Roy. Soc.* A, **151**, 494.
Thomas, D. B. 1956 Ph.D. Dissertation, University of Cambridge.

Contributions to the theory of the Pitot-tube displacement effect

By M. J. LIGHTHILL
Department of Mathematics, University of Manchester

(*Received* 8 *April* 1957)

SUMMARY

In an earlier paper the uniform shear flow past a sphere was studied, by investigating how vortex lines are deformed by the 'primary flow' (flow in the absence of shear), and deducing the 'secondary' vorticity field (first approximation for small shear). In another paper the image system associated with each element of secondary vorticity was found, whence the Biot–Savart law can be used to determine the secondary flow field by integration. The integration is here carried out for the 'downwash' (secondary flow component perpendicular to the undisturbed flow, down the velocity gradient) on the dividing streamline. Difficulties due to the infinite domain of integration and singularities of the integrand are overcome by selecting variables of integration carefully and using known analytical properties of the secondary vorticity. From the computation of downwash is inferred the first approximation (for small shear A) to the 'displacement' δ (displacement of the dividing streamline, up the velocity gradient, far upstream of the sphere). If U is the upstream flow velocity and a the radius of the sphere, the computed value of $\lim_{A\to 0}(U\delta/Aa^2)$ is 0·9.

Details of the calculation show that the secondary trailing vorticity is not an important contributor to the displacement. The downwash is due almost entirely to vorticity upstream of the sphere (Hall's earlier simplified theory gave good results, e.g., 1·24 instead of 0·9, because it concentrated on the effect of local vorticity in producing downwash); further, this produces displacement principally through its image vorticity.

The relation between theories for a sphere and experimental results on Pitot tubes (beginning with Young & Maas 1936) is discussed. Theoretical evidence on tertiary- and quartary-flow effects is used here in the light of recent work which renders the successive-approximation sequence uniformly valid at infinity. The conclusion is that the theories, taken together, are not inconsistent with the experimental evidence that (i) at values of the 'shear parameter' Aa/U at which the displacement is measurable the ratio δ/a seems to have asymptoted to an approximately constant value, and (ii) displacement is greatly reduced in supersonic flow (Johannesen & Mair 1952) or when 'sharp-lipped' tubes are used (Livesey 1956).

1. Introduction

In this paper the mechanism of the 'Pitot-tube displacement effect' is analysed by further study of the shear flow past a sphere, following on three earlier papers, "The image system of a vortex element in a rigid sphere" (Lighthill 1956 a, to be referred to hereafter as **I**), "Drift" (Lighthill 1956 b, with corrigenda in Lighthill 1957 a, to be referred to collectively as **D**), and "The displacement effect of a sphere in a two-dimensional shear flow" (Hall 1956, to be referred to as **H**).

When a parallel shear flow, such as a boundary layer or wake, is investigated with a Pitot tube (that is, a tube with the open end pointing upstream and the other end closed by a manometer), it is found that the pressure in the tube is greater than the total pressure on the streamline approaching the centre of the tube orifice; it is equal rather to the total pressure on a streamline displaced in the direction of higher velocities, by an amount δ usually known as the 'displacement of the effective centre' of the Pitot tube. For the tubes whose ratio of internal diameter d_i to external diameter d_e is 0·6, Young & Maas (1936) found that δ/d_e was scattered fairly randomly about 0·18, and Macmillan (1956) obtained an average value 0·15 for δ/d_e.

Two recently observed phenomena enhance the desirability of understanding the displacement effect physically. First, in supersonic flow, Johannesen & Mair (1952) showed that the displacement effect practically vanished in a wake for $M = 1{\cdot}96$. Understanding of this result is made vastly harder by the presence of the 'bow shock wave' in front of the Pitot tube, but in view of the considerable region of subsonic flow between that shock wave and the orifice, it is safe to say that no explanation can reasonably be attempted until the incompressible-flow phenomenon is understood.

Secondly, although Young & Maas (1936) found some indications that δ/d_e increased slightly with increase of d_i/d_e, Livesey (1956) has made experiments which indicate that there is practically no displacement when $d_i = d_e$. This condition was obtained by chamfering the front part of the tube wall to a cone-frustum shape, so that the orifice became sharp-edged. As a check on his experimental technique, Livesey obtained results for $d_i/d_e = 0{\cdot}6$ comparable with those noted above. The contrasted results are difficult to understand without a rather full discussion of the mechanism of the displacement effect.

It might be thought that useful data for such a discussion would be found by a study of the analogous two-dimensional problem, in which a two-dimensional 'Pitot channel', whose external thickness becomes $2c$ downstream of the nose, is placed in a parallel shear flow. However Hall shows (**H**, Appendix) that the displacement of the dividing streamline in this problem is given by

$$\frac{\delta}{c} = \left(\frac{U^2}{A^2c^2} + 1\right)^{1/2} - \frac{U}{Ac},$$

where $U+Ay$ is the velocity distribution in the oncoming stream*. For values of U/Ac occurring in practice, this result is approximately

$$\frac{\delta}{d_c} = \frac{\delta}{2c} = \frac{Ac}{4U} = \frac{Ad_c}{8U},$$

a value well below the experimentally determined values of the displacement for the values $Ad_c/U < \frac{1}{4}$ which are used in practice. Similar results are found for two-dimensional shear flow about cylinders of various shapes (see Mitchell & Murray 1955 as well as references in **H**). Hall shows, however, that a three-dimensional theory, which takes into account the stretching of the vortex lines of the oncoming shear flow as they pass over the body, but still neglects viscous effects, can be used to obtain displacements of the right order of magnitude. There is a simplifying approximation in Hall's work, which will be critically examined below by comparison with a theory which avoids the approximation, but the results of this examination will be found to be favourable.

Before further detailed discussion it may be worth indicating where the subject stands within hydrodynamics as a whole. It falls under the general heading 'secondary flow' which is used to describe what happens when a parallel shear flow is disturbed in a three-dimensional manner (for example by being led round a bend in a pipe or channel; or deflected by a pressure gradient transverse to the streamlines; or subjected to Coriolis force as in meteorology; or confronted with an obstacle as in the present problem). More particularly, it is used to denote the departure of the disturbed flow from a so-called 'primary flow', in which the streamlines are the same as if the original parallel flow had been uniform instead of sheared.

There are two useful ways of looking at secondary flows. In the older approach (see, for example, Goldstein 1938, chap. 2) one considers what unbalanced pressure gradients are implied by the primary flow when account is taken of inertial forces, altered in magnitude because the original parallel flow is not really uniform. The secondary flow is regarded as maintained by such pressure gradients, and limited by viscous resistance. This view of the matter, though always of qualitative value, leads to useful quantitative results only at rather low Reynolds numbers, when the inertial forces may be regarded as a small perturbation of a régime dominated by viscous resistance (Dean 1927, 1928; Cuming 1951).

In flows at high Reynolds numbers it has therefore become usual (Squire & Winter 1951; Hawthorne 1951, 1954; Hawthorne & Martin 1955; Preston 1954) to seek quantitative results by another method, namely study of the vorticity field. The technique used can be interpreted

* In the last sentence of this Appendix, note that "on the body" should read as "at infinity". (To make $\psi = 0$ the dividing streamline, ψ_1 must tend to $-\frac{1}{2}Ac^2$ as the external body surface becomes flat. But a bounded harmonic function must tend to the same limit at infinity in all directions. Hence also upstream $\psi_1 \to -\frac{1}{2}Ac^2$, so that $\psi \sim Uy + \frac{1}{2}Ay^2 - \frac{1}{2}Ac^2$ and the displacement δ of the dividing streamline $\psi = 0$ satisfies (A.9).) Also, in equation (A.8), $\frac{1}{2}A$ should read as $\frac{1}{3}Ay^3$.

geometrically as a study of how vortex elements in the original shear flow are stretched and rotated by the primary flow, yielding a 'secondary vorticity field', whose associated velocity field is the 'secondary flow'. In **D**, a mathematical approach was described which, while essentially equivalent to those of the authors cited, corresponds rather more directly to this geometrical picture.

Such a method is obviously of only approximate validity, partly because it neglects diffusion of vorticity by viscosity or turbulence, and partly because the vortex elements are in reality stretched not by the hypothetical primary flow but by the exact flow. The latter inaccuracy can in principle be reduced by calculating a 'tertiary vorticity field' by considering the stretching and rotation of vortex lines by the combined primary and secondary flows, and deducing a 'tertiary flow' from it, and one can even consider quartary flows, as Hall was able to do (**H**, p. 154) by the use of his simplifying approximation.

The vortex approach to secondary flow has so far had the greatest success with internal flows (through bends in pipes, or cascades), for which the calculation of the velocity field from the vorticity field can be fairly straightforward. With external secondary flows, such as those resulting from parallel shear flow past an obstacle, this calculation is more difficult, and work apart from Hall's (**H**) has been limited to calculations of the secondary vorticity field (Hawthorne 1954; Hawthorne & Martin 1955; and **D**, §2 and §7). The problem of how to deduce the secondary velocity field without making Hall's approximation is considered in some detail in this paper, partly to establish the value of Hall's approximation, partly to improve understanding of the effect, and partly to improve techniques for the mathematical calculation of three-dimensional, fully rotational flows.

The calculations are still confined to the case of a sphere, which can be regarded in many ways as a typical bluff obstacle. The work was consciously prepared for in **D** by the calculation of the secondary vorticity field, and in **I** by the calculation of the image system of a single vortex element in the sphere. This type of image approach, combined with the Biot–Savart law, is found to be more convenient in the present problem than any approach based on images of complete vortex lines.

The relevance of calculations for a sphere to the Pitot-tube problem is supported by the finding that vorticity downstream of the sphere contributes negligibly to the displacement effect. This also kills a plausible hypothesis, namely that secondary trailing vorticity might be largely responsible for the displacement effect, which therefore would be greatly reduced at supersonic speeds for which the trailing vorticity has no upstream influence.

A more correct physical interpretation of the results, as discussed in §4, is that in all cases the image system of the vorticity upstream of the obstacle is the main cause of the displacement. It is shown in §5 how this can be regarded as responsible for the altered situation when either a supersonic main stream or a sharp-lipped orifice is used.

2. Evaluation of the secondary downwash ahead of the sphere

The shear flow past a sphere will here be studied in the notation set out in **D**. Thus, Cartesian axes are used, with origin at the centre of the sphere, such that far upstream the velocity field is

$$v_x = U + Ay, \qquad v_y = v_z = 0, \tag{1}$$

where suffixes denote components. In addition, spherical polar coordinates r, θ, λ such that

$$x = r\cos\theta, \qquad y = r\sin\theta\cos\lambda, \qquad z = r\sin\theta\sin\lambda \tag{2}$$

are used; in these coordinates the sphere is $r = a$.

The primary flow is the irrotational flow about the sphere, associated with an upstream velocity field as in (1) but with $A = 0$. The secondary flow represents the first-order correction for non-zero A: thus, it is the term in Aa/U in an expansion in powers of that non-dimensional parameter.

The secondary vorticity field was determined in **D**, § 7. Certain asymptotic properties of the secondary velocity field were derived in **D**, § 3. Here, such further properties of it are derived as are necessary to determine the displacement of the stagnation streamline to the first order in the parameter Aa/U.

For this one must know the distribution along the line $y = z = 0$, $x < -a$ (which *is* the stagnation streamline for $A = 0$) of the secondary flow component normal to that line. This component is actually in the negative y-direction. It may be referred to as 'downwash' if we think of the upstream velocity distribution as horizontal and increasing upwards. Accordingly, we write $D(s)$ for the value of $(-v_y)$ at the point $(-s, 0, 0)$, and call $D(s)$ the 'downwash function'.

Now, the secondary flow may be calculated in three parts as explained in **D**, § 3. First, there is a part, which is the gradient of a potential ϕ_1 vanishing at infinity, and whose normal velocity component on the surface just cancels out that associated with the uniform shearing motion $v_x = Ay$, $v_y = v_z = 0$. In the case of a sphere this condition may be satisfied by a single solid harmonic (easily obtained by inspection), namely

$$\phi_1 = \frac{Aa^5xy}{3r^5}. \tag{3}$$

This part may be regarded as the velocity field due to the image system of the undisturbed vorticity field $(0, 0, -A)$ in the sphere $r = a$; we see that this image system consists of a single quadrupole at the centre. The contribution of this part to the downwash function $D(s)$ is

$$D_1(s) = \frac{Aa^5}{3s^4}. \tag{4}$$

Secondly, there is the Biot–Savart field of the 'vorticity change' $\boldsymbol{\omega}_1$, that is, the difference between the secondary vorticity field and its undisturbed value $(0, 0, -A)$. The contribution of this Biot–Savart field (**D**, (82)) to $D(s)$ is

$$D_2(s) = -\frac{1}{4\pi} \iiint_{x^2+y^2+z^2>a^2} \frac{\omega_{1x}z - \omega_{1z}(x+s)}{\{(x+s)^2+y^2+z^2\}^{3/2}}\,dxdydz. \tag{5}$$

To evaluate (5) it is convenient to change over to spherical polar coordinates, when it becomes

$$D_2(s) = \frac{1}{4\pi}\int_a^\infty \int_0^\pi \int_0^{2\pi} \times$$
$$\times \left\{ \frac{\omega_{1r}\, s\sin\theta\sin\lambda + \omega_{1\theta}(s\cos\theta + r)\sin\lambda + \omega_{1\lambda}(s + r\cos\theta)\cos\lambda}{(s^2 + 2sr\cos\theta + r^2)^{3/2}} \right\} \times$$
$$\times r^2 \sin\theta\, dr d\theta d\lambda. \quad (6)$$

Thirdly, there is a further irrotational part of the secondary velocity field, which must be added to the Biot–Savart field of $\boldsymbol{\omega}_1$ so that together they may satisfy the boundary condition on the surface of the sphere. In **I** this was shown to be simply the Biot–Savart field of a certain system of image vorticity inside the sphere. Using the term 'strength' to denote the product of the volume dV of an elementary region with the vorticity inside it, it was shown that transverse vortex elements of strengths $\omega_\theta\, dV$ and $\omega_\lambda\, dV$ have images of strengths $(-a/r)\omega_\theta\, dV$ and $(-a/r)\omega_\lambda\, dV$ respectively at the inverse point $(a^2/r, \theta, \lambda)$ while a radial vortex element of strength $\omega_r\, dV$ has an image system consisting of (i) a radial vortex element of strength $(+a/r)\omega_r\, dV$ at the inverse point, and (ii) a uniform line vortex, of strength $(-1/a)\omega_r\, dV$ per unit length, stretching between the inverse point and the origin.

It follows by comparison with (6) that the contribution of this image vorticity to the downwash function $D(s)$ is

$$D_3(s) = \frac{1}{4\pi}\int_a^\infty \int_0^\pi \int_0^{2\pi} \left[\left(\frac{a}{r}\right) \times \right.$$
$$\times \frac{\omega_{1r}\, s\sin\theta\sin\lambda - \omega_{1\theta}(s\cos\theta + a^2/r)\sin\lambda - \omega_{1\lambda}\{s + (a^2/r)\cos\theta\}\cos\lambda}{\{s^2 + 2s(a^2/r)\cos\theta + (a^2/r)^2\}^{3/2}} -$$
$$\left. - \frac{\omega_{1r}}{a}\,\frac{\sin\lambda}{s\sin\theta}\left\{ \frac{s\cos\theta + a^2/r}{\{s^2 + 2s(a^2/r)\cos\theta + (a^2/r)^2\}^{1/2}} - \cos\theta \right\} \right] r^2 \sin\theta\, dr d\theta d\lambda, \quad (7)$$

where the coefficient of $(-\omega_{1r}/a)$ inside the square brackets is obtained by integrating with respect to r from 0 to a^2/r (the value of r at the inverse point) the coefficient of ω_{1r} in the curly brackets in (6).

Now, $\omega_{1\lambda}$ takes the simple form (**D**, (81))

$$\omega_{1\lambda} = (A\cos\lambda)\left\{ 1 - \left(1 - \frac{a^3}{r^3}\right)^{-1/2} \right\}. \quad (8)$$

As a result, the terms involving $\omega_{1\lambda}$ in $D_2(s) + D_3(s)$, which may be designated as $D_\lambda(s)$, can be greatly simplified. Since

$$\int_0^\pi \frac{(s + r\cos\theta)\sin\theta\, d\theta}{(s^2 + 2sr\cos\theta + r^2)^{3/2}} = \left\{ \begin{array}{ll} 2s^{-2} & (s > r) \\ 0 & (s < r) \end{array} \right\}, \quad (9)$$

we have

$$D_\lambda(s) = \frac{1}{2s^2}\left[\int_a^s \left\{ 1 - \left(1 - \frac{a^3}{r^3}\right)^{-1/2} \right\} r^2\, dr - \int_a^s \left\{ 1 - \left(1 - \frac{a^3}{r^3}\right)^{-1/2} \right\} ar\, dr \right]$$
$$= \frac{1}{2s^2}\left[\frac{1}{3}\left\{ s^3 - a^3 - s^{3/2}(s^3 - a^3)^{1/2} - \cosh^{-1}\left(\frac{s}{a}\right)^{3/2} \right\} + 0{\cdot}850a^3 \right], \quad (10)$$

the last term (independent of s) being obtained by evaluating the infinite integral in terms of factorial functions.

The vorticity components ω_{1r} and $\omega_{1\theta}$ can be written

$$\omega_{1r} = (A\sin\lambda)F_r(r,\theta), \qquad \omega_{1\theta} = (A\sin\lambda)F_\theta(r,\theta), \tag{11}$$

where in **D**, § 7 the quantities F_r and F_θ were tabulated for points on three particular streamlines, and determined asymptotically near the axis of symmetry, near the surface of the sphere and far from the sphere. In terms of F_r and F_θ the terms involving ω_{1r} and $\omega_{1\theta}$ in $D_2(s)+D_3(s)$, which may be designated as $D_r(s)$ and $D_\theta(s)$ respectively, may be written as follows:

$$D_r(s) = \tfrac{1}{4}A\int_a^\infty\int_0^\pi F_r(r,\theta)r^2\sin\theta\,dr\,d\theta\Bigg[\frac{s\sin\theta}{(s^2+2sr\cos\theta+r^2)^{3/2}} + \\ + \left(\frac{a}{r}\right)\frac{s\sin\theta}{\{s^2+2s(a^2/r)\cos\theta+a^4/r^2\}^{3/2}} - \frac{1}{as\sin\theta}\times \\ \times\left\{\frac{s\cos\theta+a^2/r}{\{s^2+2s(a^2/r)\cos\theta+a^4/r^2\}^{1/2}}-\cos\theta\right\}\Bigg], \tag{12}$$

$$D_\theta(s) = \tfrac{1}{4}A\int_a^\infty\int_0^\pi F_\theta(r,\theta)r^2\sin\theta\,dr\,d\theta\Bigg[\frac{s\cos\theta+r}{(s^2+2sr\cos\theta+r^2)^{3/2}} - \\ -\left(\frac{a}{r}\right)\frac{s\cos\theta+a^2/r}{\{s^2+2s(a^2/r)\cos\theta+a^4/r^2\}^{3/2}}\Bigg]. \tag{13}$$

In the numerical evaluation of the integrals (12) and (13) difficulties arise from two main sources. First, there are the ordinary difficulties involved in the numerical evaluation of any integral when the domain of integration is infinite. These (as we shall see) can be overcome in the ordinary manner, because of our rather full knowledge of the behaviour of the integrands for large r/a.

The second source of difficulties is the unboundedness of the integrands. For every s there is one value of r (namely $r=s$) for which one of the denominators in (12) and (13) vanishes on $\theta=\pi$. In addition, F_r and F_θ have singularities, both on $r=a$, where F_θ is actually infinite, and on $\theta=0$, where F_r is actually infinite. Thus, there are difficulties in the neighbourhood of the whole dividing streamline ($\theta=\pi$, $r=a$, $\theta=0$).

This indicates the advantage of a change in the variables of integration. Instead of r, θ we use ρ_0, θ, where ρ_0, introduced in **D**, § 5 and defined by the equation (**D**, (60))

$$r^2\left(1-\frac{a^3}{r^3}\right)\sin^2\theta = \rho_0^2, \tag{14}$$

is constant along each streamline*. Then the integration with respect to θ can be carried out first (and here the fact that this integration is over a finite range $0<\theta<\pi$ is an advantage); the singular character of the integrands comes in only when the second integration (with respect to ρ_0)

* Stokes's stream function $\frac{1}{2}U\rho_0^2$ would do almost as well as ρ_0 as a variable of integration, but there are some small advantages in favour of ρ_0 in the present problem.

is carried out, and there it is confined to the single point $\rho_0 = 0$ which represents the whole of the dividing streamline.

To change the integrals (12) and (13) into integrals with respect to ρ_0 and θ, one has only to replace the differential product $drd\theta$ in each by

$$drd\theta = \left(\frac{\partial r}{\partial \rho_0}\right)_{\theta \text{ constant}} d\rho_0\, d\theta = \frac{r(r^3 - a^3)}{\rho_0(r^3 + \frac{1}{2}a^3)}\, d\rho_0\, d\theta. \tag{15}$$

The ranges of integration become $0 < \theta < \pi$, $0 < \rho_0 < \infty$.

The integrations with respect to θ, keeping ρ_0 constant, were carried out by Simpson's rule, with equal intervals of 10° for θ, for three values (0·25, 0·5 and 1·0) of ρ_0/a, using the values of r/a, F_r and F_θ given in **D**, table 3, for the required combinations of values of θ and ρ_0/a. At a few places, where the values of the integrands made it appear probable that Simpson's rule was being slightly strained, intermediate values were computed and used to improve the approximation.

If the result of such integration is written as $D_r(s, \rho_0)$ in the case of the integrand of $D_r(s)$, so that

$$D_r(s) = \int_0^\infty D_r(s, \rho_0)\, d\rho_0, \tag{16}$$

and similarly with D_θ, the problem remains of carrying out the integration with respect to ρ_0. This was done by using Simpson's rule in different forms for two parts of the integral, writing

$$\begin{aligned}\int_0^\infty D_r(s, \rho_0)\, d\rho_0 &= \int_0^{\frac{1}{2}a} D_r(s, \rho_0)\, d\rho_0 + \int_0^{2/a} D_r(s, \rho_0)\rho_0^2\, d(\rho_1^{-1}) \\ &\doteq \frac{1}{12}a[D_r(s, 0) + 4D_r(s, \tfrac{1}{4}a) + D_r(s, \tfrac{1}{2}a)] + \\ &\quad + \frac{1}{3a}\Big[\tfrac{1}{4}a^2 D_r(s, \tfrac{1}{2}a) + 4a^2 D_r(s, a) + \lim_{\rho_0 \to \infty}\{\rho_0^2 D_r(s, \rho_0)\}\Big].\end{aligned} \tag{17}$$

In this method one requires only those three values of $D_r(s, \rho_0)$ which were computed as described above, and the two limiting values $D_r(s, 0)$ and $\lim\{\rho_0^2 D_r(s, \rho_0)\}$. An equation similar to (17) is used also for D_θ.

Now it may be shown that both $D_r(s, 0)$ and $D_\theta(s, 0)$ are zero. This result is deduced from the detailed behaviour of F_r and F_θ as $\rho_0 \to 0$ derived in **D**, § 7 (equations (78) to (80)). The singularity at $\theta = \pi$, $r = s$ due to inverse (3/2)th powers in (12) and (13) produces no effect in $D_r(s, 0)$ because F_r vanishes on $\theta = \pi$, and none in $D_\theta(s, 0)$ because of the factor $s\cos\theta + r$ in the numerator. The singularity of F_θ on $r = a$ is cancelled out by the vanishing on $r = a$ of the term in square brackets in (13). The contribution to $D_\theta(s, 0)$ as well as to $D_r(s, 0)$ of this part of the streamline $\rho_0 = 0$ therefore vanishes, since the coefficient of $d\rho_0\, d\theta$ in the differential element (15) vanishes as $\rho_0 \to 0$ for fixed θ. Finally, the singularity in F_r as $\theta \to 0$ produces no effect in $D_r(s, 0)$ because of the vanishing as $\theta \to 0$ of the term in square brackets in (12).

The limits as $\rho_0 \to \infty$, on the other hand, do not both vanish. By (**D**, (77))

$$F_\theta \sim -\frac{1}{2}\left(\frac{a}{r}\right)^3 \cos\theta, \quad F_r \sim \left(\frac{a}{r}\right)^3 \sin\theta, \quad r \sim \rho_0 \operatorname{cosec}\theta, \tag{18}$$

as $\rho_0 \to \infty$. Hence by (13) and (15)

$$D_\theta(s, \rho_0) \sim \tfrac{1}{4}A \int_0^\pi \left\{ -\frac{1}{2}\left(\frac{a}{\rho_0}\right)^3 \sin^3\theta \cos\theta \right\} (\rho_0^2 \operatorname{cosec}^2\theta \, d\theta) \left(-\frac{a}{\rho_0 s^2} \cos\theta \sin\theta \right)$$

$$= \frac{\pi A a^4}{64 \rho_0^2 s^2}, \tag{19}$$

but

$$D_r(s, \rho_0) \sim \tfrac{1}{4}A \int_0^\pi \left\{ \left(\frac{a}{\rho_0}\right)^3 \sin^4\theta \right\} (\rho_0^2 \operatorname{cosec}^2\theta \, d\theta) \left\{ O\left(\frac{1}{r^2}\right) \right\} = O\left(\frac{1}{\rho_0^2}\right), \tag{20}$$

so that

$$\lim_{\rho_0 \to \infty} \{\rho_0^2 D_\theta(s, \rho_0)\} = \frac{\pi A a^4}{64 s^2}, \qquad \lim_{\rho_0 \to \infty} \{\rho_0^2 D_r(s, \rho_0)\} = 0. \tag{21}$$

Note that the distant transverse vorticity is effective entirely through its images in the sphere (that is, only the second term in square brackets in (13) contributes to the asymptotic result (19)); the distant radial vorticity is less effective* because its image system consists of a nearly cancelling pair of vortex elements of opposite sense.

Everything has now been found to enable $D_r(s)$ and $D_\theta(s)$ to be determined from equation (17). This has been done for $s/a = 1$ and $\sqrt{2}$, and the results are given in table 1, together with values of D_λ (see (10)) and D_1 (see (4)), the contributions from the 'ring vorticity' $\omega_{1\lambda}$ and from the image system of the undisturbed vorticity distribution. The four terms are added to produce the total downwash given in the last column.

s/a	D_r/Aa	D_θ/Aa	D_λ/Aa	D_1/Aa	Total D/Aa
1	$0{\cdot}12_7$	$0{\cdot}08_9$	0·425	0·333	0·97
$\sqrt{2}$	$0{\cdot}11_6$	$0{\cdot}04_7$	0·083	0·083	0·33

Table 1.

For comparison with these values of $D(s)$ we have for large s/a, by (**D**, (86)),

$$D(s) = (-v_{1y})_{x=-s, y=z=0} \sim \frac{A(V_b + \frac{1}{2}V_h)}{4\pi s^2} = \frac{5}{12}\left(\frac{a}{s}\right)^2 Aa, \tag{22}$$

where we have used the facts that the volume V_b of the sphere is $\frac{4}{3}\pi a^3$, and the volume V_h of fluid, whose mass is the 'hydrodynamic mass' associated with the sphere's motion, is $\frac{1}{2}V_b$. Table 1 shows that $(s/a)^2 D(s)$ is 0·97 for $s/a = 1$ and 0·66 for $s/a = \sqrt{2}$, so that it is tending fairly rapidly to the asymptotic value $\frac{5}{12} = 0{\cdot}42$ as $s/a \to \infty$.

* Actually, a more detailed analysis than that given above shows that $D_r(s, \rho_0) = O(\rho_0^{-4})$.

3. First-order displacement of the stagnation streamline

The stagnation streamline, or 'dividing streamline', must be in the plane of symmetry $z = 0$ (or $\lambda = 0$) and on it

$$v_r\, r\, d\theta - v_\theta\, dr = 0. \tag{23}$$

For the irrotational flow about a sphere this equation becomes

$$U\cos\theta\left(1-\frac{a^3}{r^3}\right) r\, d\theta + U\sin\theta\left(1+\frac{a^3}{2r^3}\right) dr = 0, \tag{24}$$

which can be put into the form

$$d\left\{r\sin\theta\left(1-\frac{a^3}{r^3}\right)^{1/2}\right\} = 0, \tag{25}$$

after multiplying through by $U^{-1}(1-a^3/r^3)^{-1/2}$. The solution of (25) that must be used is

$$r\sin\theta\left(1-\frac{a^3}{r^3}\right)^{1/2} = 0, \tag{26}$$

since other solutions give $r\sin\theta \to \infty$ as $r \to a$, which is impossible if the streamline is to meet the body. Hence $\theta = 0$ or π off the sphere $r = a$.

When $A \neq 0$ we can obtain the displacement of the upstream part $\theta = \pi$ of the stagnation streamline by modifying the v_θ term in (23) by including the downwash function $D(s)$ of § 2 in it. The term in v_r need not have a secondary flow term included, however, since it is multiplied by $r d\theta$ which is itself a small* quantity of order A (vanishing, as we have seen, for $A = 0$).

Thus, (24) is replaced by

$$U\cos\theta\left(1-\frac{a^3}{r^3}\right) r\, d\theta + \left\{U\sin\theta\left(1+\frac{a^3}{2r^3}\right) - D(r)\right\} dr = 0. \tag{27}$$

Equation (27) after multiplication by $U^{-1}(1-a^3/r^3)^{-1/2}$, an integrating factor already used above, becomes

$$d\left\{r\sin\theta\left(1-\frac{a^3}{r^3}\right)^{1/2}\right\} = \frac{D(r)\, dr}{U(1-a^3/r^3)^{1/2}}. \tag{28}$$

Hence the dividing streamline takes the form

$$r\sin\theta = \frac{1}{(1-a^3/r^3)^{1/2}} \int_a^r \frac{D(s)\, ds}{U(1-a^3/s^3)^{1/2}}, \tag{29}$$

that solution of (28) being chosen for which $r\sin\theta$ remains finite as $r \to a$. Thus, the displacement of the stagnation point on the sphere is

$$\lim_{r\to a}(r\sin\theta) = \frac{2a}{3U} D(a) = 0{\cdot}65\,\frac{Aa^2}{U}, \tag{30}$$

* Actually, $r\, d\theta$ becomes less small as $r \to a$, as the solution to be obtained shows, but since $v_r \to 0$ as $r \to a$ the argument is unaffected.

where table 1 has been used, while the displacement δ of the stagnation streamline far upstream of the sphere (the main object of our investigation) is

$$\delta = \lim_{r\to\infty}(r\sin\theta) = \frac{1}{U}\int_a^\infty \frac{D(s)\,ds}{(1-a^3/s^3)^{1/2}}. \tag{31}$$

To compute δ numerically we substitute $s = a\operatorname{cosec}\alpha$ in (31), giving

$$\frac{U\delta}{Aa^2} = \int_0^{\frac{1}{2}\pi} \frac{D(a\operatorname{cosec}\alpha)\operatorname{cosec}\alpha\cot\alpha}{Aa(1-\sin^3\alpha)^{1/2}}\,d\alpha. \tag{32}$$

If Simpson's rule with interval $\frac{1}{4}\pi$ is used in (32), we obtain

$$\frac{U\delta}{Aa^2} \doteqdot \frac{1}{12}\pi\left[\lim_{s\to\infty}\left\{\frac{s^2D(s)}{Aa^3}\right\} + 4\,\frac{D(a\sqrt{2})}{Aa}\,\frac{\sqrt{2}}{(1-2^{-3/2})^{1/2}} + \right.$$
$$\left. + \frac{D(a)}{Aa}\lim_{\alpha\to\frac{1}{4}\pi}\frac{\cos\alpha}{(1-\sin^3\alpha)^{1/2}}\right] \tag{33}$$

$$= \frac{1}{12}\pi\left\{\frac{5}{12} + 7{\cdot}036\,\frac{D(a\sqrt{2})}{Aa} + \frac{2}{3}\,\frac{D(a)}{Aa}\right\}$$

$$= \frac{1}{12}\pi(0{\cdot}417 + 2{\cdot}3_{22} + 0{\cdot}6_{47})$$

$$= 0{\cdot}8_9 = 0{\cdot}9. \tag{34}$$

The use of a large interval $\frac{1}{4}\pi$ for Simpson's rule may appear drastic, but the numerical value of the terms, not far from being in the ratio 1 : 4 : 1, indicates a smoothness in the integrand which justifies the conclusion that $U\delta/Aa^2 = 0{\cdot}9$ to one place of decimals. The integrations with respect to θ, unless 19 values had been used and a few more interpolated here and there, were likely to have caused more error than those with respect to ρ_0 or s which used 5 and 3 values respectively but had far greater smoothness in the integrands. Greater accuracy than one place of decimals is not required as the theory is only an asymptotic one for small Aa/U in any case.

It is really a quadruple integration which has been performed to get (34). One has integrated with respect to s a function part of which consisted of integrations with respect to ρ_0 and θ of functions which in **D** were derived as derivatives of the 'drift function' t, which is itself defined as an integral. The result of all this work, which it has taken three papers to expound (although the first two, **D** and **I**, each had, in addition, a more general application), is principally the numerical value (34). However, it will be seen in the next section that some useful qualitative results can also be found by studying intermediate steps of the calculation.

4. Discussion of results and comparison with Hall's theory

It is helpful to begin discussing the results of §2 and §3 by comparing them with those of Hall's much simpler theory of the same shear flow past a sphere. This is based on one principal approximate assumption (**H**, p. 145): that on the plane of symmetry $z = 0$ the velocity gradient $\partial v_z/\partial z$ takes the same value as in the primary (irrotational) flow. This

assumption determines the velocity field (v_x, v_y) in the plane of symmetry as the sum of the primary velocity field and an additional velocity field satisfying the two-dimensional equation of continuity

$$\frac{\partial v_x}{\partial x} + \frac{\partial v_y}{\partial y} = 0. \tag{35}$$

The only non-zero vorticity component

$$\omega_z = \frac{\partial v_y}{\partial x} - \frac{\partial v_x}{\partial y} \tag{36}$$

in this plane can also be determined from Helmholtz's equation

$$v_x \frac{\partial \omega_z}{\partial x} + v_y \frac{\partial \omega_z}{\partial y} = \omega_z \frac{\partial v_z}{\partial z}, \tag{37}$$

since the value which $\partial v_z/\partial z$ takes on the plane $z = 0$ has already been assumed. The two-dimensional velocity field (v_x, v_y) can then be determined without reference to conditions outside that plane, from a knowledge of its divergence and curl, from the boundary condition on the body, and suitable boundary conditions at infinity.

The latter boundary conditions have to be altered somewhat from their original form. Two-dimensional flows about obstacles have the well-known lack of uniqueness arising from arbitrariness in the circulation; Hall avoids this (tacitly, in **H**, (2.15)) by selecting only the solution in which the disturbance velocities fall off as fast as the inverse square of the distance from the origin (as indeed they must in the real flow); other solutions, with additional vorticity inside the sphere, would have disturbance velocities falling off as the inverse first power. On the other hand, to obtain existence of solutions, the condition that disturbance velocities tend to zero as $r \to \infty$ has to be applied only in a bounded interval of y (**H**, (3.44)), but again this is reasonable because the primary flow is a sensible first approximation to the motion only in such a region.

With these assumptions the equations are solved by means of a power series in the non-dimensional shear parameter Aa/U. The coefficient of Aa/U is an approximation to the secondary flow discussed in §2 and §3 above. The coefficients of $(Aa/U)^2$ and $(Aa/U)^3$, also obtained, are approximations to what may be called the tertiary and quartary flows.

In order to form an estimate of the value of Hall's approximate assumptions, we may compare his results for the secondary downwash function $D(s)$ with those obtained in §2 and §3. He gets, in our notation,

$$\frac{D(s)}{Aa} = \frac{a^3}{2s^3} + \frac{a}{s}\int_{s/a}^{\infty} \{x^{5/2}(x^3 - 1)^{-1/2} - x\}\, dx. \tag{38}$$

To check this, see **H**, equations (2.5), (2.9), (2.11), (3.16), (3.17) and (3.21); in Hall's notation, equation (38) is

$$(-v)_{\theta = 0} = UK\left(\frac{1}{2r^3} - \frac{dQ}{dr}\right). \tag{39}$$

Table 2 compares values of the secondary downwash function given by this paper and by Hall's theory (that is, by (38) above). It is seen that Hall's method of approximation does not lead to any large departure from our more exact values. His downwash is an overestimate; so, therefore, is his inferred value of $U\delta/Aa^2$, which, as deduced from (38) and (31), is 1·24. For comparison, if we integrate (31) approximately by means of equation (33), using Hall's values of $D(s)$ given in table 2, we obtain $U\delta/Aa^2 = 1{\cdot}20$. Neither result exceeds our value 0·9, obtained with far greater labour, by as much as 40%.

	$D(a)/Aa$	$D(a\sqrt{2})/Aa$	$\lim_{s\to\infty}(s^2D(s)/Aa^3)$
This paper	0·97	0·33	0·42
H	1·39	0·45	0·50

Table 2.

Now, in discussing the reasons for the success of Hall's approach to the problem of estimating secondary downwash and the displacement effect, it must be remembered that he uses the correct secondary vorticity field in the plane $z = 0$. (For, in calculating ω_z to the first approximation, one may legitimately put $\partial v_z/\partial z$ in (37) equal to its primary-flow value; and indeed Hall's expression for ω_z in the plane $z = 0$ agrees with our equation (8).) His secondary flow field in that plane, however, is simply *one* velocity field which satisfies the boundary condition and has the right vorticity in the plane (to be precise, it is the one whose two-dimensional divergence vanishes). In reality, the secondary velocity field can be determined only from the complete secondary vorticity field, both on the plane and off, as in § 2 above. It is easily checked that the two-dimensional divergence of this field in the plane $z = 0$ will not in general be zero.

Thus, Hall's assumptions are equivalent to the view that the main thing is to pick a velocity field which has the right vorticity locally, on the assumption that the vorticity field near the plane $z = 0$, with its image vorticity, will be much more potent in generating the velocity distribution on $z = 0$ than is the vorticity field away from $z = 0$ (and, in particular, the secondary trailing vorticity) in combination with *its* images. Now, this statement was already verified far upstream of the body in **D**, § 3 and corrigenda, from which it appeared that such an approach would give a value of the secondary downwash only 20% above the exact value far upstream, as is now confirmed by the results in table 2. For it was shown (**D**, (19) and (23)) that the velocity field far upstream which results directly from the local vorticity distribution is asymptotically

$$\frac{A(V_b+V_h)}{4\pi}\left(-\frac{y}{r^3},\frac{x}{r^3},0\right), \tag{40}$$

but that the complete asymptotic form includes also a term associated with the trailing vorticity, which (**D**, (86)) changes the $V_b + V_h$ in the downwash

implied by (40) into $V_b + \frac{1}{2}V_b$, as was used in (22) above. Thus in the case of a sphere (for which $V_b = \frac{1}{2}V_b$) expression (40) is an overestimate by exactly 20%, which identifies it with Hall's result in this region.

Nearer the sphere itself Hall's theory still gives reasonably good results for the secondary downwash. To explain this it is desirable to find out how much of the secondary downwash calculated at $s/a = 1$ and $\sqrt{2}$ in § 2 comes from trailing vorticity alongside and downstream of the sphere, which was ignored in Hall's theory.

In addition, there is an independent interest in asking how much contribution comes from trailing vorticity in the region where a turbulent wake would be found in the real flow, because of course the secondary vorticity distribution which has been used would be seriously inaccurate in this region. Accordingly, the contributions to $D(a)$ and $D(a\sqrt{2})$ from vorticity components ω_{1r} and $\omega_{1\theta}$ on parts of the streamlines $\rho_0/a = 0{\cdot}25$ and $0{\cdot}5$ with $\theta < 90^\circ$, and on parts of the streamline $\rho_0/a = 1$ with $\theta < 45^\circ$, were separately evaluated. Their contribution to $U\delta/Aa^2$ was found to be exclusively negative, but amounted only to $-0{\cdot}06$ altogether. There is some indication here that the applicability of the solution will not be much affected by the inaccuracy of the assumed distribution of vorticity in the wake.

The remaining contributions to $U\delta/Aa^2$ from ω_{1r} and $\omega_{1\theta}$ are all positive; examination shows, however, that the principal contributions come from fairly near the upstream axis $\theta = \pi$. For example, positive contributions from the region $\theta < 120^\circ$ amount to $+0{\cdot}06$, just cancelling the (also small) negative contribution from the wake region.

It is concluded that trailing vorticity cannot be regarded as responsible for the downwash on the axis upstream of the sphere, and this is compatible with the good accuracy of Hall's approximation. Physically, the result is due mainly to cancellation of the effect of trailing vortices by the effect of their image vortices.

Having examined the detailed computations to dispose of the suggestion that trailing vorticity is responsible for the displacement effect, we may now ask what, physically speaking, *is* principally responsible for it. Again, the computation in § 2 and § 3 appears to give a clear answer, namely: of the remaining vorticity and its images, the images make the main contribution to the downwash function $D(s)$ and so to the displacement effect.

To show this, one repeats the calculation of § 2 and § 3 with the terms due to ω_{1r} and $\omega_{1\theta}$ for $\theta < 120^\circ$ omitted (these terms were described above as due to trailing vorticity, and their net contribution to $U\delta/Aa^2$ was found to be zero), and divides the remaining terms into those due to vorticity outside the sphere and those due to image vorticity. Then the contribution to $U\delta/Aa^2$ of the former is found to be 0·08 and the contribution of the latter 0·81.

Actually, the vorticity outside the sphere makes its contribution almost wholly in the region far upstream; in fact the result $\lim_{s\to\infty}\{s^2D(s)/Aa^2\} = \frac{5}{12}$ is entirely due to vorticity outside the sphere, and this contributes 0·11 to

$U\delta/Aa^2$ in the calculation. On the other hand, downwash near the sphere is almost entirely due to image vorticity; the downwash at $s/a = 1$ due to vorticity outside the sphere is only $0{\cdot}15Aa$ (compare $0{\cdot}82Aa$ due to image vorticity), and that at $s/a = \sqrt{2}$ is $-0{\cdot}03Aa$ (compare $0{\cdot}36Aa$ due to image vorticity); their combined contribution to $U\delta/Aa^2$ is $-0{\cdot}03$.

To sum up the results of this section, the expected effect of trailing vorticity (or more precisely of all the vorticity ω_{1r} and $\omega_{1\theta}$ for $\theta < 120°$) is cancelled out by that of its image vorticity; the effect of the remaining vorticity outside the sphere, on the other hand, is small compared with that of its image vorticity.

The images of the undisturbed vorticity distribution $(0, 0, -A)$, and of the 'ring-vortex' part $\omega_{1\lambda}$ of the change from the undisturbed distribution, are especially potent in producing downwash, as is obvious geometrically from the rule for constructing image vortices, and they account for a part $0{\cdot}68$ in $U\delta/Aa^2$. The images of the vortex elements ω_{1r} and $\omega_{1\theta}$ in $\theta > 120°$ by contrast account for only $0{\cdot}13$.

5. The Pitot-tube problem discussed in the light of the results for a sphere

Now, calculations like those of this paper are difficult to apply to the problem of the Pitot-tube displacement effect, both because of the substantial difference of shape between a sphere and a Pitot tube, and because the calculated amount of the secondary flow, and hence also of the displacement, increases linearly with the shear parameter Aa/U; by contrast, in the range of Aa/U at which experiments have proved possible, the displacement has been found to vary little with Aa/U.

On the first difficulty, Hall points out (**H**, p. 146) that, if a sphere were used as a Pitot tube, then, provided the round opening in the front of the sphere were large enough* to include the displaced position of the stagnation point (see (30) above for our estimate of this position), the pressure measured would be close to the stagnation pressure on the dividing streamline. He goes on to argue that this 'spherical Pitot tube' would in many ways be equivalent to an ordinary Pitot tube of somewhat smaller diameter. This is well borne out by the subsequent work of Livesey (1956), who tested a Pitot tube with a hemispherical nose and a ratio $d_i/d_e = 0{\cdot}5$ of the internal and external diameters. The studies of § 4 indicate that the shape of the front of the tube, which agrees with that of the sphere, is more important than that of the rear (which extends as a long cylinder instead of being terminated), since the trailing vorticity is unimportant, and so this tube is probably a lot closer than conventional ones are to the ideal 'spherical Pitot tube'. (The main difference between the secondary flows in the two cases will be further discussed at the end of this section.) The measured displacement was $0{\cdot}10d_e$, as compared with $0{\cdot}16d_e$ obtained by Livesey

* He notes that a small hole would in any case be inacceptable because of the resulting sensitivity to yaw.

(as well as by other workers) on tubes of the form used by Young & Maas (1936). This observed difference is in agreement with Hall's suggestion.

Hall then goes on to meet the second difficulty by saying that the displacement function which we have to explain is not a constant, but rather is of the form

$$\frac{\delta}{a} = C\,\mathrm{sgn}\left(\frac{Aa}{U}\right), \tag{41}$$

where $\mathrm{sgn}\,x$ is $+1$ when $x > 0$ and is -1 when $x < 0$. (For the displacement is in the direction y increasing if $A > 0$ and in the direction y decreasing if $A < 0$.) In (41) the observed value of the constant C is about 0·2 (since the external diameter d_e of the 'spherical Pitot tube' just discussed is $2a$). Now, the discontinuous behaviour (41) is not plausible on theoretical grounds, and it is much more reasonable to suppose that the true behaviour is something like

$$\frac{\delta}{a} = C\tanh\left(\lambda\frac{Aa}{U}\right), \tag{42}$$

say (where any odd function tending to 1 at $+\infty$ could really be substituted for the tanh), but that λ is large enough so that the tanh takes the value $+1$ or -1 for all Aa/U at which accurate measurement is possible (and indeed for small Aa/U the effect measured is so small that the experimental points become intolerably scattered). If (42) were correct the limit of $U\delta/Aa^2$ as $Aa/U \to 0$ (found in § 3 to be 0·9) would be $C\lambda$, so that values $C = 0{\cdot}2$ and $\lambda = 4{\cdot}5$ would be consistent with the results of this paper.

To test these ideas one should find the next term in the expansion of δ/a in powers of Aa/U, which according to (42) would be

$$\frac{\delta}{a} = C\left\{\lambda\frac{Aa}{U} - \frac{1}{3}\lambda^3\left(\frac{Aa}{U}\right)^3 + \ldots\right\} = 0{\cdot}9\frac{Aa}{U} - 6{\cdot}1\left(\frac{Aa}{U}\right)^3 + \ldots \tag{43}$$

with the values of C and λ just suggested. The evaluation of the next term therefore requires a study of both the tertiary and quartary flows (that is, both the square and cube terms in the expansion of the velocity field in powers of Aa/U).

Accordingly, Hall evaluates these, with the aid of his basic approximation (described above at the beginning of § 4). After fairly lengthy calculations, he obtains for the displacement effect

$$\frac{\delta}{a} = 1{\cdot}24\frac{Aa}{U} - 1{\cdot}18\left(\frac{Aa}{U}\right)^3 + \ldots . \tag{44}$$

The coefficient of $(Aa/U)^3$ is of the right sign, but is five times too small for agreement with (43). Now, some of this disagreement may be due to selection of the special function tanh in (42); if one took simply a cubic levelled off constant beyond its maximum, the coefficient 6·1 in (43) would be replaced by 2·7. However, even with this form, the effect of quartary upwash on the displacement is still definitely underestimated by Hall's theory.

This is hardly surprising. In the first place, the cumulative error in applying Hall's approximation three times to obtain successively the secondary, tertiary and quartary flows must greatly exceed the error in applying it once only, which already produced an error in the displacement of the order of 30%. Again, Hall's approximation gives erroneously only the divergence, not the curl, of the secondary flow field in the plane of symmetry; but both divergence and curl will be erroneous in the case of the tertiary and quartary flows.

A more clear-cut argument, which also appears to explain the sign of the error in Hall's calculation, is provided by some discussion in **D**, § 3, which is greatly amplified and extended in a forthcoming paper (Lighthill 1957 b).

There it is shown that far upstream the tertiary flow tends to zero more slowly than the secondary flow, and that similarly the quartary flow is greater in magnitude than the tertiary (not, in fact, tending to zero at all). Hall's equations give a smaller order of magnitude for the quartary upwash, at least far upstream, than that indicated by the exact theory. This indicates that the true reduction of the displacement by the quartary flow may be greater than Hall predicts.

Actually, the successive-approximation sequence is not uniformly valid for large r. In this region the disturbances can best be treated as a small perturbation of the exact parallel flow, which leads to their expression as a Hankel transform of suitable solutions of the steady inviscid case of the Orr–Sommerfeld equation for the shear layer.

The solution so obtained can be represented as the sum of secondary, tertiary, quartary flows and so on, with downwashes of orders s^{-2}, s^{-1}, 1, respectively, only for moderately small s. For larger s the downwash behaves as a more complicated function, which ultimately falls off like s^{-1} as $s \to \infty$. The solution of this paper which assumes that the falling-off is like s^{-2} all the way therefore overestimates the displacement. It can be shown (Lighthill 1957 b) that an approximate form of the correction to δ due to departure from the secondary flow for large s is

$$\frac{a^3}{8U} \int_{-\infty}^{\infty} \frac{1}{y} \frac{dA}{dy}\, dy, \tag{45}$$

where the shear A has been supposed a function of y (measured from an origin at the centre of the sphere). This term of order a^3 is negative, and is intermediate in order between the secondary flow term $0{\cdot}9Aa^2/U$ of this paper and Hall's quartary-flow term of order a^4. This again gives a reason for the fairly rapid turning over of the graph of δ/a against Aa^2/U.

There is one more difficulty in the comparison between the theory for the sphere and the experimental results, which can be investigated effectively in the light of the theory just described. It can take two forms.

First, if an actual sphere were used as a Pitot tube, the fact that the sphere experiences drag, and has the wake associated with its drag, modifies the upstream character of the primary irrotational flow, especially far from the

body. There it is asymptotic not to a 'doublet' motion but to that due to a source of strength $D/\rho U$, where D is the drag. Accordingly the upstream behaviour assumed in our solution is incorrect. The weight of this objection should not, however, be overestimated. For a sphere of radius a the doublet strength is $2\pi Ua^3$, while the source strength even under the high-drag conditions obtaining with laminar separation (with, say, $C_D = \frac{1}{2}$) is only $\frac{1}{4}\pi Ua^2$. Hence the source produces a velocity reduction upstream of the body greater than that due to the doublet for $r > 16a$ only, so that it could hardly be expected to be important.

Secondly, for a real Pitot-tube form, the upstream behaviour of the primary irrotational flow will again be asymptotically that of a source, this time of strength πUa^2, where a is the external radius. Obviously it is more questionable in this case whether the results calculated for the sphere are applicable, even though the Pitot tube may have a hemispherical nose, because of the larger source strength. In both cases the problem is made more serious by the result (**D**, (29)), which gives

$$D(s) \sim \frac{Am}{4\pi Us}, \tag{46}$$

where m is the source strength. If the downwash really satisfied (46), then the integral (31) for the displacement would be logarithmically infinite.

However, it is shown in the forthcoming paper already mentioned that, when the solution for large s is replaced by a uniformly valid approximation, a finite value for δ emerges. It is shown that the displacement so obtained is the same as that deduced from the secondary flow alone if, in the latter, the integration be carried only to the value $s = s_c$, described as the secondary-flow cut-off. In other words the displacement is the same as if the secondary flow penetrated only a distance s_c ahead of the source. The distance s_c is of the order of the width of the shear layer; an approximation to it is given by

$$\log s_c = \frac{1}{2A(0)} \int_{-\infty}^{\infty} \left(-\frac{dA}{dy} \operatorname{sgn} y \right) \log |y| \, dy, \tag{47}$$

which makes s_c in a sense a 'geometric mean' of the difference in y-coordinate between points in the shear layer and the source.

These considerations lead to a term

$$\frac{Am}{4\pi U} \log \frac{s_c}{a} = \frac{a^2}{8U} \int_{-\infty}^{\infty} \left(-\frac{dA}{dy} \operatorname{sgn} y \right) \log \frac{|y|}{a} \, dy \tag{48}$$

in the expansion of δ in powers of a, where in (48) the value of m appropriate to a solid Pitot tube of external diameter $d_e = 2a$ has been inserted. The term (48) of order $a \log a$ in δ/a is in addition to the previously found term of order a. The logarithmic term certainly is a non-negligible addition in this case; when the integral is as much as $2A$, it would increase the coefficient of Aa/U by about a quarter. In the other case, when only the source resulting from the wake drag is present, the effect is not very important. In both cases,

however, the effect is not a complete change of order of magnitude but rather a mere quantitative increase.

To sum up, we may state as the main conclusion of this section that the original Young & Maas suggestion of a discontinuous functional dependence (41) of δ/a on Aa/U is without theoretical support. All the theories agree in predicting a continuous functional dependence, which one can only assume (in the light of experimental results) becomes slowly-varying for values of $|Aa/U|$ in excess of a fairly modest limit, an assumption which in the light of the full discussion is seen to be not inconsistent with the theories.

We may ask, in conclusion, whether the work of this paper gives any explanation of two results which were noted as especially interesting in the introduction: the great reduction of the displacement effect with supersonic flow (Johannesen & Mair 1952) or with sharp-lipped tubes (Livesey 1956). Certainly no precise answer is possible in either case, but it is probably relevant to both facts that, as shown in § 4, the image vorticity is the main contributor to the diplacement effect.

Thus, in supersonic flow about a Pitot tube, the extent of regions of vorticity whose image vorticity could affect the downwash on the dividing streamline is much reduced—partly because the region of subsonic flow is cut off by a shock wave a short distance upstream of the orifice, and partly because the flow on streamlines as far away from the axis as $\rho_0/a = 1$ (which were found in the calculations of § 2 to make substantial contributions to the downwash) becomes supersonic very soon, and ceases to have a domain of influence which includes the dividing streamline.

Similarly, one may imagine that the ideal Pitot tube with internal and external diameters equal (to which Livesey's sharp-lipped tube is a good approximation) produces very little displacement because image vorticity in such a tube is reduced, both in magnitude and in effectiveness for producing displacement. For, first, the *undisturbed* vorticity distribution $(0, 0, -A)$ has no image vorticity at all in this case. In other words, the 'first part' of the secondary flow, as defined in **D**, § 3 and in § 2 above (and which for a sphere has the potential (3)), vanishes, since the uniform shearing motion by itself possesses no velocity component normal to the surface.

As to the image system of the vorticity change $\boldsymbol{\omega}_1$, one may note that this will include a uniform vorticity $(0, 0, +A)$ from some point of the tube downstream inside the tube; for in this region all motion, and hence also all vorticity, is doubtless absent. However, the effect of this vorticity trapped inside the tube is negligible outside it; even in the corresponding two-dimensional case it falls off exponentially, by a factor of $e^{\pi} = 23$ in one diameter.

Thus, we are led finally to ask about the effect of such *disturbance* vorticity as is placed similarly to that which produced the displacement in the case of a sphere. As in that case, the effect of the trailing vorticity will be cancelled out by the effect of its images; and the vorticity upstream of the Pitot tube may be expected to make its effect largely through its image vorticity. However, since there is no room inside the surface in the case of a shape like

this, the image vorticity must be rather remote—in mathematical language, it is on another sheet of a Riemann surface (of three dimensions). Accordingly, its image effect upstream may be expected to be less than in the case of a more full-bodied shape.

Again, we have not explained the results by the theory, but merely shown that the theory is not inconsistent with them. Clearly, much more work will be required before theories of shear flow become fully satisfactory and widely applicable. However, the attempt to achieve this end seems to be worth making.

References

Cuming, H. G. 1951 The secondary flow of a viscous incompressible fluid in motion through curved pipes, *Aero. Res. Counc., Lond., Rep.* no. 13979.

Dean, W. R. 1927 *Phil. Mag.* (7), **4,** 208.

Dean, W. R. 1928 *Phil. Mag.* (7), **5,** 673.

Goldstein, S. (Ed.) 1938 *Modern Developments in Fluid Dynamics.* Oxford University Press.

Hall, I. M. 1956 *J. Fluid Mech.* **1,** 142 (referred to in the text as **H**).

Hawthorne, W. R. 1951 *Proc. Roy. Soc.* A, **206,** 374.

Hawthorne, W. R. 1954 *J. Aero. Sci.* **21,** 588.

Hawthorne, W. R. & Martin, Moira E. 1955 *Proc. Roy. Soc.* A, **232,** 184.

Johannesen, N. H. & Mair, W. A. 1952 *J. Aero. Sci.* **19,** 785.

Lighthill, M. J. 1956 a *Proc. Camb. Phil. Soc.* **52,** 317 (referred to in the text as **I**).

Lighthill, M. J. 1956 b *J. Fluid Mech.* **1,** 31. } These two papers are referred to
Lighthill, M. J. 1957 a *J. Fluid Mech.* **2,** 311. } collectively in the text as **D**.

Lighthill, M. J. 1957 b *J. Fluid Mech.* **2** (in the press).

Livesey, J. L. 1956 *J. Aero. Sci.* **23,** 949.

Macmillan, F. A. 1956 Experiments on pitot tubes in shear flow, *Aero. Res. Counc., Lond., Rep.* no. 18235.

Mitchell, A. R. & Murray, J. D. 1955 *Z. angew. Math. Phys.* **6,** 223.

Preston, J. H. 1954 *Aero. Quart.* **5,** 218.

Squire, H. B. & Winter, K. G. 1951 *J. Aero. Sci.* **18,** 271.

Young, A. D. & Maas, J. N. 1936 *Aero. Res. Counc., Lond., Rep. & Mem.* no. 1770.

On the existence of higher than normal detonation pressures

By DONALD R. WHITE
General Electric Company Research Laboratory, Schenectady, New York

(*Received* 25 *March* 1957)

With the increasing popularity of combustion driving in strong shock tube experiments, the possibility of detonation must be considered seriously. In addition to the extreme and relatively well-known conditions associated with a detonation, there exists a phase during the transition from a flame to a detonation during which pressures and velocities of propagation can exist which are higher than those associated with the fully formed detonation. This has been discussed theoretically by Oppenheim (1952) and has been shown experimentally by several workers. A luminous front having a higher than detonation velocity has been observed by Bone, Fraser & Wheeler (1936) and others. J. B. Smith (1949), using calibrated burst diaphragms at the end of a pipe, has observed reflected pressures in fuel gas–air, acetylene–air, and hydrogen–air mixtures which were approximately four times greater than those associated with a reflected normal detonation. Turin & Huebler (1951), using quartz pressure transducers in the side of a tube, observed pressures during this transition process about three and a half times higher than those at a later time when detonation was fully developed. They worked with Toledo natural gas. Mooradian & Gordon (1951) also have clear indications of this phenomenon with hydrogen–air mixtures.

Tube length	Peak pressure	Time to half maximum pressure	Impulse
24 ft.	no detonation	—	—
32 ft.	2600 lb./in.^{2}	200 microsec	0·8 lb. sec/in.^{2}
47 ft.	710 lb./in.^{2}	1000 microsec	1·0 lb. sec/in.^{2}

Table 1.

Several experiments have been run in this laboratory using a quartz pressure transducer (SLM model PZ 14) mounted in the end flange of a $3\frac{1}{4}$ in. square tube. A stoichiometric hydrogen–air mixture at atmospheric pressure was ignited near one end of the tube with a spark plug, and the pressure on the other end of the tube was measured as a function of time. This pressure record was then integrated between the time of impact and the time the pressure dropped to 150 lb./in.^{2} abs. to obtain the impulse applied to the end of the tube during this interval. The pressure level corresponding to constant volume combustion is about 120 lb./in.^{2} abs., and that due to a reflected normal detonation wave is on the order of 500 or 600 lb./in.^{2}. Our measurements are given in table 1.

The 32 ft. length was marginal with respect to occurrence of this over-detonation when the ignition was at the extreme end. However, moving the spark plug 32 in. from the end resulted in this over-detonation on each run at this length. Over-detonation was accompanied by a much more substantial noise than was detonation, like the difference between blows by a sledge hammer and a carpenter's hammer.

This over-detonation phenomenon may have escaped the attention of some experimenters using combustion driving in shock tube experiments. It must be noted that not only are the limits for the occurrence of detonation rather uncertain, but also that the first departure from the expected constant volume combustion may result in a pressure loading much more severe than that which would result from a fully developed detonation. The long distances noted above do not offer comfort since the use of oxygen instead of air greatly reduces the formation distance for detonation. This hazard may be reduced by using a number of points of ignition and by choosing a gas loading sequence such that the mixture does not go through a condition which is more readily detonable than the final mixture desired (i.e. loading of hydrogen last).

References

Bone, W. A., Fraser, R. P. & Wheeler, W. H. 1936 *Phil. Trans.* A, **235,** 29.

Mooradian, A. J. & Gordon, W. E. 1951 *J. Chem. Phys.* **19,** 1166.

Oppenheim, A. K. 1952 Gas dynamic analysis of the development of gaseous detonation and its hydraulic analogy. *Fourth Symposium on Combustion,* p. 471. Williams & Wilkins.

Smith, J. B. 1949 Explosion pressures in industrial piping systems. Paper presented before the International Acetylene Association; copies available from Eng. Div., Factory Mutual Labs, Boston, Mass.

Turin, J. J. & Huebler, J. 1951 *Report Comm. Industr. Commer. Gas Res., Project I.G.R.*–59. Amer. Gas Assn.

REVIEWS

Viscous Flow Theory, I—Laminar Flow, by SHIH-I PAI. Princeton: D. Van Nostrand Co., 1956. 384 pp. $7.75 or 58*s*.

In the study of real fluids, this has been the half-century of boundary layer theory. It is remarkable how Prandtl's discovery still dominates research in viscous flow, as it has done since 1904, though one may suspect that the possible extensions of boundary layer theory are at last nearly exhausted, and that the really exciting discoveries await us in problems in which the boundary layer, if present at all, is but one component of the flow field. Oseen swam against this current for years, not finding it necessary in his *Hydrodynamik* of 1927 even to mention Prandtl or his Grenzschicht. But with a few other exceptions the history of viscous flow theory since the turn of the century has been in large part the record of the development of boundary layer theory, following paths that to a remarkable extent were at least sketched in outline by Prandtl and his students in the first few pioneering years.

It is perhaps not surprising, then, that the book under review, which is the first of a two-part work on viscous flow theory (the second being devoted to turbulent flow), is concerned mainly with the theory of the laminar boundary layer. Indeed, aside from two short and rather disappointing chapters on other topics, it is devoted entirely to a thoroughly modern survey of laminar boundary layer theory, together with the requisite introductory chapters. It is not intended to be a comprehensive treatise in the style of Schlichting's *Grenzschicht-Theorie*, but a textbook for advanced students of engineering and aerodynamics. The account is purely theoretical, with no enlightenment ever sought from experiment.

The great virtue of the book is that it is the first to assign a central role to compressibility and heat conduction. In this respect it is strongest where Schlichting's treatise is weakest; for, even in the expanded English translation, Schlichting considers an incompressible fluid from the outset, and defers to the advent of high-speed flight only in two appended chapters. (Goldstein's *Modern Developments in Fluid Dynamics*, written as it was at the dawn of the age of compressibility, could not reasonably have attempted a unified treatment of compressibility and heat conduction.) To be sure, Dr. Pai is forced more often than not to retrench in view of mathematical complexity, and to consider a particular problem only in the special case of incompressible flow. But his eye is constantly on the compressible fluid. This is undoubtedly the modern approach, to be taken by future writers.

If one thus breaks with tradition and starts from the Navier–Stokes equations for a compressible heat-conducting gas, it is imperative that he understand precisely how compressibility enters the problem, and how the often necessary specialization to incompressible flow is to be made. The supersonic aerodynamicist, who automatically associates compressibility with Mach number, may be surprised to realize that for a heat-conducting fluid there is a second way in which compressibility can appear. No matter how slight the Mach number, heating of a body will induce a

temperature field in the flow and consequent variations of density. Unfortunately, such important distinctions are not always clearly made in the present book. Nor are they perhaps entirely clear to the author, who remarks (p. 49): "Another current practice in finding the temperature distribution approximately is to drop the viscous dissipation terms in the energy equation, and then to solve for the temperature distribution. Strictly speaking, such an approximation is not logical, because the terms of heat conduction and vicous dissipation are of the same order of magnitude. But for practical purposes, when both the velocity of the flow and the temperature gradients are small, such an approximation seems to give reasonably good results."

Now the fact of the matter is that conduction and dissipation are not of the same order of magnitude in general, and that there are important classes of problems in which it is an entirely logical approximation to drop the dissipation term (and the more so the larger the temperature gradients). Consider for definiteness a stream of perfect gas flowing at Mach number M past a heated body. Introducing dimensionless variables in the energy equation (or solving an example) shows that both the dissipation and the enthalpy changes due to pressure gradients are proportional to M^2. Hence dissipation and also pressure terms in the energy equation can be neglected strictly at $M = 0$ or approximately when M^2 is very small. If, in addition, the maximum temperature difference ΔT is small compared with the temperature T itself, then density variations are slight, and to a first approximation the momentum and energy equations are not coupled, so that the heat is transported by the incompressible velocity field. (This is readily verified by expanding all flow quantities in powers of $\Delta T/T$ and retaining only linear terms.)

If the body is insulated (the thermometer problem), viscous dissipation is the only source of heat, so that a problem exists only for $M > 0$. If M^2 is small, the heat is again carried by the incompressible velocity field to a first approximation. The combined problem in which heat is supplied both by transfer from the body and by dissipation can be handled with a double series expansion, which shows that to a first approximation for small $\Delta T/T$ and M^2 the solution of the thermometer problem can simply be added to the solution of the heat transfer problem for $M = 0$, and that non-linearities as well as coupling between the momentum and energy equations arise only in the second-order terms.

It should be pointed out that the above conclusion that dissipation is strictly negligible at $M = 0$ holds only for flows with a definite stream. In problems of free convection the dissipation can be neglected only as a first approximation for slight heating, because the velocities are proportional to $\Delta T/T$ and the dissipation is consequently of order $(\Delta T/T)^2$. It must be admitted that these matters are not well explained in most existing books on viscous flow theory, or in many research papers. (They are very carefully discussed in Lagerstrom's forthcoming article on laminar flow in the Princeton series, and briefly but precisely in Lighthill's paper in *Proc. Roy. Soc.* A, vol. 202, 1950, p. 359.)

The first hundred pages of the present book are introductory in nature, covering basic thermodynamics and kinetic theory, the laws of friction and heat conduction, the derivation of the equations of motion, a number of illustrative exact solutions (mainly incompressible), dynamic similitude, and a general discussion of the Navier–Stokes equations, including Burgers' model, linearization, and the limits of low and high Reynolds number. There follows a short chapter on slow motion, which has a curiously old-fashioned tone. Indeed, there are no references to work done since 1910, which is a pity, since the realm of Stokes and Oseen flow is one in which some interesting discoveries have recently been made, with more expected to follow.

The main bulk of the book, some 200 pages, is devoted to a generally admirable survey of laminar boundary layer theory. This is the field of the author's own research, is clearly where his heart lies, and is by far the strongest part of the book. The emphasis is on compressible flow where possible, including such recent matters as the hypersonic boundary layer and interaction with a shock wave. Successive chapters treat the boundary layer equations, exact solutions, approximate methods, axisymmetric and three-dimensional boundary layers, unsteady boundary layers (including a sketch of the stability theory), and boundary layers with suction and injection. Aside from Kuerti's survey in the second volume of *Advances in Applied Mechanics*, there is no comparable summary of compressible laminar boundary layer theory, and I would recommend it with only minor quibbles. I would only protest that more than the necessary two boundary conditions are provided for the energy equation on pages 148–149, and that of these the requirement of equal normal temperature gradients in the gas and body at their juncture is incorrect. (Note also the unfortunate typographic loss, on page 178, of a radical sign in Blasius' famous formula for flat-plate skin friction.) In particular, the author displays considerable skill in summarizing the various complicated extensions to a compressible fluid of the Kármán–Pohlhausen approximation.

He breaks away from the boundary layer approximation again in the last chapter, which is entitled " Linearized theory of viscous compressible fluid ". Although mainly a survey of Lagerstrom, Cole, and Trilling's study of compressible Oseen flow, it also includes, among other incidentals, an overly-condensed account of Kuo's second approximation to Blasius' solution for the boundary layer on a finite flat plate, from which the main result—the numerical coefficient of the second term (it is $a_2 = 4{\cdot}12$)—is unaccountably omitted. Unfortunately, the author has thought it necessary to copy some ten pages of his book literally word for word from the report of Lagerstrom *et al.* (In his only major departure from that text, he thoroughly garbles the characteristic condition for a second-order partial differential equation.) Now it is perhaps a matter of taste whether one chooses to expound another's theory by quoting him verbatim and at length; this seems to be a growing trend in the literature of fluid mechanics, for I have found three well-known writers doing so within the last year. But it is certainly another, and quite indefensible, matter when the present author

concocts introductory pages that are ostensibly his own by assembling a pastiche of sentences and paragraphs lifted from the Lagerstrom report.

This is, then, a book with some serious flaws, written in a style that is often derivative, and concerned more with examples than ideas. Despite its title, it concentrates on the boundary layer approximation to the virtual exclusion of other facets of viscous flow theory. Yet, admitting these limitations, it is the best available survey of laminar boundary layer theory from the modern point of view. The student who arms himself also with at least the first of Goldstein's two masterly volumes, to provide the physical insight and appeal to experiment that the present book lacks, should find it a useful guide to that subject. M. D. VAN DYKE

Molecular Flow of Gases, by G. N. PATTERSON. New York: John Wiley & Sons, 1956. 217 pp. $7.50 or 60*s*.

The molecular viewpoint in studies of gas flows is by no means a new area of interest. It goes back at least to the studies of Kundt, Warburg and Maxwell (1875–1879) on low-speed slip flow, and the later work of Knudsen and Smoluchowski (1910–1911) on low-speed free molecule flow. However, the increase in the amount of research in molecular gas flows since World War II is most impressive. Over and above a proportionate share of the post-war growth of all branches of science, the increasing importance of the molecular viewpoint in many problems has attracted the attention of more and more scientists from the disciplines of physics, chemistry and astronomy.

There is a wide range of problems requiring a consideration of the molecular structure of moving gases. Such considerations are necessary in the study of colliding galaxies, supernovae, stellar atmospheres, and meteors, in the development of high-speed, long-range missiles, in the development of controlled thermonuclear reactions, and in the study of shock-induced chemical reactions. An illustration of the kind of problem to be dealt with is provided by a simple shock transition. For weak shock waves in a moderately dense monatomic gas, the shock transition zone (the region between the shock front and the attainment of equilibrium in the shocked state) is so thin as to defy detailed experimental study, the gas behaves ideally, and the transition can be dealt with adequately by regarding it as a discontinuity in a continuum fluid flow problem. Conservation laws are here sufficient for a determination of the change in flow properties across the transition. At low densities in a monatomic gas the density profile through the shock thickens in proportion to the increased mean free path in the gas, for a certain number of collisions are required for equilibration of translational energy of the molecules. (It is interesting to note here that a shock profile derived from the Navier–Stokes equation with the continuum viewpoint represents the observed transitions better than the best solutions of the Boltzmann equation yet available.) With stronger shocks in a diatomic gas the transition zone is thickened further, as the gas requires many more collisions to equilibrate rotational and

vibrational degrees of freedom than to equilibrate translational kinetic energy. Here we must not only consider the Boltzmann equation with inelastic collisions, but must modify the ideal gas form of the internal energy to include thermodynamic properties of the specific gas under study, in order to specify correctly the final equilibrium state. For still stronger shocks we must include molecular dissociation, ionization and other gas phase reactions. Much work needs to be done before we understand on a theoretical basis even such a basic problem as the shock transition in molecular gas flows.

There appear to be several stages of sophistication involved in considering gas flows on a molecular basis. There is firstly a purely kinetic viewpoint in which one assumes elastic collisions and a model for the intermolecular forces in the gas. If the collisions cause at most a small deviation from a Maxwell velocity distribution, then one can use the Boltzmann equation and the Maxwell equations of transfer to develop the fluid equations of motion, including transport properties. Boundary conditions at a surface in the flow also may be developed on this basis. A more sophisticated development would describe gas flows under the condition that the molecular collisions are inelastic. Here the collisions not only alter materially the velocity distribution function, but involve energy transfer into internal excitation, dissociation, ionization, recombination, and so on. In a still more sophisticated analysis one might attempt (although whether it would be profitable to do so is debatable) to deal with turbulent flows, in which one might combine consideration of microscopic, random molecular motions with the ordered motion in eddies having dimensions of many gas mean free paths. Other more complex flow problems include the motion of highly ionized gases involving collective behaviour due to long range forces, and the motion of very dense gases in which one may not be able to limit the analysis to bimolecular collisions only and in which collisions may not be isentropic because of the finer details of intermolecular forces.

Professor Patterson's book is concerned primarily with the first stage of sophistication mentioned above. The book has as its stated purpose the provision of a transition from the continuum to the molecular viewpoint in fluid mechanics, and provides perhaps as elementary an introduction to the kinetic theory of non-uniform gases as can reasonably be expected for those interested principally in fluid mechanics. It might be read with profit by those who would later undertake study of such works as *Mathematical Theory of Non-Uniform Gases* by Chapman and Cowling or *Molecular Theory of Gases and Liquids* by Hirschfelder, Curtiss and Bird.

The book begins with a brief discussion of basic concepts in kinetic theory, including an introduction to the Boltzmann integro-differential equation and the Maxwell transfer equation. A very clear discussion is given of molecular collisions. Next the author describes the solution of these equations for gases represented by perfectly elastic spherically symmetric particles, having no internal degrees of freedom. Collisions of such particles do not alter the velocity distribution function, the

gas is in a steady state, and the Boltzmann equation leads directly to the Maxwellian velocity distribution. The transfer equation then leads to the equations of isentropic flow. Properties of a Maxwellian gas are then discussed. As part of the isentropic flow discussion the author develops at some length the non-stationary expansion wave.

The major part of the book is devoted to slightly non-isentropic flows, i.e. flows in which small gradients in composition, temperature, and density occur, and in which the velocity distribution function deviates slightly from the Maxwellian. To describe such flows one assumes a repulsive force field for a point particle having no internal degrees of freedom. Using a method due to Grad, the author obtains a perturbation solution to first order of the Boltzmann equation for a gas not in a shady state. The resulting transport properties are similar to the Chapman–Enskog result. The theory is then applied to weak shock transitions and boundary layer flows. Comparisons are made with experimental studies of slightly non-isentropic flows. A very brief discussion is given of the flow alterations resulting from real gas effects, i.e. internal excitation of atoms and molecules, dissociation, ionization, etc. Finally there is a description of the present state of the theory of slip flow and of free molecule flows. Appendices include some mathematical relations which occur in kinetic theory problems, a discussion of first-order ordinary and partial differential equations, and a concise statement of the procedure leading to the Chapman–Enskog result and the Burnett approximation.

Several features and flaws of the book invite comment. The author has achieved his goal of giving an introduction to the flow of gases with molecular structure. The discussion of molecular collisions and the development of the flow of rarified gases are presented with particular clarity. The exposition of expansion waves and characteristics is unnecessarily long, not too pertinent to the main thesis of the book, and the material covered is readily available to the reader elsewhere. The discussion of gas flows in which molecules are excited, dissociated or ionized, or in which chemical reactions may occur, is much too brief. What discussion is given is cursory and fails to convey to the reader what can be accomplished by an analysis of high temperature and high velocity flows in terms of thermodynamics and chemical kinetics. For example, one finds the familiar equilibrium constant applied to a dissociation reaction referred to as "a characteristic quantity relevant to dissociation". The appendices could be eliminated without any particular loss to the book, except that the brief mention of the Burnett approximation might profitably be expanded and incorporated into the text as part of a discussion of the general problem of dealing with the Boltzmann equation. The author does not even hint that there is at present considerable interest in the molecular description of the flow of conducting gases in magnetic fields.

The flaws mentioned nevertheless are minor, and do not detract seriously from the general worth of the book as a useful text for introduction of the student of gas dynamics to the molecular viewpoint.

R. A. Alpher

JOURNAL OF
FLUID MECHANICS

—o—

Orders originating

in

UNITED STATES OF AMERICA

and

CANADA

should be sent to the sole agents

ACADEMIC PRESS INC.

111 Fifth Avenue,

New York, 3,

N.Y., U.S.A.

JOURNAL OF FLUID MECHANICS
Volume 2, Part 5 July 1957

CONTENTS

On the generation of waves by turbulent wind
by O. M. PHILLIPS 417

A cross-flow theory for the normal force on inclined bodies of revolution of large thickness ratio
by R. N. COX 446

The laminar and turbulent mixing of jets of compressible fluid. Part I Flow far from the orifice
by L. J. CRANE and D. C. PACK 449

Turbulent transport of heat and momentum from an infinite rough plane
by T. H. ELLISON 456

An experimental investigation of a wall jet
by P. BAKKE 467

Turbulent convection over a heated horizontal surface
by D. B. THOMAS and A. A. TOWNSEND 473

Contributions to the theory of the Pitot-tube displacement effect
by M. J. LIGHTHILL 493

On the existence of higher than normal detonation pressures
by DONALD R. WHITE 513

Reviews 515